

EXPRESSION, PURIFICATION AND CHARACTERIZATION OF A
DROSOPHILA MELANOGASTER MANNOSIDASE ORTHOLOGOUS TO
DROSOPHILA MELANOGASTER GOLGI MANNOSIDASE II

by

HEATHER ANNE STRACHAN

(Under the Direction of Kelley Moremen)

ABSTRACT

Drosophila melanogaster Golgi Mannosidase IIb (dGMIIb) is a class II (CAZy GH38) α -mannosidase involved in the processing of N-glycan structures in the insect secretory pathway. The enzyme activity of this 140-145 kDa protein is stimulated by cobalt, sensitive to furanose inhibitor mimics (swainsonine and 1,4-di-deoxy-mannitol), and has a pH optimum of 6.0. dGMIIb is an ortholog of the well-characterized *Drosophila melanogaster* Golgi Mannosidase II (dGMII). The preferred natural substrate for dGMII is GlcNAcMan₅GlcNAc₂ asparagine (N)-linked proteins, whereas the preferred natural substrate for dGMIIb is Man₅GlcNAc₂. dGMII has been crystallized and its active site extensively studied as a potential target for inhibition in cancer therapeutics. Modeling of dGMIIb using the crystal structure of dGMII as a template reveals differences in the GlcNAc - binding “anchoring site” which may account for the distinct substrate specificities of these processing enzymes.

INDEX WORDS: *Drosophila melanogaster* Golgi Mannosidase IIb, *Drosophila melanogaster* Golgi mannosidase II, α mannosidase II and α mannosidase IIb

EXPRESSION, PURIFICATION AND CHARACTERIZATION OF A
DROSOPHILA MELANOGASTER MANNOSIDASE ORTHOLOGOUS TO
DROSOPHILA MELANOGASTER GOLGI MANNOSIDASE II

by

HEATHER ANNE STRACHAN

B.S., University of Central Florida, 2001

A Thesis Submitted to the Graduate Faculty of The University of Georgia in
Partial Fulfillment of the Requirements for the Degree

MASTER OF SCIENCE

ATHENS, GEORGIA

2009

© 2009

Heather Anne Strachan

All Rights Reserved

EXPRESSION, PURIFICATION AND CHARACTERIZATION OF A
DROSOPHILA MELANOGASTER MANNOSIDASE ORTHOLOGOUS TO
DROSOPHILA MELANOGASTER GOLGI MANNOSIDASE II

by

HEATHER ANNE STRACHAN

Major Professor: Kelley Moremen

Committee: Michael Pierce
Michael Tiemeyer

Electronic Version Approved:

Maureen Grasso
Dean of the Graduate School
The University of Georgia
December 2009

DEDICATION

I would like to dedicate this body of work to all scientists, for the future development of selective cancer therapeutics and the continuing pursuit of scientific endeavors for the betterment of humanity.

ACKNOWLEDGEMENTS

I would like to acknowledge my partner, Dean Moniz, for all his love and patience. His contribution to the completion of my research in the form of support is immeasurable.

I would also like to acknowledge my major professor Kelley Moremen as an excellent mentor, as well as past and present members of my lab Rozalyn, Alison, Trisha, Yong, Lu, Harminder, Narendra, Khanita, Steve, Chaeho, and Zhifeng, for their intellect and insight, which contributed to the completion of my research.

TABLE OF CONTENTS

| | Page |
|--|------|
| ACKNOWLEDGEMENTS | v |
| LIST OF TABLES..... | viii |
| LIST OF FIGURES | ix |
| CHAPTER | |
| 1 LITERATURE REVIEW..... | 1 |
| α -Mannosidases: Classification and Biochemical Characteristics..... | 8 |
| Glycosyl hydrolase Enzymatic Mechanisms | 11 |
| Golgi Mannosidase II: A Target for Cancer Therapeutics | 14 |
| Glycan Processing in the Golgi apparatus: Biochemical Redundancies | 15 |
| <i>Drosophila</i> Golgi Mannosidase II | 20 |
| References..... | 32 |
| 2 EXPRESSION, PURIFICATION AND CHARACTERIZATION OF A <i>DROSOPHILA MELANOGASTER</i> MANNOSIDASE ORTHOLOGOUS TO <i>DROSOPHILA MELANOGASTER</i> GOLGI MANNOSIDASE II | 44 |
| Abstract..... | 45 |
| Introduction | 46 |
| Results | 50 |
| Discussion..... | 60 |

| | | |
|---|----------------------------|----|
| | Materials and Methods..... | 62 |
| | References..... | 72 |
| 3 | DISCUSSION..... | 79 |
| | References..... | 85 |

LIST OF TABLES

| | Page |
|---|------|
| Table 1.1: Characteristics of Eukaryotic Processing and Catabolic α -Mannosidases | 89 |
| Table 2.1: Protein Purification Table | 98 |
| Table 2.2: K_m and K_i Data with 4MU-Man Substrate and Selected Inhibitors.... | 102 |
| Table 2.3: K_m Data with Natural Substrates | 104 |
| Table 2.4 Comparison of Natural Substrate Affinities Normalized to 4MU-Man | 105 |

LIST OF FIGURES

| | Page |
|--|------|
| Figure 1.1: Partial Scheme for Mammalian N-linked Biosynthesis & Catabolism | 87 |
| Figure 1.2: Dendrogram of Selected Glycosyl Hydrolase Family 38 Enzymes ... | 90 |
| Figure 1.3: Co-crystal Structures of dGMII with Small Inhibitors | 91 |
| Figure 1.4: Three Binding Pockets for Specific Substrate Interactions with dGMII | 93 |
| Figure 1.5: The Anchoring Site | 94 |
| Figure 1.6: Superimposed bLysMan and dGMII..... | 95 |
| Figure 2.1: 4MU-Man Activity Over Induction Period of Four Days..... | 96 |
| Figure 2.2: Phenyl Sepharose Purification..... | 97 |
| Figure 2.3: Nickel-NTA Purification..... | 98 |
| Figure 2.4: Determination of Optimum pH for Catalytic Activity | 100 |
| Figure 2.5: Metal Cation Requirement | 101 |
| Figure 2.6: HPLC Chromatograms Depicting Natural Substrate | 103 |
| Figure 2.7: Homology Modeling of dGMIIb and SfMII | 106 |
| Figure 2.8: Comparison of Binding Regions in Homology Models and Superimposed Structure | 110 |
| Figure 2.9: The Active Site..... | 112 |
| Figure 2.10: The Holding Site | 114 |
| Figure 2.11: The Anchoring Site | 115 |
| Figure 2.12 Constructs Used for Expression | 117 |

CHAPTER 1

LITERATURE REVIEW

A General Overview of N-linked Glycosylation

Asparagine-linked oligosaccharides are made in the secretory compartments of all eukaryotic cells. The synthesis and maturation of these oligosaccharides occurs in the endoplasmic reticulum (ER), the Golgi complex, trans-Golgi network, and the transport vesicles between the compartments of these cells (Kornfeld and Kornfeld 1985; Moremen, Trimble et al. 1994). Biosynthesis happens in four stages; the first three stages are well conserved between organisms (Moremen 2002). The first stage of the pathway involves the synthesis of a membrane-bound dolicholpyrophosphate precursor by enzymes located on both sides of the ER membrane (Moremen 2002). This precursor is synthesized at first on the cytoplasmic face of the ER membrane and then the synthesis is completed on the luminal side of the membrane. The second stage in the pathway involves the transfer of the completed core oligosaccharide from the dolicholpyrophosphate carrier through the action of an oligosaccharide transferase complex that generates an amide linkage to asparagine residues in Asn-X-Ser/Thr glycosylation sequons on newly created polypeptides as they are translocated to the luminal side of the ER membrane (Helenius and Aebi 2001;

Moremen 2002; Roth 2002). In the third stage of the pathway, the oligosaccharide undergoes trimming by ER glucosidases I and II, and ER mannosidase I (ERMI) and in some cases ER Mannosidase II (ERMII), to form a $\text{Man}_8\text{GlcNAc}_2$ oligosaccharide structure from a $\text{Glc}_3\text{Man}_9\text{GlcNAc}_2$ structure (Moremen 2000; Moremen 2002). These three early steps in N-glycan biosynthesis that occur in the ER, including the production of the dolichol-oligosaccharide precursor and cycles of glucose removal and re-addition that are closely involved in protein folding and quality control, are conserved among most eukaryotic organisms (Figure 1.1). The fourth, and final, stage of N-linked oligosaccharide biosynthesis occurs in the Golgi complex and involves the branching and addition of the glycans by Golgi glycosyltransferases (Moremen 2002). This final stage is the most diverse stage among eukaryotes and produces the wide spectrum of N-linked oligosaccharides seen in different cell and tissue types (Varki 1998; Moremen 2002).

In fungal organisms, after the generation of the $\text{Man}_8\text{GlcNAc}_2$ structure, up to 15 mannose or more residues are added to this structure to produce high-mannose N-glycans that are the majority of N-glycans found in these organisms (Moremen, Trimble et al. 1994). In contrast, metazoan organisms, which are the focus of this body of work, processing of N-glycans to a $\text{GlcNAcMan}_3\text{GlcNAc}_2$ core structure occurs with a conservation of the next three biosynthetic steps that include Golgi mannosidase I (GMI), GlcNAc Transferase I (GnTI) and Golgi Mannosidase II (GMII). GMI and its isoforms, cleave three mannose residues from the $\text{Man}_8\text{GlcNAc}_2$ structure to produce a $\text{Man}_5\text{GlcNAc}_2$ structure. An N-

acetylglucosamine (GlcNAc or Gn) residue is then added by GnTI. This is the first enzyme needed to create hybrid type N-glycans. Two more mannose residues are removed by GMII in the medial Golgi compartment to produce a $\text{GlcNAcMan}_3\text{GlcNAc}_2$ core structure (Moremen 2000; Moremen 2002). In mammals GlcNAc transferase II (GnTII) acts on the GMII product to create complex N-glycans, which are the most abundant glycans in vertebrates.

Four more GlcNAc transferases (III-VI) are found in mammals, and up to six branches have been observed on the pentasaccharide core in mammalian glycoproteins. GlcNAc transferases compete for hybrid and/or complex N-glycans. For example, GlcNAc Transferase III (GnTIII) competes with GMII and GnTII by adding a bisecting β 4 linked GlcNAc to the β -linked mannose residue on the pentasaccharide core in mammalian glycoproteins. GnTIII inhibits the addition of a β 6-linked GlcNAc by GlcNAc Transferase V (GnTV) and a core α 6-fucose linkage by α 6-fucosyltransferase. Arthropods, in contrast to mammals, have an N-acetylglucosaminidase that removes the GlcNAc residue of the GMII product, $\text{GlcNAcMan}_3\text{GlcNAc}_2$, to produce a “paucimannosidic” N-glycan with a $\text{Man}_3\text{GlcNAc}_2$ oligosaccharide structure. In arthropods, $\text{GlcNAcMan}_3\text{GlcNAc}_2$ is the substrate for additional α 3- and α 6- fucosyltransferases (α 3 core fucose linkages are not found in mammals) that create the paucimannosidic glycans $\text{Man}_3\text{GlcNAc}_2\text{Fuc}_6$ and $\text{Man}_3\text{GlcNAc}_2\text{Fuc}_{3,6}$, after the action of N-acetylglucosaminidase. Paucimannosidic glycans are the most abundant glycans found in arthropods and only a very small amount of complex structures are found. In mammals complex type structures are more prevalent, while high

mannose structures are less abundant and paucimannose glycans are extremely low abundance.

The primary focus of this proposal is a pair of isozymes of Golgi mannosidase II in *Drosophila*, Golgi Mannosidase II (dGMII) and *Drosophila* Golgi Mannosidase IIb (dGMIIb), enzymes that are involved in processing N-glycans to trimmed core structures in insect cells. These studies provide insights into the machinery of glycan maturation in insect cells and, by comparison to processing enzymes in mammals, reveals the structural basis for substrate recognition.

Glycosylation and Human Genetic Disease

Carbohydrates are the most structurally diverse and complex biopolymers in biological systems (Lowe and Marth 2003). It is predicted that 1% of genes in the mammalian genome are involved in carbohydrate biosynthesis and modification (Lowe and Marth 2003). Most extracellular proteins contain asparagine-linked (N-linked) oligosaccharides (N-linked glycans or N-glycans) as a result of post-translational modification (Varki 1993). Proteins that have these oligosaccharide modifications include enzymes, hormones, secreted proteins, cell surface receptors, immunoglobulins, and viral antigens (Varki 1993). The carbohydrates attached to these different proteins have been found to influence interactions with their environment and many important biological events including protein folding, localization, immunogenicity, bioactivity, and adhesion characteristics (Moremen 2000). Secreted and cell surface N-glycans play

important roles in cell to cell communication during development, immune response, hormonal response, inflammatory response, viral infection, arthritis, and metastasis of oncogenically transformed cells (Feizi 1985; Varki 1993; Moremen 2000). The structural diversity and complexity of N-glycans allows for the wide range of functions exhibited by these glycoconjugates and is essential for proper functioning in metazoan organisms (Moremen 2002).

The post-translational modification of glycosylation is important in many interactions including cell-to-cell communication and signaling during development and immune response. Disorders of glycosylation have become recognized as the cause of a growing number of genetic diseases (Lowe and Marth 2003). In elucidating the roles of complex-type N-glycans over the last 25 years, researchers have developed a variety of approaches to study the biological effects of these oligosaccharide linkages. These studies include generating defective enzymes in mouse models through gene disruptions, analyzing genotypes in humans that have defects in the enzymes involved in biosynthesis and catabolism of N-glycans, and inhibiting these enzymes with glycosidase inhibitors in cell culture (Moremen 2002). From these studies it has been found that malfunctions in the earlier, most conserved, steps of glycosylation are more harmful to the organism than disruptions later in the pathway (Haltiwanger and Lowe 2004). For example, *Mgat1* is the gene that encodes GnTI, which enables hybrid and complex glycosylation. When this gene is disrupted only high mannose structures can be formed. *Mgat1* null embryos have defects in vascularization, neural tube development and *situs inversus* of

the early heart. As a result, null embryos die *in utero* by embryonic day 9.5 (Ioffe, Liu et al. 1996). This embryonic developmental period is related to the first trimester in humans where interactions between cells and signaling occurs and promotes important changes in the embryo's morphology (Wang, Tan et al. 2001). This demonstrates the importance of hybrid and complex glycosylation in cell differentiation in embryogenesis. In contrast, if the gene that encodes GnTII (*Mgat2*) is disrupted, human and mouse embryos develop and survive past birth (Wang, Tan et al. 2001). GnTII allows for the formation of complex glycans; in *Mgat2* null animals the majority of N-glycans formed are hybrid type. Hybrid-type N-glycans are sufficient for the completion of embryogenesis, but abnormal development leads to symptoms including failure to thrive, psychomotor retardation, immune dysfunction, osteopenia, blood coagulopathies, gastrointestinal abnormalities and ventricular septal heart defects. In humans, an enzymatic deficiency in GnTII is caused by an autosomal recessive defect in the *MGAT2* gene and is classified as a type II congenital disorder of glycosylation (CDG), CDG-IIa. Type II CDGs involve defects in the trimming and processing of N-glycans in the late endoplasmic reticulum or the Golgi.

Hereditary erythoblastic multinuclearity with a positive acidified serum (HEMPAS) or congenital dyserythropoietic anemia type II is characterized by ineffective erythropoiesis, bone marrow erythroid multinuclearity, dysmorphic facial features, abnormalities in erythroid membranes and deposition of iron in the secondary tissues. Humans with this disorder have mild to severe anemia and an enlargement of the spleen (Moremen 2002). Most N-glycans in HEMPAS

patients are of hybrid type containing no biantennary complex oligosaccharides with extended polylactosamine structures on proteins. HEMPAS patients have been shown to have varying deficiencies in GMII between individuals (Fukuda 1999; Moremen 2002), although one report suggests potential deficiencies in GnTII and β 1,4 Gal T (Gal T – galactosyl transferase) (Fukuda 1999). A second GMII isozyme has been identified with similar substrate specificity (see below) that probably accounts for why HEMPAS symptoms are mild compared to CDG IIa. In CDG IIa there is a systemic effect from GnTII deficiency compared to the restricted effect in erythroid cells in human HEMPAS patients resulting from GMII deficiency. A mouse model of GMII deficiency (*α M-II* null) was generated and exhibited many characteristics similar to HEMPAS patients, primarily in erythroid cells, but did not display other HEMPAS phenotypes, including multinucleated erythroid cells, problems with the spleen or liver, or iron deposits in tissues. There was an absence of complex N-glycan structures on erythroid cells, but non-erythroid cells had a minor variation in the degree of complex N-glycans. The formation of complex N-glycans was not blocked by the GMII gene disruption, demonstrating the existence of a bypass route allowing the formation of complex-type structures. This bypass route is now believed to be accomplished by Golgi Mannosidase IIx (GMIIx) (Chui, Oh-Eda et al. 1997; Oh-Eda, Nakagawa et al. 2001). The profound phenotypes that accompany defects in GnTI, GnTII, and GMII can be contrasted to a disruption of the gene that encodes GlcNAc Transferase III (GnTIII), *Mgat3*, downstream in the pathway,

where no developmental defects have been described (Priatel, Sarkar et al. 1997; Bhattacharyya, Bhaumik et al. 2002).

α -MANNOSIDASES: CLASSIFICATION AND BIOCHEMICAL CHARACTERISTICS

Mannosidases involved in the biosynthesis and catabolism of N-glycans have been divided into three broad classes based on sequence comparisons, specificities for substrates, protein molecular weights, localization in the cell, cation requirements, and mechanisms of enzymatic action (Henrissat 1991; Henrissat and Bairoch 1993; Henrissat and Bairoch 1996; Henrissat and Davies 1997; Henrissat 1998; Moremen 2000; Bourne and Henrissat 2001). Exo-mannosidases, mannosidases that cleave mannose residues from the non-reducing terminus of the glycan, make up two of the mannosidase classes. The other class is an endomannosidase that can cleave the glycosidic linkage between two internal α 1,2-linked mannose residues (Lubas and Spiro 1987; Lubas and Spiro 1988; Spiro, Bhoyroo et al. 1997; Moremen 2000).

Class I mannosidases

Class I mannosidases (CAZy glycosyl hydrolase family 47 (Henrissat 1991) require Ca^{2+} for their enzymatic activity, are susceptible to inhibition by pyranose substrate mimics deoxymannojirimycin and kifunensine, and cleave α 1,2-mannose linkages on $\text{Man}_9\text{GlcNAc}_2$ processing intermediates. They

accomplish mannosidase hydrolysis by an inverting enzymatic mechanism. The enzymes in this family have a conserved catalytic domain that is comprised of a 440 to 510 amino acid ($\alpha\alpha$)₇ barrel structure (Lal, Pang et al. 1998; Vallee, Karaveg et al. 2000; Vallee, Lipari et al. 2000; Moremen 2002). This family of enzymes is found in the early secretory pathway of the ER and the Golgi where the enzymes are involved in glycoprotein biosynthesis, protein folding, and quality control (Moremen 2000; Helenius and Aebi 2004). Class I mannosidases are not the focus of the studies in this thesis.

Class II mannosidases

Class II mannosidases (CAZy glycosylhydrolase family 38 (Henrissat and Bairoch 1996) are comprised of a group of enzymes that cleave mannose residues from the non-reducing terminus of N-glycans during biosynthesis in the ER and Golgi complex and catabolism in the lysosomes and cytosol (Moremen 2002). This class of mannosidases is the focus of this thesis (Figure 1.2). Class II mannosidases are defined by a relatively large protein molecular weight (110-135 kDa), sensitivity to furanose transition state analogs like swainsonine and 1,4-dideoxy-1,4-imino-D-mannitol, a varying cation requirement of Zn²⁺ or Co²⁺, an ability to cleave glycosidic linkages by a retaining enzymatic mechanism, and a region of conserved sequence predominantly associated with the catalytic domain residues (Henrissat 1991; Henrissat and Bairoch 1993; Henrissat and Bairoch 1996; Henrissat and Davies 1997; Henrissat 1998; Moremen 2000; Bourne and Henrissat 2001). Each enzyme in this class can be differentiated by

its distinctive features of localization in the cell, optimum pH, substrate specificity, and metal ion requirement (Moremen 2002). In mammals, there are at least five different Class 2 mannosidases (Moremen 2002). The first enzyme is Golgi mannosidase II (GMII). This enzyme is involved in glycoprotein biosynthesis for the cleavage of $\text{GlcNAcMan}_5\text{GlcNAc}_2$ to $\text{GlcNAcMan}_3\text{GlcNAc}_2$, has a pH optimum around 5.5, is stimulated by zinc and is localized to Golgi membranes (Tabas and Kornfeld 1978; Harpaz and Schachter 1980; Tulsiani, Harris et al. 1982; Moremen, Touster et al. 1991) (Figure 1.1). The protein structure of *Drosophila melanogaster* Golgi mannosidase II (dGMII) has been solved (van den Elsen, Kuntz et al. 2001) and will be discussed further below. The second enzyme isoform is a GMII homolog that is called Golgi mannosidase IIx (GMIIx) (Misago, Liao et al. 1995). This enzyme is involved in glycan processing in the Golgi complex of cells, has a pH optimum around 5.5, and is thought to be an alternative route to complex N-linked glycosylation in the absence of GMII (Chui, Oh-Eda et al. 1997; Oh-Eda, Nakagawa et al. 2001; Hato, Nakagawa et al. 2006) and appears to have a similar substrate specificity as GMII. The third enzyme is the broad specificity lysosomal α -mannosidase (LysMan), a catabolic mannosidase with a broad substrate specificity and low pH optimum (~ 4.5) that is found in the lysosomes of cells (al Daher, de Gasperi et al. 1991; DeGasperi, al Daher et al. 1991; Daniel, Winchester et al. 1994; Liao, Lal et al. 1996; Merkle, Zhang et al. 1997). The protein structure of bovine (*Bos taurus*) lysosomal mannosidase (bLysMan) has been solved, but at a pH in which the protein was not active (Heikinheimo, Helland et al. 2003). The fourth enzyme is a lysosomal

core-specific α 1,6 mannosidase with a low pH optimum (\sim 4.0) that is involved in catabolism of glycans in the lysosomes (Park, Meng et al. 2005). The fifth Class 2 enzyme is a soluble or cytoplasmic mannosidase that is a catabolic mannosidase with a neutral pH optimum (\sim 6.5), stimulated by Co^{2+} and found in cytosol of mammalian cells (Shoup and Touster 1976; Bischoff, Moremen et al. 1990). A proteolytically cleaved form of this enzyme, called ER mannosidase II (ERMII), has been detected in the ER and is thought to be involved in the early steps of glycoprotein biosynthesis (Weng and Spiro 1993; Weng and Spiro 1996).

There are other enzymes that have been classified as Class 2 enzymes but not fully characterized. These include *S. frugiperda* Golgi Mannosidase II (SfGMII) (Kawar, Karaveg et al. 2001), *Drosophila melanogaster* Golgi Mannosidase IIb (dGMIIb), and a Co^{2+} stimulated α -mannosidase found in rat liver microsomes (Monis, Bonay et al. 1987; Bonay and Hughes 1991; Bonay, Roth et al. 1992) (Table 1.1).

GLYCOSYL HYDROLASE ENZYMATIC MECHANISMS

Glycosyl hydrolases are a group of enzymes that hydrolyze the glycosidic bond between two or more carbohydrates or between a carbohydrate and a non-carbohydrate. The continuously updated online database for carbohydrate active enzymes (CAZy) classifies 115 families of glycosyl hydrolases based on their amino acid sequence similarities (Cantarel, Coutinho et al. 2009). Glycoside hydrolases can also be characterized based on the stereochemical outcome of

their hydrolytic enzymatic mechanism as either “retaining” or “inverting” according to the anomeric configuration of the sugar product. In both retaining and inverting mechanisms, the hydrolysis of the glycosidic bond occurs through a general acid catalysis mechanism that uses one amino acid residue to act as a proton donor to the glycosidic oxygen and a second residue as either a nucleophile (retaining enzymes) or catalytic base to activate a water nucleophile (inverting enzymes) (Davies and Henrissat 1995). A third mechanism has been found for N-acetylhexosamine-glycosidic cleavage, where the acetyl group acts as a nucleophile in substrate-assisted catalysis (Terwisscha van Scheltinga, Armand et al. 1995). In most glycosyl hydrolases, the catalytic amino acids have been found to be aspartate and/or glutamate.

Retaining mechanisms

Retaining glycosyl hydrolases catalyze cleavage of glycosidic bonds through a double displacement mechanism that leads to retention of the anomeric configuration of the released monosaccharides (Vocadlo, Davies et al. 2001). The carboxylates involved in catalysis sandwich the glycosidic bond in the active site and are positioned $\sim 5.5 \text{ \AA}$ apart. The proton donor is within hydrogen bonding distance of the glycosidic oxygen and the side chain nucleophile is in close vicinity of the sugar anomeric carbon. In the first step of catalysis, one of the carboxylic acids acts as a general acid catalyst by donating a proton to the glycosidic oxygen. Coincident with glycosidic bond cleavage a covalent intermediate is formed by nucleophilic attack of the carboxylate side

chain to the anomeric carbon of the glycone and the aglycone departs. Next, a water diffuses into the active site and the side chain of the general acid now acts as a general base to abstract a proton from the water nucleophile, which subsequently attacks at the C-1 position of the enzyme-associated covalent intermediate, hydrolyzing the glycosyl-enzyme intermediate (Davies and Henrissat 1995; Vocadlo, Davies et al. 2001) to generate a product with the same anomeric configuration as the original substrate. Using X-ray crystallized complexes with fluorinated sugar analogs, 5-fluoro- β -L-gulosyl fluoride (5FGulF) (Figure 3.3) and 2-deoxy-2-fluoro- α -mannosyl fluoride (2FManF) (Numao, Kuntz et al. 2003), the Withers lab has demonstrated that dGMII employs a covalent intermediate during its retaining enzymatic mechanism.

Inverting Mechanisms

Inverting glycoside hydrolases catalyze the cleavage of glycosidic bonds through a direct displacement of the leaving group by water, inverting the configuration of the anomeric carbon. In the inverting reaction mechanism, the carboxylates involved in catalysis are on opposite sides of the glycosidic bond similar to the retaining mechanism, while they are further apart (~ 8 - 10 Å) to accommodate a water molecule in the active site. The proton donor is within hydrogen-bonding distance of the glycosidic oxygen and a water molecule is situated between the nucleophilic base and the sugar. In the catalysis, an enzyme carboxyl group acts as a general the base and abstracts a proton from the water nucleophile coincident with the protonation of the glycosidic oxygen by

a second carboxylate acting as a general acid. This single nucleophilic substitution occurs through an oxycarbonium ion-like transition state before generating a product with an opposite anomeric configuration as the substrate.

GOLGI MANNOSIDASE II: A TARGET FOR CANCER THERAPEUTICS

In some tumor cells, large polylectosamine extensions on N-glycan structures have been found to influence cell adhesion characteristics and contribute to metastasis. These polylectosamine extensions are due to an upregulation of GnTV that adds a β 1,6 linked GlcNAc to the α 1,6-linked core mannose in N-linked glycan biosynthesis (Dennis, Granovsky et al. 1999). Inhibition of an enzyme upstream in the N-glycan biosynthetic pathway from GnTV, by treatment with swainsonine, has been found to alter adhesion characteristics and metastasis in these tumor cells. Swainsonine strongly inhibits GMII, an enzyme that initiates the first committed step in creating complex-type oligosaccharides on glycoconjugates (Tulsiani, Harris et al. 1982). GMII has a very restricted substrate specificity (Tabas and Kornfeld 1978; Harpaz and Schachter 1980; Tulsiani, Hubbard et al. 1982) and inhibition leads to the formation of hybrid-type N-glycan structures (Tulsiani, Harris et al. 1982) and a decrease in the amount of complex structures in animal cells (Chui, Oh-Eda et al. 1997). Swainsonine also inhibits other class II mannosidases, including two lysosomal mannosidases. When the broad specificity lysosomal mannosidase and α 1,6 specific lysosomal mannosidase are inhibited, a phenocopy of a genetic

lysosomal storage disease, called alpha-mannosidosis, is created (Tulsiani, Hubbard et al. 1982; Novikoff, Touster et al. 1985). In this disease, a large number of oligosaccharides that are normally degraded by the lysosomal α -mannosidases accumulate in large storage vacuoles (Tulsiani, Broquist et al. 1984). This effect is reversible with discontinued treatment of swainsonine (Goss, Baker et al. 1995; Goss, Reid et al. 1997). A more selective inhibitor for GMII would be useful in altering metastasis and adhesion characteristics of tumor cells without creating the phenocopy of alpha-mannosidosis in patients.

GLYCAN PROCESSING IN THE GOLGI APPARATUS: BIOCHEMICAL REDUNDANCIES

GnTI transfers a GlcNAc residue to $\text{Man}_5\text{GlcNAc}_2$ N-linked glycans in N-linked glycan biosynthesis creating hybrid glycans. When the gene that encodes GnTI (*Mgat1*) is disrupted, the generation of complex and hybrid glycans is eliminated leaving only high mannose glycans. This loss of complex and hybrid glycans results in embryonic death (Ioffe and Stanley 1994; Metzler, Gertz et al. 1994).

GMII acts on the hybrid substrate created by GnTI and catalyzes the first committed step in the biosynthesis of complex N-glycans; therefore when GMII is disrupted hybrid-type glycans would still be formed by GnTI. The elimination of the GMII reaction would be expected to decrease complex glycosylation. However, when a gene disruption of the GMII gene was made in mice, the

homozygous null mice generated complex N-glycans in all cells except erythrocytes and resulted in a relatively mild phenotype (Chui, Oh-Eda et al. 1997).

Cleavage of the GlcNAcMan₅GlcNAc₂ glycan by GMII generates the substrate for GnTII, GlcNAcMan₃GlcNAc₂ (Harpaz and Schachter 1980; Tulsiani, Hubbard et al. 1982; Moremen, Trimble et al. 1994). When a gene disruption is made in the gene that encodes GnTII (*Mgat2*) there is a decrease in the amount of complex glycans (Wang, Tan et al. 2001) and an increase in hybrid glycans. The loss of complex glycosylation results in development through embryogenesis, but severe systemic effects lead to perinatal lethality.

The severity of phenotype in GnTII null animals is contradicted by the mild effects of disruption of GMII. The loss of GMII would be expected to block complex glycosylation completely and create at least similar phenotypes and complications as seen in the GnTII deficiency. However, a gene disruption of the GMII resulted in a relatively mild phenotype compared to the GnTII deficiency (Chui, Oh-Eda et al. 1997). This led to speculation that an alternate processing enzyme could bypass the GMII enzymatic step. An α -mannosidase activity was detected in wild type and GMII null cells that could enzymatically cleave Man₅GlcNAc₂-PA to produce Man₃GlcNAc₂-PA in the presence of cobalt and was called α -mannosidase III (Man III) (Chui, Oh-Eda et al. 1997). This enzyme did not act on GlcNAcMan₅GlcNAc₂-PA and was less sensitive to swainsonine than GMII. This Man III activity was not cloned and could have been one of three α -mannosidases that have been partially characterized and further described

below: 1) Golgi Mannosidase IIx (GMIIx) (Misago, Liao et al. 1995), 2) an enzyme characterized in BHK cells and purified from rat liver (Monis, Bonay et al. 1987; Bonay and Hughes 1991; Bonay, Roth et al. 1992), or 3) an ER/cytosolic mannosidase (Monis, Bonay et al. 1987; Bischoff, Moremen et al. 1990; Weng and Spiro 1993; Grard, Herman et al. 1996; Weng and Spiro 1996; Yamashiro, Itoh et al. 1997).

GMIIx is an isozyme of GMII (Misago, Liao et al. 1995) that is activated by cobalt and inhibited by swainsonine. When the gene encoding this protein (*Man2a2*) was disrupted in mice it resulted in male sterility (Akama, Nakagawa et al. 2002). There has been some evidence that this enzyme can cleave $\text{Man}_6\text{GlcNAc}_2$ to $\text{Man}_4\text{GlcNAc}_2$ without the prior action of GnTI (Oh-Eda, Nakagawa et al. 2001) in the Golgi complex (Misago, Liao et al. 1995; Oh-Eda, Nakagawa et al. 2001) but more recent data indicate a substrate specificity similar to GMII (see below).

The α -mannosidase characterized in BHK cells and purified from rat liver (Monis, Bonay et al. 1987; Bonay and Hughes 1991; Bonay, Roth et al. 1992), is stimulated by cobalt and is somewhat resistant to swainsonine. This enzyme can cleave $\text{Man}_5\text{GlcNAc}_2$ to $\text{Man}_3\text{GlcNAc}_2$ but does not hydrolyze pNP- α -mannosidase.

ER/cytosolic α -mannosidases could also be involved in an alternative pathway in mice. These enzymes are stimulated by cobalt, are somewhat resistant to swainsonine, and can cleave $\text{Man}_5\text{GlcNAc}$ to $\text{Man}_3\text{GlcNAc}$. ER/cytosolic mannosidases are more efficient in the catalysis of glycans with

only one GlcNAc residue on the reducing end and seem to be involved in catabolism instead of biosynthesis of N-linked glycans (Monis, Bonay et al. 1987; Bischoff, Moremen et al. 1990; Grard, Herman et al. 1996; Weng and Spiro 1996; Yamashiro, Itoh et al. 1997).

Recently, a double knockout of GMII and GMIIx was generated and the mouse model did not create any complex glycans (Akama, Nakagawa et al. 2006). These mice did not survive embryonic development. This evidence confirms that GMIIx is the alternate biosynthetic pathway for GMII in mammals, but more detailed biochemical evidence still needs to be shown concerning the substrate specificity of GMIIx. However, unpublished data has demonstrated that human GMIIx has a preference for cleaving GlcNAcMan₅GlcNAc₂ over Man₅GlcNAc₂ similar to GMII (Singh and Moremen, personal communication). If GMIIx has the same substrate specificity as GMII, the Man₅GlcNAc₂ cleaving activity seen in GMII null animals is still a mystery. It is not known why there would be an activity in mammals for cleavage of Man₅GlcNAc₂ that does not function as a bypass of the GMII biosynthetic step.

Most processed N-linked glycans found in insects are paucimannosidic, or truncated high mannose structures. These glycans consist of a tri- or tetra-mannosylchitobiosyl core structure that often includes core fucosylation (Man₄GlcNAc₂ (M4N2) or Man₃GlcNAc₂ (M3N2) with or without an α 1,6-linked fucose and/or an α 1,3-linked fucose). The steps required in creating these paucimannosidic glycans require the prior action of GnTI. This was determined by creating GnTI null mutations of the gene that encodes this enzyme, *Mgat1*, in

Drosophila (Sarkar, Leventis et al. 2006). In these null flies there was a severe decrease in M3N2F⁶ (F⁶ = α 1,6-linked fucose) to an almost undetectable level and a decrease in M3N2F³ (F³ = α 1,3-linked fucose) with a corresponding increase in Man₅GlcNAc₂ (M5N2) structures due to the fact that the production of these final enzymatic products require the prior action of GnTI. The phenotypes associated with this mutation was male sterility due to failure to mate, sluggishness with a >95% reduction in movement, premature death, and fused lobes of the mushroom β lobes in the brain (fused lobes).

Due to the fact that the majority of paucimannosidic glycans do not have a non-reducing terminal GlcNAc residue, an N-Acetylglucaminidase was hypothesized to be involved in N-linked glycan processing in flies. A protein termed FDL was found to hydrolyze GlcNAc specifically attached to the α 1,3-linked mannose of the core pentasaccharide N2M3N2 as well as NM3N2. When a FDL deletion mutant was created, *Df(2R)achi²*, there was a 7-fold decrease in the creation of paucimannosidic glycans in *Drosophila*. This causes a significant reduction in M3N2 and M3N2F⁶, which is believed to contribute to abnormal brain development where the mushroom β lobes are fused (fused lobes) in viable mutants.

When analyzed by mass spectrophotometry M3N2F⁶ is decreased by 83% in FDL null and >98% in GnTI null flies. M3N2 also significantly decreased by 73% in FDL null and 59% in GNTI null flies. There was a large increase in high mannose structures (M9N2 – M6N2) in both mutations. M5N2 decreased by 54% in FDL null flies, however this glycan increased by 47% in GnTI null flies.

NM3N2F⁶ (where GlcNAc is attached to the α 1,3-linked mannose branch) is a major glycan in FDL null flies. It is speculated that the large decrease of M3N2 and M3N2F⁶ in both FDL and GnTI null flies contribute to the fused lobes phenotype. The presence of unusually high amounts of high mannose glycans may also contribute to this phenotype. The residual amount of M3N2 and M3N2F⁶ paucimannosidic glycans in GnTI null flies implicates a GnTI independent mannosidase. Evidence of this activity has been seen in other invertebrates as described below.

A Co⁺² dependent Man₅GlcNAc cleaving activity has been detected in *Spodotera fruigiperda* (Sf9) insect cells, and termed SfMII. This enzyme is sensitive to swainsonine, is activated by cobalt, and can hydrolyze pNP- α -mannosidase and Man₅GlcNAc₂ to form the product Man₃GlcNAc₂, but cannot hydrolyze GlcNAcMan₅GlcNAc₂ (the restricted substrate for GMII). This enzyme has a neutral pH optimum and is localized in the Golgi in the same intracellular distribution as GMII (Kawar, Karaveg et al. 2001). SfMII has a close sequence similarity to *Drosophila melanogaster* Golgi Man IIb (dGMIIb) (NP_650494) suggesting dGMIIb is the SfMII homologue in *Drosophila* cells (Sarkar, Leventis et al. 2006).

DROSOPHILA GOLGI MANNOSIDASE II

Drosophila melanogaster Golgi α -mannosidase II (dGMII) cloning and sequence analysis was first performed by Foster, et al. in the Roberts' lab (Foster, Yudkin et al. 1995). Using a cDNA library from embryos, the library was

probed by in situ hybridization with a ^{32}P -labeled *EcoRI* fragment of murine GMII (mGMII) encoding a 3350 bp open reading frame (ORF) with some 5' and 3' untranslated DNA (Moremen and Robbins 1991). The fragment that hybridized the strongest with the mouse probe was subcloned into pUC9 and sequenced. This sequenced fragment displayed 60% identity and 75% similarity to mGMII, and after this analysis, the remainder of dGMII was sequenced. Sequence analysis of dGMII showed that the cDNA was 3926 bp long, with one ORF composed of 3327 bp. This ORF predicted a polypeptide of 1108 amino acids corresponding to a molecular weight of 127 kDa. A short positively charged N-terminus typical of Type II transmembrane proteins was found upstream of a short hydrophobic region predicted to be a non-cleavable signal sequence. The dGMII ORF sequence was compared to other mannosidases; mGMII, *Dictyostelium discoideum* lysosomal mannosidase (*DdLM*), rat ER mannosidase (rERM) and yeast vacuolar mannosidase (yVM). dGMII has a 41% identity and 61% similarity to mGMII, 50% similarity to *DdLM*, and some similarity to rERM and yVM. Similarity was mainly restricted to a 210 amino acid region within the hydrophilic C-terminal domain of these proteins. dGMII was mapped to a single site on the right arm of the 3rd chromosome, 85D14-18 by *in situ* hybridization of polytene chromosome squashes.

Additional characterization of dGMII was performed in the Roberts lab in 1999 by Rabouille, et al. (Rabouille, Kuntz et al. 1999). Three clones were obtained from the Berkley *Drosophila* Genome project (Hartl, Nurminsky et al. 1994) that mapped to the 85D region. A dGMII cDNA probe hybridized to only

one 6 kb *EcoRI* fragment from DS05016 (85D11-17) and was then subcloned into the *EcoRI* site of pUC18. After PCR analysis, a 6 kb insert was sequenced to determine intron and exon organization of the *dGMII* gene. The complete sequence was deposited at GenEMBL accession number AJ 132715. *dGMII* and *mGMII* sequences were cloned into a pProtA expression vector including a SV40 early gene promoter and an N-terminal secretion signal sequence from rat stromelysin. These constructs were used for transient expression in CHOP cells. The expressed ProtA-GMII fusions contained the predicted catalytic domain. The cytosolic and transmembrane domain including a portion of the “stalk” that connects the transmembrane domain to the catalytic domain was absent from the fusions (a larger portion of the stalk was present in *mGMII* compared to *dGMII*). Secreted recombinant enzyme was isolated from cell culture medium using IgG sepharose fast flow beads that bound the Prot-A-fusion. Expression of bound pProtA fusions were analyzed using a standard western blot technique utilizing rabbit IgG as the primary antibody and horseradish peroxidase conjugated to goat anti rabbit IgG as the secondary antibody.

The presence of α -mannosidase activity was determined using the synthetic substrate pNP-Man for the enzymes bound to the IgG sepharose beads. *dGMII* and *mGMII* both showed α -mannosidase activity. The optimal pH for *dGMII* was found to be 5.7 in these studies, which is similar to other GMIIIs (Kaushal, Szumilo et al. 1990; Moremen, Touster et al. 1991; Ren, Castellino et al. 1997). *dGMII* was strongly inhibited by swainsonine with an IC_{50} between 12 and 20 nM. *dGMII* was found to have no metal ion dependency or activation

when tested with MgCl₂, CaCl₂, MnCl₂, ZnSO₄, NiSO₄, BaCl₂, LiCl₂, and NaCl up to 10 mM. EDTA also had no effect on activity under these same conditions. In contrast, dGMII was strongly inhibited by CuSO₄ with an IC₅₀ of 25 μM (Rabouille, Kuntz et al. 1999).

Antibodies to a synthetic peptide of dGMII, consisting of 14 carboxyterminal amino acids, was produced by coupling this peptide to ovalbumin and introducing the final product into rabbits. The anti-dGMII serum was characterized by analyzing WT embryos overexpressing dGMII with western blot techniques. dGMII was also expressed in Sf9 cells and the anti-dGMII serum was tested for its ability to detect dGMII using western blot techniques. Both of these tests provided positive results that the anti-dGMII serum was interacting with dGMII (Rabouille, Kuntz et al. 1999).

This anti-serum was then used to examine the cellular distribution of dGMII in S2 cells using immunofluorescence microscopy in a single labeling experiment. This data detected a typical punctate pattern indicative of the Golgi, but the localization pattern was different than mammalian Golgi membranes (Burke, Griffiths et al. 1982), (Nilsson, Pypaert et al. 1993). A number of double labeling experiments were performed with anti-dGMII serum and well-established Golgi markers (syntaxin 5 (Hui, 1997 #222), Gos28 (Nagahama, Orci et al. 1996), and delta subunit from AP-3 coat complex (Simpson, Peden et al. 1997)). The best example of co-localization was between dGMII and the delta subunit. S2 cells were then fixed, processed for cryo immunoelectron microscopy, sectioned and labeled with dGMII anti-serum and detected by Protein A coupled

to 10nm gold particles. This labeling technique showed dGMII to localize to the Golgi, but also localization was seen in the ER, cisternae and endosomes. Immunolabeling was also performed on embryos in a single labeling experiment with anti dGMII serum as well as immunogold labeling. This data showed dGMII to be localized mostly to the Golgi but some labeling was also seen in the ER. A truncated dGMII was constructed which contained the transmembrane domain, cytoplasmic domain, and stalk region. A construct that included the truncated dGMII and a triple HA tag was transfected into S2 cells and double labeled with anti-dGMII serum (to detect protein expressed natively) and anti-HA (to detect the transiently transfected construct). Co-localization of the antibodies was observed with endogenous dGMII, which showed that the truncated form of dGMII was sufficient for localization (Rabouille, Kuntz et al. 1999).

Phenotypic analysis of overexpression of the *dGMII* gene has also been determined. A P-element insertion (*PdL(3)19B3*) was made in the 5'-UTR of the gene that encodes *dGMII* (Landis, Bhole et al. 2001). A tet-on promoter was inserted upstream of the mannosidase gene that induced overexpression of the enzyme following the addition of DOX. In these studies, the overexpression of *dGMII* resulted in rough eye phenotype and increased life span. A gene disruption screen was performed by Lukacsovich, et al. (Lukacsovich, Asztalos et al. 2001) using a P-element gene trap method to create a lethal insertion in the gene at the chromosomal location 89A1-5. When published, this gene was identified as corresponding to α -mannosidase II, and was cited by Landis, et al. as a gene disruption in the *dGMII* gene. However, 89A5 is the chromosomal

location for the *dGMIIb* gene, not *dGMII*. It is not clear whether the lethality caused from the gene disruption was solely due to the disruption of the *dGMIIb* gene or if this disruption affected other genes in that chromosomal location which may be involved in survival.

In addition to the biochemical and genetic data compiled for dGMII, a recombinant form of dGMII has been crystallized using X-ray crystallography. dGMII was first crystallized in 2001 by van den Elsen, et al. with a resolution of 2.14 Å (van den Elsen, Kuntz et al. 2001). This was the first structure of a GH38 mannosidase. DGMII was co-crystallized with known inhibitors swainsonine (SWA) at 1.87 Å (Figure 1.3.2) resolution and deoxymannojirimycin (DMNJ) at 1.69 Å resolution (Figure 1.3.1). These crystal structures gave insight into the tertiary protein structure and important sites involved in catalysis in GMII.

The N-terminal domain (N-terminal α/β domain) of dGMII is made up of 16 α helices surrounding an inner core of three β sheets. The three β sheets are composed of 11 β strands that are mostly parallel. The N-terminal α/β domain is stabilized by disulfide bonds from 3 cysteines that are well conserved between species.

The C-terminal region of dGMII is comprised of a 3 helix bundle and is connected to the N-terminal α/β domain by a zinc binding site. This C-terminal region also contains immunoglobulin-like domains, including a small β sandwich of 12 antiparallel strands and a 21 β -strand structure.

The active site of dGMII is represented by a small cavity next to an extended surface pocket in the N-terminal α/β domain. The residues in this large

surface exposed patch are highly conserved between GMII species. The active site harbors a Zn^{2+} ion, which is involved in ionic interactions and transition state stabilization (Figures 1.3.1 – 1.3.3). Co-crystals of dGMII and inhibitors occupying the putative active site reveal hydrophobic interactions with aromatic residues forming the walls of the small cavity. These inhibitors are stabilized by hydrogen bonds and interactions with the Zn^{2+} ion. The positions of each inhibitor is stabilized by hydrogen bonds between carboxylic oxygens of Asp472 (Figures 1.3.1 and 3.2). DMNJ is involved in additional hydrogen bonds via water molecules with the NH_2 nitrogen of Arg228, the hydroxyl oxygen of Tyr269, the backbone carbonyl oxygen of Arg876, and the OD1 oxygen of Asp204 (Figure 1.3.1). The co-crystals with bound inhibitors provide insight into residues involved in catalysis as well as residues and a Zn^{2+} ion important in stabilization and positioning of the mannose residues for hydrolysis by dGMII's retaining mechanism (Figures 1.3.1 and 1.3.2).

DGMII has a retaining mannosyl hydrolase mechanism. Asp204 is the catalytic nucleophile in this mechanism and Asp341 is the catalytic acid/base. The dGMII crystal structure not only gave insight into the nucleophile, acid/base, and Zn^{2+} ion involved in catalysis, but also made it possible to propose a GlcNAc binding site, which has been shown to impart the unique glycan substrate specificity for the enzyme. A 2-methyl-2,4-pentanediol (MPD) molecule, used as a cryoprotectant in the crystallization process, was found to be bound in a loop region close to the active site (Figures 1.3.1 – 1.3.3). When MPD was replaced by the cryoprotectant glycerol, the glycerol molecule also occupied the same

region. Glycerol has previously been shown to mimic the binding of sugar residues in glycosyl hydrolases. The binding of both cryoprotectants in the same region led to the hypothesis that this region may comprise the β 1,2-GlcNAc binding site. Modeling of GlcNAcMan₅GlcNAc₂ with the dGMII crystal structure led to the hypothesis that GlcNAc binding in this region may act as an anchor, stabilizing the interaction of the rest of the flexible glycan for efficient catalysis. This model also proposed an order of mannose cleavage, where the first mannose to be cleaved would be the α 1,6 mannose residue followed by and 180° rotation around the flexible core α 1,6 mannose linkage, to allow cleavage of the second α 1,3 mannose residue.

The hydrolysis of these mannosyl residues occurs via a retaining mechanism, but until recently it was unclear whether the transition state occurred via an oxycarbonium ion intermediate or a covalent intermediate. In 2003, the Rose and Withers groups collaborated to use structural analysis and bound fluorinated analogues to analyze this retaining mechanism (Numao, Kuntz et al. 2003). In their studies they produced three different covalent glycosyl-enzyme intermediates with dGMII, two with 5-fluoro- β -L-gulosyl fluoride (5FGulF), and one with 2-deoxy-2-fluoro- α -D-mannosyl fluoride (2FManF).

The crystal structures that were produced with the mechanism-based inactivator, 5FGulF, trapped a covalent glycosyl enzyme intermediate with *wt* dGMII (1QWN) (Figure 1.3.3) at 1.2 Å resolution and a D341N acid/base catalyst mutant (1QWU) at 2.03 Å resolution. The covalent intermediate was found to be distorted in a ¹S₅ skew boat conformation in both crystals. The crystal structure

bound with the 2FManF (1QX1) of the covalent intermediate formed during hydrolysis by the dGMII D341N mutant, was solved at a resolution of 1.3 Å. This manno-configured inactivator was chosen for crystallization as well as 5FGulF because this compound has a natural C-5 configuration that was thought to reflect the conformation of the intermediate formed during natural mannose hydrolysis, unlike 5FGulF which is the C-5 epimer of mannosides and also has a fluorine atom attached to its C-5 position. However, the backbone of solved structures of 2FManF and 5FGulF did not change significantly when crystallized and all three structures were found to be in a 1S_5 skew boat conformation. This is hypothesized to be the conformation adopted during hydrolysis of α -mannosidases by dGMII, and most likely other GMII. These co-crystals suggest that the retaining mechanism for GMII operates via a covalent glycosyl-enzyme intermediate.

In 2008, the Rose group co-crystallized a dGMII inactive nucleophile mutant (D204A) with GlcNAcMan₅GlcNAc at 1.4 Å resolution (3CZN) (Figure 1.4) (Shah, Kuntz et al. 2008). In this structure the β 1,2-GlcNAc was found to occupy the putative “anchoring site” ~14 Å away from the mannosyl residues to be hydrolyzed at the site previously occupied by mpd and glycerol. As predicted, the binding of this GlcNAc residue anchored the rest of the glycan across an active site cleft to correctly position the α 1,6 Man residue for catalysis. The anchoring effect could be seen in comparison to a co-crystal structures previously produced with a chemically synthesized Man₅GlcNAc moiety (3BVV),

where the glycan occupied the space in a way that was unfavorable for catalysis (Zhong, Kuntz et al. 2008).

The co-crystal with GlcNAcMan₅GlcNAc (Figure 1.4) revealed an additional interaction in a binding pocket 9 Å away from the D204A residue. The amino acid residues in this region interacted with the α 1,3 mannose residue stabilizing it in a “holding site” prior to the cleavage of the α 1,6 mannose residue. Steric restrictions of the “holding site” favor the initial binding of the α 1,6 mannose residue in the catalytic site. This indicates that it is the holding site that determines the order of mannose cleavage by dGMII. The information gathered from this co-crystal structure suggests that three sites are involved in substrate recognition and catalysis, 1) the holding site, which interacts with the α 1,3 mannose residue second in line to be cleaved, 2) the active site, where the first α 1,6 mannose residue cleavage occurs firstly followed by the cleavage of the α 1,3 mannose residue, and 3) the anchoring site, that interacts with the essential β 1,2-GlcNAc positioning the glycan in a favorable, stable way for efficient catalysis.

Closer analysis of the GMII anchoring site shows that β 1,2-GlcNAc is stably bound in this pocket (Figure 1.5), forming strong stacking interactions with Tyr267, while its acetyl group interacts with Trp299 and Pro298 which forms a hydrogen bond with a conserved histidine, His273. The synthetic Man₅GlcNAc glycan binds readily to the catalytic and holding sites similar to GlcNAcMan₅GlcNAc, but due to the lack of the anchoring GlcNAc, the oligosaccharide extends out of the active site allowing a core mannose to interact

with Asp873, which compromises cleavage of this glycan by 80 - fold or greater (Zhong, Kuntz et al. 2008). Study of this anchoring site is a promising avenue for understanding GMII substrate recognition.

The crystal structure of a related family 38 glycosylhydrolase (GH38), *Bovus taurus* lysosomal mannosidase (bLysMan), was solved by Heikinheimo et al. (Heikinheimo, Helland et al. 2003). The active site cleft of bLysMan has numerous conserved residues compared to dGMII and also contains a Zn²⁺ ion. However, the active site cleft of bLysMan is 8 Å wider than dGMII's and there is a lack of sequence conservation at both the holding and anchoring sites. In fact, the anchoring site seems to be missing in the bLysMan structure (Figure 1.6). The absence of the GlcNAc anchoring site is a key difference between dGMII and bLysMan and accounts for the restricted substrate specificity for the former enzyme. Lysosomal mannosidase (LysMan) is not equipped to cleave oligosaccharides containing this GlcNAc residue, but has a broad substrate specificity for high mannose oligosaccharides.

The high sequence conservation of active site residues in GH38 enzymes suggests a similar mechanism for hydrolyzing mannose residues. The presence of an anchoring site in dGMII for the GlcNAc residue appears to impart the unique specificity of GMII to its substrate. It is this anchoring site that sets GMII apart from other GH38 enzymes.

The studies in the following thesis will describe the identification, expression, purification, and characterization of the *Drosophila melanogaster* Man IIb (dGMIIb) and comparison with dGMII and the human lysosomal α -

mannosidase (hLysMan). Several similarities were found between dGMIIb and dGMII, yet substrate specificity studies indicate recognition of $\text{Man}_5\text{GlcNAc}_2$ substrates over $\text{GlcNAcMan}_5\text{GlcNAc}_2$ indicating a significant difference in the anchoring site and in the substrate binding site of the enzyme (Figure 1.6).

REFERENCES

- Akama, T. O., H. Nakagawa, et al. (2002). "Germ cell survival through carbohydrate-mediated interaction with Sertoli cells." Science **295**(5552): 124-7.
- Akama, T. O., H. Nakagawa, et al. (2006). "Essential and mutually compensatory roles of {alpha}-mannosidase II and {alpha}-mannosidase IIx in N-glycan processing in vivo in mice." Proc Natl Acad Sci U S A **103**(24): 8983-8.
- al Daher, S., R. de Gasperi, et al. (1991). "The substrate-specificity of human lysosomal alpha-D-mannosidase in relation to genetic alpha-mannosidosis." Biochem J **277 (Pt 3)**: 743-51.
- Bhattacharyya, R., M. Bhaumik, et al. (2002). "Truncated, inactive N-acetylglucosaminyltransferase III (GlcNAc-TIII) induces neurological and other traits absent in mice that lack GlcNAc-TIII." J Biol Chem **277**(29): 26300-9.
- Bischoff, J., K. Moremen, et al. (1990). "Isolation, characterization, and expression of cDNA encoding a rat liver endoplasmic reticulum alpha-mannosidase." J Biol Chem **265**(28): 17110-7.
- Bonay, P. and R. C. Hughes (1991). "Purification and characterization of a novel broad-specificity (alpha 1----2, alpha 1----3 and alpha 1----6) mannosidase from rat liver." Eur J Biochem **197**(1): 229-38.

- Bonay, P., J. Roth, et al. (1992). "Subcellular distribution in rat liver of a novel broad-specificity (alpha 1----2, alpha 1----3 and alpha 1----6) mannosidase active on oligomannose glycans." Eur J Biochem **205**(1): 399-407.
- Bourne, Y. and B. Henrissat (2001). "Glycoside hydrolases and glycosyltransferases: families and functional modules." Curr Opin Struct Biol **11**(5): 593-600.
- Burke, B., G. Griffiths, et al. (1982). "A monoclonal antibody against a 135-K Golgi membrane protein." Embo J **1**(12): 1621-8.
- Cantarel, B. L., P. M. Coutinho, et al. (2009). "The Carbohydrate-Active EnZymes database (CAZy): an expert resource for Glycogenomics." Nucleic Acids Res **37**(Database issue): D233-8.
- Chui, D., M. Oh-Eda, et al. (1997). "Alpha-mannosidase-II deficiency results in dyserythropoiesis and unveils an alternate pathway in oligosaccharide biosynthesis." Cell **90**(1): 157-67.
- Daniel, P. F., B. Winchester, et al. (1994). "Mammalian alpha-mannosidases-- multiple forms but a common purpose?" Glycobiology **4**(5): 551-66.
- Davies, G. and B. Henrissat (1995). "Structures and mechanisms of glycosyl hydrolases." Structure **3**(9): 853-9.
- DeGasperi, R., S. al Daher, et al. (1991). "The substrate specificity of bovine and feline lysosomal alpha-D-mannosidases in relation to alpha-mannosidosis." J Biol Chem **266**(25): 16556-63.
- Dennis, J. W., M. Granovsky, et al. (1999). "Glycoprotein glycosylation and cancer progression." Biochim Biophys Acta **1473**(1): 21-34.

- Feizi, T. (1985). "Demonstration by monoclonal antibodies that carbohydrate structures of glycoproteins and glycolipids are onco-developmental antigens." Nature **314**(6006): 53-7.
- Foster, J. M., B. Yudkin, et al. (1995). "Cloning and sequence analysis of GmII, a *Drosophila melanogaster* homologue of the cDNA encoding murine Golgi alpha-mannosidase II." Gene **154**(2): 183-6.
- Fukuda, M. N. (1999). "HEMPAS. Hereditary erythroblastic multinuclearity with positive acidified serum lysis test." Biochim Biophys Acta **1455**(2-3): 231-9.
- Goss, P. E., M. A. Baker, et al. (1995). "Inhibitors of carbohydrate processing: A new class of anticancer agents." Clin Cancer Res **1**(9): 935-44.
- Goss, P. E., C. L. Reid, et al. (1997). "Phase IB clinical trial of the oligosaccharide processing inhibitor swainsonine in patients with advanced malignancies." Clin Cancer Res **3**(7): 1077-86.
- Grard, T., V. Herman, et al. (1996). "Oligomannosides or oligosaccharide-lipids as potential substrates for rat liver cytosolic alpha-D-mannosidase." Biochem J **316 (Pt 3)**: 787-92.
- Haltiwanger, R. S. and J. B. Lowe (2004). "Role of glycosylation in development." Annu Rev Biochem **73**: 491-537.
- Harpaz, N. and H. Schachter (1980). "Control of glycoprotein synthesis. Processing of asparagine-linked oligosaccharides by one or more rat liver Golgi alpha-D-mannosidases dependent on the prior action of UDP-N-

- acetylglucosamine: alpha-D-mannoside beta 2-N-acetylglucosaminyltransferase I." J Biol Chem **255**(10): 4894-902.
- Hartl, D. L., D. I. Nurminsky, et al. (1994). "Genome structure and evolution in Drosophila: applications of the framework P1 map." Proc Natl Acad Sci U S A **91**(15): 6824-9.
- Hato, M., H. Nakagawa, et al. (2006). "Unusual N-glycan structures in alpha-mannosidase II/IIx double null embryos identified by a systematic glycomics approach based on two-dimensional LC mapping and matrix-dependent selective fragmentation method in MALDI-TOF/TOF mass spectrometry." Mol Cell Proteomics **5**(11): 2146-57.
- Heikinheimo, P., R. Helland, et al. (2003). "The structure of bovine lysosomal alpha-mannosidase suggests a novel mechanism for low-pH activation." J Mol Biol **327**(3): 631-44.
- Helenius, A. and M. Aebi (2001). "Intracellular functions of N-linked glycans." Science **291**(5512): 2364-9.
- Helenius, A. and M. Aebi (2004). "Roles of N-linked glycans in the endoplasmic reticulum." Annu Rev Biochem **73**: 1019-49.
- Henrissat, B. (1991). "A classification of glycosyl hydrolases based on amino acid sequence similarities." Biochem J **280 (Pt 2)**: 309-16.
- Henrissat, B. (1998). "Glycosidase families." Biochem Soc Trans **26**(2): 153-6.
- Henrissat, B. and A. Bairoch (1993). "New families in the classification of glycosyl hydrolases based on amino acid sequence similarities." Biochem J **293 (Pt 3)**: 781-8.

- Henrissat, B. and A. Bairoch (1996). "Updating the sequence-based classification of glycosyl hydrolases." Biochem J **316 (Pt 2)**: 695-6.
- Henrissat, B. and G. Davies (1997). "Structural and sequence-based classification of glycoside hydrolases." Curr Opin Struct Biol **7(5)**: 637-44.
- Ioffe, E., Y. Liu, et al. (1996). "Essential role for complex N-glycans in forming an organized layer of bronchial epithelium." Proc Natl Acad Sci U S A **93(20)**: 11041-6.
- Ioffe, E. and P. Stanley (1994). "Mice lacking N-acetylglucosaminyltransferase I activity die at mid-gestation, revealing an essential role for complex or hybrid N-linked carbohydrates." Proc Natl Acad Sci U S A **91(2)**: 728-32.
- Kaushal, G. P., T. Szumilo, et al. (1990). "Purification to homogeneity and properties of mannosidase II from mung bean seedlings." Biochemistry **29(8)**: 2168-76.
- Kawar, Z., K. Karaveg, et al. (2001). "Insect cells encode a class II alpha-mannosidase with unique properties." J Biol Chem **276(19)**: 16335-40.
- Kornfeld, R. and S. Kornfeld (1985). "Assembly of asparagine-linked oligosaccharides." Annu Rev Biochem **54**: 631-64.
- Lal, A., P. Pang, et al. (1998). "Substrate specificities of recombinant murine Golgi alpha1, 2-mannosidases IA and IB and comparison with endoplasmic reticulum and Golgi processing alpha1,2-mannosidases." Glycobiology **8(10)**: 981-95.

- Landis, G., D. Bhole, et al. (2001). "High-frequency generation of conditional mutations affecting *Drosophila melanogaster* development and life span." Genetics **158**(3): 1167-76.
- Liao, Y. F., A. Lal, et al. (1996). "Cloning, expression, purification, and characterization of the human broad specificity lysosomal acid alpha-mannosidase." J Biol Chem **271**(45): 28348-58.
- Lowe, J. B. and J. D. Marth (2003). "A genetic approach to Mammalian glycan function." Annu Rev Biochem **72**: 643-91.
- Lubas, W. A. and R. G. Spiro (1987). "Golgi endo-alpha-D-mannosidase from rat liver, a novel N-linked carbohydrate unit processing enzyme." J Biol Chem **262**(8): 3775-81.
- Lubas, W. A. and R. G. Spiro (1988). "Evaluation of the role of rat liver Golgi endo-alpha-D-mannosidase in processing N-linked oligosaccharides." J Biol Chem **263**(8): 3990-8.
- Lukacsovich, T., Z. Asztalos, et al. (2001). "Dual-tagging gene trap of novel genes in *Drosophila melanogaster*." Genetics **157**(2): 727-42.
- Merkle, R. K., Y. Zhang, et al. (1997). "Cloning, expression, purification, and characterization of the murine lysosomal acid alpha-mannosidase." Biochim Biophys Acta **1336**(2): 132-46.
- Metzler, M., A. Gertz, et al. (1994). "Complex asparagine-linked oligosaccharides are required for morphogenic events during post-implantation development." Embo J **13**(9): 2056-65.

- Misago, M., Y. F. Liao, et al. (1995). "Molecular cloning and expression of cDNAs encoding human alpha-mannosidase II and a previously unrecognized alpha-mannosidase II isozyme." Proc Natl Acad Sci U S A **92**(25): 11766-70.
- Monis, E., P. Bonay, et al. (1987). "Characterization of a mannosidase acting on alpha 1----3- and alpha 1----6-linked mannose residues of oligomannosidic intermediates of glycoprotein processing." Eur J Biochem **168**(2): 287-94.
- Moremen, K. W. (2000). -Mannosidases in Asparagine linked Oligosaccharide Processing and Catabolism, Wiley and Sons.
- Moremen, K. W. (2002). "Golgi alpha-mannosidase II deficiency in vertebrate systems: implications for asparagine-linked oligosaccharide processing in mammals." Biochim Biophys Acta **1573**(3): 225-35.
- Moremen, K. W. and P. W. Robbins (1991). "Isolation, characterization, and expression of cDNAs encoding murine alpha-mannosidase II, a Golgi enzyme that controls conversion of high mannose to complex N-glycans." J Cell Biol **115**(6): 1521-34.
- Moremen, K. W., O. Touster, et al. (1991). "Novel purification of the catalytic domain of Golgi alpha-mannosidase II. Characterization and comparison with the intact enzyme." J Biol Chem **266**(25): 16876-85.
- Moremen, K. W., R. B. Trimble, et al. (1994). "Glycosidases of the asparagine-linked oligosaccharide processing pathway." Glycobiology **4**(2): 113-25.
- Nagahama, M., L. Orci, et al. (1996). "A v-SNARE implicated in intra-Golgi transport." J Cell Biol **133**(3): 507-16.

- Nilsson, T., M. Pypaert, et al. (1993). "Overlapping distribution of two glycosyltransferases in the Golgi apparatus of HeLa cells." J Cell Biol **120**(1): 5-13.
- Novikoff, P. M., O. Touster, et al. (1985). "Effects of swainsonine on rat liver and kidney: biochemical and morphological studies." J Cell Biol **101**(2): 339-49.
- Numao, S., D. A. Kuntz, et al. (2003). "Insights into the mechanism of *Drosophila melanogaster* Golgi alpha-mannosidase II through the structural analysis of covalent reaction intermediates." J Biol Chem **278**(48): 48074-83.
- Oh-Eda, M., H. Nakagawa, et al. (2001). "Overexpression of the Golgi-localized enzyme alpha-mannosidase IIx in Chinese hamster ovary cells results in the conversion of hexamannosyl-N-acetylchitobiose to tetramannosyl-N-acetylchitobiose in the N-glycan-processing pathway." Eur J Biochem **268**(5): 1280-8.
- Park, C., L. Meng, et al. (2005). "Characterization of a human core-specific lysosomal {alpha}1,6-mannosidase involved in N-glycan catabolism." J Biol Chem **280**(44): 37204-16.
- Priatel, J. J., M. Sarkar, et al. (1997). "Isolation, characterization and inactivation of the mouse *Mgat3* gene: the bisecting N-acetylglucosamine in asparagine-linked oligosaccharides appears dispensable for viability and reproduction." Glycobiology **7**(1): 45-56.
- Rabouille, C., D. A. Kuntz, et al. (1999). "The *Drosophila* GMII gene encodes a Golgi alpha-mannosidase II." J Cell Sci **112 (Pt 19)**: 3319-30.

- Ren, J., F. J. Castellino, et al. (1997). "Purification and properties of alpha-mannosidase II from Golgi-like membranes of baculovirus-infected *Spodoptera frugiperda* (IPLB-SF-21AE) cells." Biochem J **324** (Pt 3): 951-6.
- Roth, J. (2002). "Protein N-glycosylation along the secretory pathway: relationship to organelle topography and function, protein quality control, and cell interactions." Chem Rev **102**(2): 285-303.
- Sarkar, M., P. A. Leventis, et al. (2006). "Null mutations in *Drosophila* N-acetylglucosaminyltransferase I produce defects in locomotion and a reduced life span." J Biol Chem **281**(18): 12776-85.
- Shah, N., D. A. Kuntz, et al. (2008). "Golgi alpha-mannosidase II cleaves two sugars sequentially in the same catalytic site." Proc Natl Acad Sci U S A **105**(28): 9570-5.
- Shoup, V. A. and O. Touster (1976). "Purification and characterization of the alpha-D-mannosidase of rat liver cytosol." J Biol Chem **251**(13): 3845-52.
- Simpson, F., A. A. Peden, et al. (1997). "Characterization of the adaptor-related protein complex, AP-3." J Cell Biol **137**(4): 835-45.
- Spiro, M. J., V. D. Bhoyroo, et al. (1997). "Molecular cloning and expression of rat liver endo-alpha-mannosidase, an N-linked oligosaccharide processing enzyme." J Biol Chem **272**(46): 29356-63.
- Tabas, I. and S. Kornfeld (1978). "The synthesis of complex-type oligosaccharides. III. Identification of an alpha-D-mannosidase activity

- involved in a late stage of processing of complex-type oligosaccharides." J Biol Chem **253**(21): 7779-86.
- Terwisscha van Scheltinga, A. C., S. Armand, et al. (1995). "Stereochemistry of chitin hydrolysis by a plant chitinase/lysozyme and X-ray structure of a complex with allosamidin: evidence for substrate assisted catalysis." Biochemistry **34**(48): 15619-23.
- Tulsiani, D. R., H. P. Broquist, et al. (1984). "The similar effects of swainsonine and locoweed on tissue glycosidases and oligosaccharides of the pig indicate that the alkaloid is the principal toxin responsible for the induction of locoism." Arch Biochem Biophys **232**(1): 76-85.
- Tulsiani, D. R., T. M. Harris, et al. (1982). "Swainsonine inhibits the biosynthesis of complex glycoproteins by inhibition of Golgi mannosidase II." J Biol Chem **257**(14): 7936-9.
- Tulsiani, D. R., S. C. Hubbard, et al. (1982). "alpha-D-Mannosidases of rat liver Golgi membranes. Mannosidase II is the GlcNAcMAN5-cleaving enzyme in glycoprotein biosynthesis and mannosidases Ia and IB are the enzymes converting Man9 precursors to Man5 intermediates." J Biol Chem **257**(7): 3660-8.
- Vallee, F., K. Karaveg, et al. (2000). "Structural basis for catalysis and inhibition of N-glycan processing class I alpha 1,2-mannosidases." J Biol Chem **275**(52): 41287-98.

- Vallee, F., F. Lipari, et al. (2000). "Crystal structure of a class I alpha1,2-mannosidase involved in N-glycan processing and endoplasmic reticulum quality control." Embo J **19**(4): 581-8.
- van den Elsen, J. M., D. A. Kuntz, et al. (2001). "Structure of Golgi alpha-mannosidase II: a target for inhibition of growth and metastasis of cancer cells." Embo J **20**(12): 3008-17.
- Varki, A. (1993). "Biological roles of oligosaccharides: all of the theories are correct." Glycobiology **3**(2): 97-130.
- Varki, A. (1998). "Factors controlling the glycosylation potential of the Golgi apparatus." Trends Cell Biol **8**(1): 34-40.
- Vocadlo, D. J., G. J. Davies, et al. (2001). "Catalysis by hen egg-white lysozyme proceeds via a covalent intermediate." Nature **412**(6849): 835-8.
- Wang, Y., J. Tan, et al. (2001). "Modeling human congenital disorder of glycosylation type IIa in the mouse: conservation of asparagine-linked glycan-dependent functions in mammalian physiology and insights into disease pathogenesis." Glycobiology **11**(12): 1051-70.
- Weng, S. and R. G. Spiro (1993). "Demonstration that a kifunensine-resistant alpha-mannosidase with a unique processing action on N-linked oligosaccharides occurs in rat liver endoplasmic reticulum and various cultured cells." J Biol Chem **268**(34): 25656-63.
- Weng, S. and R. G. Spiro (1996). "Endoplasmic reticulum kifunensine-resistant alpha-mannosidase is enzymatically and immunologically related to the cytosolic alpha-mannosidase." Arch Biochem Biophys **325**(1): 113-23.

- Weng, S. and R. G. Spiro (1996). "Evaluation of the early processing routes of N-linked oligosaccharides of glycoproteins through the characterization of Man₈GlcNAc₂ isomers: evidence that endomannosidase functions in vivo in the absence of a glucosidase blockade." Glycobiology **6**(8): 861-8.
- Yamashiro, K., H. Itoh, et al. (1997). "Purification and characterization of neutral alpha-mannosidase from hen oviduct: studies on the activation mechanism of Co²⁺." J Biochem (Tokyo) **122**(6): 1174-81.
- Zhong, W., D. A. Kuntz, et al. (2008). "Probing the substrate specificity of Golgi alpha-mannosidase II by use of synthetic oligosaccharides and a catalytic nucleophile mutant." J Am Chem Soc **130**(28): 8975-83.

CHAPTER 2

EXPRESSION, PURIFICATION AND CHARACTERIZATION OF A DROSOPHILA MELANOGASTER MANNOSIDASE ORTHOLOGOUS TO DROSOPHILA MELANOGASTER GOLGI MANNOSIDASE II¹

¹ Heather A. Strachan, Douglas A. Kuntz, David R. Rose, and Kelley W. Moremen. To be submitted to *Glycobiology*.

ABSTRACT

Drosophila melanogaster Golgi Mannosidase IIb (dGMIIb) is a class II (CAZy GH38) α -mannosidase involved in the processing of N-glycan structures of the insect secretory pathway. The enzyme activity of this 140-145 kDa protein is stimulated by cobalt, sensitive to furanose inhibitor mimics (swainsonine and 1,4-di-deoxy-mannitol), and has a pH optimum of 6.0. dGMIIb is an ortholog of the well-characterized *Drosophila melanogaster* Golgi Mannosidase II (dGMII). The preferred natural substrate for dGMII is GlcNAcMan₅GlcNAc₂ asparagine (N)-linked to proteins, whereas the preferred natural substrate for dGMIIb is Man₅GlcNAc₂. dGMII has been crystallized and its active site extensively studied for leads into a potential target for inhibition in cancer therapeutics. Modeling of the active site of dGMIIb on the structure of dGMII indicates alterations in the GlcNAc – binding, “anchoring site”, can account for the differences in substrate specificity for these processing enzymes.

INTRODUCTION

Golgi mannosidase II (GMII) is an enzyme involved in the processing of asparagine (N) – linked glycans on newly formed glycoproteins (Moremen 2000; Moremen 2002). This process is highly conserved in eukaryotes. GMII resides in the Golgi apparatus where it cleaves two mannose residues from GlcNAcMan₅GlcNAc₂ N-glycan structures (GlcNAc, N-acetylglucosamine; Man, mannose) to form GlcNAcMan₃GlcNAc₂ (Figure 1.1). This enzymatic step acts as the committed step in the biosynthesis of complex N-glycans. GMII has a unique specificity for its substrate, the exoglycosidic cleavage of non-reducing terminal α 1,3 and α 1,6 mannose residues from GlcNAcMan₅GlcNAc₂, which is believed to be imparted by the requirement for the non-reducing terminal β 1,2-linked GlcNAc residue in GlcNAcMan₅GlcNAc₂ N-glycans. Multiple studies have been performed to understand the active site preference of *Drosophila melanogaster* GMII (dGMII), including the crystal structure determination of the enzyme in the presence of inhibitors and substrate analogs (van den Elsen, Kuntz et al. 2001; Numao, Kuntz et al. 2003; Shah, Kuntz et al. 2003; Chen, Kuntz et al. 2006; Kumar, Kuntz et al. 2008; Kuntz, Tarling et al. 2008; Shah, Kuntz et al. 2008). Small molecule inhibitors previously shown to inhibit GMII were co-crystallized with dGMII and occupied the active site pocket in coordination with a Zn²⁺ ion that is also believed to be involved in catalysis (Figure 1.3) (van den Elsen, Kuntz et al. 2001). In addition to the substrate binding to the active site, an additional binding site for the cryoprotectant 2-methyl-2,4-pentanediol (MPD), or glycerol, was found in a loop region adjacent to

the active site. Glycerol had previously been found to mimic carbohydrate residues by occupying sugar binding site in glycosylhydrolases and authors hypothesized that the cryoprotectant interaction with the active site loops reflected a β 1,2-GlcNAc binding site (Schmidt, Schlacher et al. 1998; Vallee, Lipari et al. 2000). Subsequent crystallization of a dGMII active site nucleophile mutant (D204A) with GlcNAcMan₅GlcNAc confirmed their hypothesis when the GlcNAc residue was found bound in this site (Figures 1.4) (Shah, Kuntz et al. 2008). The structure of dGMII co-crystallized with GlcNAcMan₅GlcNAc revealed three sites involved in catalysis (Figure 1.4). In addition to the active site and GlcNAc binding site (anchor site), an α 1,3 linked Man residue in the substrate occupied a site adjacent to the active site. The α 1,6 linked Man residue occupied the active site during the ordered cleavage reaction. This latter binding pocket has been termed the “holding site”. The anchoring and holding sites are believed to stabilize the flexible glycan substrate for efficient catalysis in the active site.

GMII is known to be inhibited by furanose transition state mimics like swainsonine (SWA) (Tulsiani, Harris et al. 1982) and 1,4-di-deoxy-1,4-imino-D-mannitol (DIM) (Winchester, al Daher et al. 1993). Swainsonine was used in early clinical trials as a cancer therapeutic due to its potency as an inhibitor of GMII and its drug solubility. Swainsonine was shown to decrease the overproduction of large oligosaccharide structures found in tumor cells associated with altered adhesion characteristics, metastasis, and poor clinical prognosis. These large extended β 1,6 linked poly lactosamine branches were

found to be a result of the upregulation of GlcNAc Transferase V (GnTV), and enzyme downstream of GMII (Dennis, Granovsky et al. 1999). Effective, soluble inhibitors have not been found for GnTV and have lead scientists to target GMII for inhibition. In an effort to develop a specific inhibitor for GMII, dGMII has been co-crystallized with a variety of inhibitors and GMII has been extensively screened *in vitro* for potential candidate inhibitors (Winchester, al Daher et al. 1993; van den Elsen, Kuntz et al. 2001; Numao, Kuntz et al. 2003; Shah, Kuntz et al. 2003; Li, Kawatkar et al. 2004; Siriwardena, Strachan et al. 2005; Wen, Yuan et al. 2005; Chen, Kuntz et al. 2006; Kawatkar, Kuntz et al. 2006; Chen and Pinto 2007; Englebienne, Fiaux et al. 2007; Kumar, Kuntz et al. 2008; Kuntz, Tarling et al. 2008; Shah, Kuntz et al. 2008; Zhong, Kuntz et al. 2008; Kuntz, Zhong et al. 2009). A specific inhibitor for GMII, that does not affect other glycosylhydrolase family 38 enzymes in the biosynthetic and catabolic N-linked glycosylation pathway, has not yet been developed. Characteristics of glycosylhydrolase 38 enzymes include high sequence similarity (especially in proposed active site regions), sensitivity to furanose inhibitor mimics, relatively large protein molecular weights and low to neutral pH optima depending upon enzyme subcellular localization (Henrissat 1991; Henrissat and Bairoch 1993; Henrissat and Bairoch 1996; Henrissat and Davies 1997; Henrissat 1998; Moremen 2000; Bourne and Henrissat 2001). The high sequence conservation, similar mechanisms of action, and similar inhibition characteristics provide difficulty for finding selective inhibitors. The key to developing selective GH38 mannosidase inhibitors is a more complete understanding of the unique

substrate specificities of the enzyme isoforms. For GMII, this means fully characterizing the holding and anchoring sites in substrate recognition and contrasting these substrate binding elements with related enzymes that have different substrate specificities. An enzyme with cleavage specificity for $\text{Man}_5\text{GlcNAc}_2$ has been found in crude extracts in mammals, but has never been cloned and fully characterized (Monis, Bonay et al. 1987; Bischoff, Moremen et al. 1990; Bonay and Hughes 1991; Bonay, Roth et al. 1992; Weng and Spiro 1993; Misago, Liao et al. 1995; Grard, Herman et al. 1996; Weng and Spiro 1996; Yamashiro, Itoh et al. 1997; Oh-Eda, Nakagawa et al. 2001). However, an enzyme with a specificity for cleavage of $\text{Man}_5\text{GlcNAc}_2$ has been identified in *Spodotera frugiperda*, termed SfMII (Kawar, Karaveg et al. 2001). This enzyme was later purified and tested with a variety of high mannose and hybrid oligosaccharides. It was found that unlike mammalian or *Drosophila* GMII, SfMII preferred $\text{Man}_5\text{GlcNAc}_2$ as a substrate rather than $\text{GlcNAcMan}_5\text{GlcNAc}_2$. This enzyme was shown in to be sensitive to inhibition by swainsonine, required cobalt for enzymatic activity, and had a neutral pH optimum. Localization studies with confocal microscopy and fluorescent tags localized this enzyme to the Golgi. While this data identified an enzyme in *Spodotera frugiperda* with a preference for $\text{Man}_5\text{GlcNAc}_2$ over $\text{GlcNAcMan}_5\text{GlcNAc}_2$, more extensive study is required to differentiate this enzyme from GMII and be useful in inhibitor development.

Sequence similarity searches to dGMII identified an additional ortholog in the *Drosophila* genome with a high sequence similarity to SfMII. The latter protein had not been cloned, expressed, purified or characterized. We chose this

protein for further study to determine its role in N-linked glycan processing in *Drosophila melanogaster*. Detailed substrate specificity and inhibitor studies have been performed using the purified recombinant enzyme. Substrate specificity studies indicate that this enzyme has many characteristics in common with SfMII.

RESULTS

Sequence Relationships of dGMIIb to Glycosylhydrolase Family 38

Members of the CAZy glycosylhydrolase family 38 (GH38) α -mannosidase family have a PFAM signature peptide sequence, called Glyco_hydro_38, that exists in the NH₂-terminal region of the protein (Henrissat 1998). This motif has been identified in *Drosophila melanogaster*, *Spodoptera frugiperda*, *Caenorhabditis elegans*, as well as bacterial, archael, fungal, mouse and human sequences. A collection of these sequences was used to create a dendrogram to represent the glycosylhydrolase family (Fig 1.2).

Four sequence clades are evident in this dendrogram of the GH38 family (Fig 1.2). The “Golgi Mannosidase II” clade represents α -mannosidase enzymes involved in the processing of glycoproteins (Moremen, Touster et al. 1991; Misago, Liao et al. 1995; Moremen 2000; Moremen 2002). The “Core Specific Lysosomal Mannosidase” clade is represented by α -mannosidases involved in glycoprotein catabolism that have a substrate specificity for core-linked α 1,6 mannosides (Park, Meng et al. 2005). The “Lysosomal Mannosidase Broad

Specificity” clade is represented by α -mannosidases involved in glycoprotein catabolism, harboring a much broader substrate specificity than the Core Specific Lysosomal Mannosidase or Golgi mannosidase clade (Liao, Lal et al. 1996; Merkle, Zhang et al. 1997; Nilssen, Berg et al. 1997). The “Heterogeneous Ancestral” clade is a varied collection of enzymes involved in dolichol-oligosaccharide turnover and the breakdown of glycans on glycoproteins that have failed ER quality control and ended up in the cytosol to be degraded. Orthologs in this heterogeneous clade have been found in such diverse organisms as bacteria, fungi, and archea; suggesting an ancestral origin to this clade. A comparison of a handful of glycosyl hydrolase family 38 (GH38) mannosidases and their unique characteristics can be seen in Table 1.1.

Representatives of *Drosophila* GH38 enzymes can be found in every clade shown in Figure 1.2, except the “Heterogeneous Ancestral” clade. The focus of this study revolves around the “Golgi Mannosidase” clade where dGMII and dGMIIb reside. In this clade dGMIIb diverges from dGMII and is branched closest with SfMII. This branching pattern suggests that dGMIIb and SfMII are closely related in sequence and possibly function. The likelihood that dGMIIb is a functional homolog of SfMII with a similar substrate specificity – distinct from dGMII’s substrate specificity – provides interest in determining the role of dGMIIb in N-linked glycan processing in *Drosophila*.

Recombinant Protein Expression in S2 Cells

The catalytic portion of *Drosophila melanogaster* Golgi mannosidase IIb (dGMIIb) (NM_142237) was identified using a sequence comparison of known GMIIb and SfGMIIb by comparison to a catalytically active proteolytically resistant hydrophilic 110,000 dalton digestion product of rat GMII (Moremen and Touster 1986). The catalytic domain of rat GMII was then purified and compared to an intact 124,000 dalton α -mannosidase II subunit demonstrating that the intact and cleaved forms were kinetically indistinguishable (Moremen, Touster et al. 1991). Multiple sequence alignments of mouse, human and fly GMII catalytic domains previously purified enabled a coding region to be defined for dGMIIb. This coding region was codon-optimized for *Drosophila* expression in S2 cells. The coding region encoding the catalytic domain was generated by gene synthesis (GeneArt) and cloned into pMT-Bip-V5-HisA (Invitrogen) using BglIII and NotI restriction sites along with an 8x His tag for affinity chromatography. The absence of the cytoplasmic tail and transmembrane domain found in the full length dGMIIb allowed the protein to be secreted into the medium for easy harvesting due to the incorporation of the BiP secretion signal.

The pMT-BiP-V5-HisA/dGMIIb expression construct does not encode an antibiotic resistant gene for stable transformants of S2 insect cells culture. Therefore, this vector was co-transfected with a construct, pCoBlast that confers blasticidin resistance to transformed cells for the production of stable lines. A construct that expresses an inducible form of GFP, pMT-BiP-V5-HisA/GFP, was

also used in co-transfection experiments to verify calcium phosphate transfection efficiency and copper induction of recombinant products.

Stable transformants were produced by calcium phosphate co-transfection method using a combination of pCoBlast and pMT-BiP-V5-HisA/dGMIIb. After a 24 hour incubation with transfection components, the cells were washed and resuspended in fresh media plus ~20 ug/mL blasticidin and the media was changed every 4-5 days until blasticidin resistant cells appeared and mock transfected cells died. The process of creating stable, blasticidin-resistant lines took 3-4 weeks, after which they were passaged into new tissue culture vessels (T25 tissue culture treated flasks). After 1 week the cells were tested for activity and optimum induction time (Figure 2.1). The scale up of stable transformants from T25 flasks to T175 flasks took ~ 4 – 6 weeks before large scale induction and purification was performed.

The recombinant expression of dGMIIb was induced by addition of copper sulfate to the S2 insect cell cultures and the recombinant product was isolated as a secreted protein from conditioned media of blasticidin-resistant stably transfected S2 cell lines. The optimal induction period was determined by monitoring enzyme activity using a 4MU-Man substrate and detection of the dGMIIb visualization of a His tag associated with dGMIIb recombinant product by immunoblotting over a 4-day time course of induction. Enzyme activity data indicated that the optimal time for induction of enzyme expression was 2-3 days (Figure 2.1).

Conditioned media from the induced cell cultures were harvested and dGMIIb was partially purified by Phenyl–Sepharose (Figure 2.2) and Ni²⁺-NTA affinity chromatography (Figures 2.3). 4MU-Man was used as a substrate to detect mannosidase activity during purification. In some protein isolations, serum-free media was used during the induction of protein expression (Table 2.1) to avoid contamination of fetal bovine serum (FBS).

During purification over the Phenyl-Sepharose column the specific activity increased 6.7-fold and the total activity increased 15%, presumably as a result of the removal of inhibitory contaminants in the conditioned media. Ni²⁺-NTA affinity chromatography led to an additional 5.7-fold enrichment of purification (total 38-fold purification). This purification led to a preparation where dGMIIb was the major component by SDS-PAGE (Figure 2.3.2) and was used for further characterization studies. This sample was comparable to a purified enzyme sample (kindly provided by Doug Kuntz - identical in sequence to dGMIIb minus five amino acids at the N-terminus) producing the same enzymatic results when characterized in parallel studies. Purification further using gel filtration to separate this protein by its molecular weight could possibly increase the fold purification and is suggested for future studies of this enzyme.

pH Optimum, Metal Activation and Inhibition Studies with dGMIIb

The pH optimum of recombinant *Drosophila melanogaster* Golgi mannosidase IIb (dGMIIb) was compared with dGMII and the human broad

specificity lysosomal α mannosidase, *Homo sapiens* lysosomal mannosidase (hLysMan). The optimal pH for enzymatic activity for these three enzymes was 5.0 ± 0.2 for dGMII, 5.5 ± 0.2 for dGMIIb, and 4.0 ± 0.2 for hLysMan (Figure 2.4). The neutral pH optimum of dGMIIb implies that this enzyme is more likely to reside in the Golgi apparatus or ER rather than the acidic lysosomal compartment.

Due to the fact that some GH38 mannosidases are stimulated by divalent cations, we tested the effects of various cations (1 mM each) on enzyme activity for dGMII, dGMIIb, and hLysMan at the optimal pH for each enzyme. The cations showed little or no effect for either dGMII or hLysMan in an 1 hour incubation at 37°C. The effect of EDTA treatment (1 mM) was also tested for all three enzymes and was shown to have little to no effect on mannosidase activity. DGMIb, on the other hand, was activated 6-fold by MnCl_2 , 18-fold by FeCl_2 and 35-fold by CoCl_2 (Figure 2.5.1). Under the enhancement of cobalt the pH optimum of dGMIIb shifted to 6.0 ± 0.2 (Figure 2.5.2). The effect of CoCl_2 on mannosidase activity distinguishes dGMIIb from dGMII and hLysMan, which are not affected significantly by the cations tested, despite the role of the divalent cation in substrate binding based on the crystal structures. We anticipate that the tight binding of the cation by the enzyme precludes extraction and chelation of the ion during EDTA treatment as seen previously (Karaveg, Siriwardena et al. 2005).

The inhibition characteristics of dGMII, dGMIIb, and hLysMan were tested using 4MU-Man as a substrate (Table 2.2). SWA and DIM are previously

characterized GH38 mannosidase inhibitors. The K_i s for dGMII, dGMIIb, and hLysMan using swainsonine as an inhibitor were 0.30 μ M, 0.07 μ M, and 0.50 μ M, respectively. The K_i s for dGMII, dGMIIb, and hLysMan with DIM were 2.30 μ M, 0.03 μ M, and 4.90 μ M, respectively. In both cases dGMIIb is more sensitive to inhibition than dGMII and hLysMan. This difference in sensitivity to inhibition by dGMII may be due to a different transitional state conformation or a difference in the bound ion in comparison to the other enzymes.

KIF and DMNJ have previously been characterized as GH47 inhibitors, although weak inhibition of GH38 α -mannosidases have been detected. The K_i s for dGMII, dGMIIb, and hLysMan with KIF are 2.30 mM, 28 μ M, and 34 μ M, respectively. The K_i s of dGMII, dGMIIb, and hLysMan with DMNJ are 580 μ M, 73 μ M, and 625 μ M, respectively. The sensitivity of dGMIIb to KIF is closer to the effect seen on hLysMan, however dGMIIb is more sensitive to DMNJ than hLysMan. This difference in sensitivity can possibly be exploited for inhibitor design.

Natural Substrate Cleavage by dGMII, dGMIIb, and hLysMan

The preferred natural substrate for dGMIIb was determined using GlcNAcMan₅GlcNAc₂-PA and Man₅GlcNAc₂-PA substrates followed by separation of the enzymatic products by HPLC and comparing these results to dGMII and hLysMan controls. To confirm that the respective recombinant enzyme was responsible for substrate cleavages parallel reactions were carried out in the presence of the mannosidase inhibitor, swainsonine, or the

hexosaminidase inhibitor, N-phenylcarbamate (PUGNAc), at concentrations that inhibited the respective enzyme activities. Figure 2.6 shows the enzymatic reactions at 1 and 4 hour incubation time points. dGMIIb cleaves $\text{Man}_5\text{GlcNAc}_2\text{-PA}$ at 1 and 4 hours, however it does not cleave $\text{GlcNAcMan}_5\text{GlcNAc}_2\text{-PA}$ after 1 hour of incubation. Increased enzyme concentrations or prolonged incubation times led to minor cleavage of the latter substrate indicating that the preferred substrate for dGMIIb is $\text{Man}_5\text{GlcNAc}_2\text{-PA}$, but with increased enzyme (or time) dGMIIb can cleave $\text{GlcNAcMan}_5\text{GlcNAc}_2\text{-PA}$ with less efficiency. dGMII cleaves $\text{GlcNAcMan}_5\text{GlcNAc}_2\text{-PA}$ at 1 and 4 hours incubation, and does not cleave $\text{Man}_5\text{GlcNAc}_2\text{-PA}$ under the same conditions. However, at a higher enzyme concentration tested, dGMII was shown to cleave $\text{Man}_5\text{GlcNAc}_2\text{-PA}$ after a 4-hour incubation. These data confirm the preferred substrate for dGMII is $\text{GlcNAcMan}_5\text{GlcNAc}_2\text{-PA}$. hLysMan cleaves $\text{Man}_5\text{GlcNAc}_2\text{-PA}$ at 1 and 4 hours of incubation. hLysMan did not cleave $\text{GlcNAcMan}_5\text{GlcNAc}_2\text{-PA}$ after 1 hour, but did produce minor cleavage products with increased enzyme or time confirming that the preferred substrate for hLysMan is $\text{Man}_5\text{GlcNAc}_2\text{-PA}$.

Substrate Affinity and Catalytic Rate Analysis of dGMII, dGMIIb, and hLysMan

The K_m s for dGMII, dGMIIb, and hLysMan with the 4MU-Man substrate were determined as 4.90 ± 2.60 mM, 0.90 ± 0.10 mM, and 0.80 ± 0.40 mM, respectively. K_m data was also gathered for these enzymes with their preferred natural substrates (Table 2.3). dGMII had a K_m of 89.60 μM using the

GlcAcMan₅GlcNAc₂-PA substrate, while dGMIIb had a K_m of 77.40 μ M using the Man₅GlcNAc₂-PA substrate. Similarly, hLysMan had a K_m of 85.80 μ M using Man₅GlcNAc₂-PA substrate. While all of these K_m values are similar, they also indicate higher substrate affinities for the glycan substrates compared to the 4MU-Man substrate with a synthetic aglycone, which had K_m values approaching the mM range. Interestingly, the affinity of dGMII for its natural substrate (GlcAcMan₅GlcNAc₂) was not higher than the affinities for the other enzymes for their respective substrates. The data indicate that while the GlcNAc-binding “anchoring site” is critical for the unique substrate specificity of dGMII, it did not appear to lead to an increased substrate affinity for the enzyme. This suggests that the GlcNAc plays a larger part in efficiency of catalysis rather than improving substrate affinity. The co-crystal structure generated with GlcNAcMan₅GlcNAc occupying the substrate recognition site as well as the glycan substrate kinetic studies described here and below suggest that the GlcNAc residue plays a role in the catalytic efficiency of GMII by favorably anchoring the N-glycan in the glycan binding cleft.

In contrast to direct kinetic analysis of natural glycan substrates by the respective enzymes, when enzyme turnover rates were normalized to the rates of cleavage of 4MU-Man it was surprising to find that the rate of cleavage of the preferred substrate for dGMII (GlcNAcMan₅GlcNAc₂-PA) was 150-fold greater than the rate of cleavage by hLysMan and its preferred substrate (Man₅GlcNAc₂-PA). Similarly, the rate of cleavage of its preferred substrate by dGMII was 175,000-fold greater than the cleavage of the preferred substrate by dGMIIb

(Table 2.4). These data may just reflect the relative efficiency of cleavage of small synthetic substrate by the respective enzymes and call into question the use of the latter substrate in normalization of kinetic data on the glycan substrates.

Modeling of dGMIIb and SfMII and Comparison with the Structures for dGMII and bLysMan

Using the dGMII crystal structure with bound GlcNAcMan₅GlcNAc₂ (PDB id: 3CZN) as a scaffold we generated a structural model for dGMIIb and SfMII (Figure 2.7), using the DeepView/Swiss-Pdb Viewer and the Swiss Model server (Guex and Peitsch 1997). We then aligned the modeled structure with dGMII and bLysMan and compared the sequence and residues that comprise the active site, the anchoring site and the holding site (Figures 2.7 - 2.11). The “active” and “holding sites” seem well conserved between dGMII, dGMIIb and SfMII and less conserved in bLysMan (Figures 2.7 – 2.10), but there is a striking difference in the “anchoring site” of dGMII (Figures 2.11.1 and 2.11.2) with all enzymes compared. The dGMIIb model appears to have a pocket in the vicinity of the “anchoring site”, but lacks an important His273 residue that directly interacts with the GlcNAc residue in the dGMII co-crystal structure and important loop region residues, Trp299 and Pro298, that stabilize the histidine residue (Figure 2.11.1). The dGMIIb model also lacks an important residue that may be involved in stacking interactions with the GlcNAc, Tyr267, and hydrogen bonding with the

core β 1,4 linked mannose residue in the GlcNAcMan₅GlcNAc ligand (Figure 2.11.2) The bLysMan model appears to completely lack an “anchoring site” seen in the dGMII co-crystal (Figures 2.8 – 2.11). The “anchoring site” is the largest difference between the dGMII crystal structure and bLysMan crystal structure, which suggests that this binding region provides the unique substrate specificity for GMII. Due to the fact that dGMIIb prefers the Man₅GlcNAc₂-PA substrate to GlcNAcMan₅GlcNAc₂-PA, but appears to have a loop region in the modeled structure, comparing these loop regions could aid in the development of specific inhibitors of GMII (Figure 2.11).

DISCUSSION

We have shown that dGMIIb is a ~140-145 kDa GH38 α -mannosidase with characteristics similar to other enzymes in this family. *Drosophila melanogaster* has protein representatives in the Golgi mannosidase and broad specificity lysosomal mannosidase clades, but not in the heterogeneous ancestral clade or recently characterized core specific lysosomal mannosidase clade. dGMIIb is a member of the Golgi Mannosidase clade rooted closely to SfMII, an enzyme previously characterized from *Spodoptera frugiperda* (Kawar, Karaveg et al. 2001). dGMIIb is similar in substrate specificity to SfMII in that it preferentially cleaves Man₅GlcNAc₂-PA to Man₃GlcNAc₂-PA, but cleaves GlcNAcMan₅GlcNAc₂-PA with poor efficiency, is stimulated by cobalt, is sensitive

to SWA, and has a neutral pH optimum. This enzyme is also sensitive to DIM and DMNJ. Thus, dGMII is likely an ortholog of SfMII.

The dGMIIb structural model displays a significant difference in the “anchoring site” compared to the dGMII co-crystal structure (Figures 2.8, 2.11). Although the dGMIIb model appears to have a pocket in the vicinity of the “anchoring site”, it does not have the His273 residue found in dGMII that directly interacts with the GlcNAc residue in the dGMII co-crystal structure or the loop region residues Trp299 and Pro298 that interact with His273. The dGMIIb model is also missing a Tyr residue possibly involved in stacking interactions with the GlcNAc residue and hydrogen bonding interactions with the core β 1,4 linked mannose residue. These differences could be key in providing the unique substrate specificity for dGMII in glycan processing.

Residual amounts of paucimannosidic glycans in GnTI and FDL (N-Acetylglucosaminidase) null flies led to the hypothesis that an N-glycan processing enzyme existed in flies which was independent of the enzymatic action of GnTI. We believe that dGMIIb is the GnTI independent enzyme in the N-glycan processing pathway, which can bypass the GMII step (although with reduced efficiency) and is the cause of residual paucimannosidic glycans seen in these mutants. Further research must be conducted to confirm this hypothesis in null flies. However, the data indicate that dGMIIb can cleave $\text{Man}_5\text{GlcNAc}_2$ to $\text{Man}_3\text{GlcNAc}_2$ independent of the action of GnTI.

MATERIALS AND METHODS

Expression of *Drosophila Melanogaster* Golgi Mannosidase IIb

A synthetic gene, composed of a sequence corresponding to the catalytic portion of dGMIIb (NM_142237 encoding residues EEQ – SEV from NP_650494) containing an 8x His tag at the N-terminus was codon optimized for insect cell expression and assembled by GeneArt Inc. (Regensburg, Germany) from synthetic oligonucleotides. The gene fragment was cloned into pMT-Bip-V5-HisA (Invitrogen) using BglIII and NotI restriction sites to result in a coding region encoding the catalytic domain of dGMIIb with an attached His tag for affinity chromatography. GeneArt verified the sequence of the final construct. The maps of this and two other constructs used in these experiments, pCoBlast and pMT/BiP/V5-His/GFP (Invitrogen), can be seen in Figure 2.12.

The final DNA constructs were transfected into Top 10 *E.coli* cells and large-scale plasmid preparations were isolated by Qiagen Maxi Prep kits using standard methods. The final DNA preparation was quantitated by spectrophotometry (NanoDrop).

These constructs were introduced into *Drosophila* Schneider 2 (S2) cells (gift from Rose and Kuntz – University of Toronto) using a standard calcium phosphate transfection method with reagents from Invitrogen. The cells were cultured for transfection by seeding 3×10^6 S2 cells/mL into 6 well tissue culture treated plate (Corning). Each well contained 3 mL of S2 cells in Schneider's *Drosophila* S2 medium (Gibco) supplemented with 10% fetal bovine serum (FBS)

(Gibco) (complete medium). These cells were incubated at 28°C until they reached a density of $2-4 \times 10^6$ cells/mL (corresponds to log phase growth). Cell counts were performed following addition of Trypan Blue (Gibco) and using a hemacytometer to determine the viability of the cultures. The incubation time needed to reach the appropriate density varied from 16 hours to 2 days. The cells were then split again into a second 6 well plate to produce cultures for stable cell transfection. After the cells reached log phase the cells were transfected with the appropriate DNA construct.

For each well to be transfected the following transfection mix was prepared: 36 μ L of 2 M CaCl_2 , 19 μ g of pMT/BiP/V5-His/dGMI**b**, 1 μ g pMT/BiP/V5-His/GFP, and 1 μ g of pCoBlast, and was combined with tissue culture sterile water to a final volume of 300 μ L (solution A). Solution B consisted of 300 μ L of 2x (50 mM HEPES, 1.5 mM NaH_2PO_4 , 280 mM NaCl, pH 7.1) HBS per well to be transfected. Solution A was added slowly, dropwise to solution B with continuous mixing to ensure production of a fine precipitate for efficient transfections. The combined solution was incubated for 30 minutes and up to 6 hours to further allow a fine precipitate to be formed. The solution was mixed and added dropwise to the cells in the 6 well plates containing Schneider's medium, swirling after each drop for consistent mixing. The cells were incubated for 24 hours and then washed by centrifugation and resuspension 2 times with complete medium. After the last wash, the cells were resuspended in complete growth media containing 20 μ g/mL blasticidin (American Scientific Chemicals) (blasticidin resistance was enabled by cotransfection with the pCoBlast vector),

replated into the same wells that they were transfected in, and incubated at 28°C. The media was replaced every 4-5 days until antibiotic resistant colonies appeared and all the mock transfected cells died (~3-4 weeks). The blasticidin-resistant cells were expanded by replating into new plates with selective medium, (Schneider S2 cell media containing 10% FBS and 20µg/mL blasticidin) and split when the density of the cells reached 6-20x10⁶ cells/mL. The cells were maintained in selective medium and moved into T25 flasks for scaling-up and testing expression. Cells in T25 flasks were tested for protein expression when they reached log phase and were ≥ 90% viable. Stable, blasticidin-resistant cell lines were induced with 500 µM copper sulfate (Sigma). The induced secreted protein was harvested after 2-3 days. There was a significant increase in 4MU-Man activity between the cells transfected with the dGMIIb and pCoBlast constructs versus cells only transfected with the pCoBlast vector alone (Figure 2.1).

To test that the 4MU-Man activity corresponded to the construct of interest, Western blotting was performed to visualize the His tag associated with the recombinant product. The induced samples were denatured by boiling in SDS sample buffer (45 mM Tris HCl, pH 6.8; 1% SDS, 10% glycerol, and 50mM DDT), and loaded onto a 1.5mm gel with 5% stacking and 8% resolving gel, and run for 45 minutes at 150-200 V in SDS running buffer (25 mM Tris, 192 mM Glycine, 0.1% SDS, pH 8.3). This gel was then used for transfer of the protein to a PVDF (Immobilon) membrane in 25mM Tris, pH 8.3, 192 mM glycine, 20% methanol and ddH₂O at 100mA for 2-2.5 hours at 4°C. The membrane was then

blocked in 5% fat free milk in 10mM Tris, 150 mM NaCl, 0.02% Tween and ddH₂O (TBST) overnight at 4°C. After blocking, the membrane was then washed 3 times with TBST and then incubated with a monoclonal anti-His antibody conjugated with alkaline phosphatase (Alpha Diagnostic International) (1:1000 dilution) in 1% milk TBST for 45 minutes. The membrane was washed 3 times with TBST and then developed in a solution of 0.15 mg/mL 5-bromo-4-chloro-3-indolyl phosphate (BCIP), 0.3 mg/mL p-nitroblue tetrazolium chloride (NBT), 100mM Tris buffer, and 5mM MgCl₂ (BCIP/NBT Sigma Fast) and TBST for 2 minutes or until the tagged protein started to become barely visible. The membrane continued to develop while drying at room temperature. A band of the His tagged recombinant proteins, dGMIIb or GFP, were visible in co-transfected samples, while no band was visible in the mock transfection (Figure 2.1.2). The stably transfected cell lines were then scaled up into T75 flasks and later T175 flasks for large-scale expression. Later purification of this media revealed a large amount of BSA contamination. To troubleshoot this problem, a subset of these cell lines was adapted to EXCELL 420 serum-free media (SFM) containing 17.5 µg/mL blasticidin. These cells were also scaled up into T175 flasks. After the induction of the cell lines in SFM samples for 2-3 days, the dGMIIb conditioned media was then harvested by decanting media, clarified by centrifugation 3 times at 1000-1200 rpm remove cells and cell debris. This media was then used for protein purification.

Purification of Drosophila Melanogaster Golgi Mannosidase IIb

After the harvesting and clarification of the dGMIIb conditioned media, the media was adjusted to 1M $(\text{NH}_4)_2\text{SO}_4$ (JT Baker). The equilibrated, conditioned media was then loaded on a Phenyl-Sepharose (GE Healthcare) column equilibrated with 1 M $(\text{NH}_4)_2\text{SO}_4$, 50 mM NaH_2PO_4 , pH 7 (JT Baker). The column was washed with 1 M $(\text{NH}_4)_2\text{SO}_4$, 50 mM NaH_2PO_4 , pH 7, and then washed with 50 mM NaH_2PO_4 , pH 7. The protein was eluted with an ethylene glycol (JT Baker) gradient from 0-60% (protein eluted at 60%). Fractions containing mannosidase activity were collected (Figure 2.2) for further purification.

Ni-NTA (Qiagen) column chromatography was performed taking advantage of the 8x His tag encoded by the pMT-Bip-V5-HisA dGMIIb construct. The Ni-NTA column was equilibrated with 300 mM NaCl, 25 mM HEPES at pH 7.4. The pooled fractions from the Phenyl-sepharose purification step were diluted 5-fold with column buffer containing 300 mM NaCl (JT Baker), 25 mM HEPES (Sigma), pH 7.4, and loaded at a flow rate of 1 mL/min. The recombinant protein was then eluted with a gradient of 0-100% 500 mM imidazole (Sigma) in column buffer. Fractions containing mannosidase activity were collected (Figure 2.3) and concentrated with an Amicon 50 YM30 or YM50 millipore membrane exchanged into 300 mM NaCl, 25 mM HEPES at pH 7.4. A protein purification table (Table 2.1) shows each enzyme enrichment during the purification protocol.

Optimum pH for Catalytic Activity

The catalytic domains of dGMII (NP_524291.2, GI:24645354, kindly provided by Doug Kuntz, Department of Medical Biophysics, University of Toronto, Toronto, ON, Canada), dGMIIb, and hLysMan (NP_000519.2 GI:51873064, kindly provided by Lu Meng, Department of Biochemistry and Molecular Biology, Complex Carbohydrate Research Center, University of Georgia, Athens, GA) were assayed in citrate/phosphate (McIlvaine 1921) buffer ranging from a pH of 2.5 – 8.0. The enzymatic reaction components (3 mM 4 MU-Man, 20 mM NaH₂PO₄, 10 mM citric acid, enzyme and dH₂O) were assembled in 96 well flat-bottomed black plates (Corning) on ice and then incubated at 37°C for 1 hour. The enzyme reactions were stopped by addition of 150 mM sodium carbonate pH 12.7 and read immediately on a Spectramax Gemini XS fluorometer. The optimum pH for enzymatic activity was determined by plotting the nmoles of 4MU-Man cleaved/min for each pH value (Figure 2.4).

Metal Cation Requirements

To test the effect of different cations on dGMIIb activity, the enzyme was incubated with 3 mM 4 MU-Man, 20 mM NaH₂PO₄, 10 mM citric acid, dH₂O and 1 mM of a metal cation at 37°C for 1 hour. The enzymatic reactions were prepared in 96 well flat-bottomed plates and assembled on ice before incubating. The reaction was stopped with 150 mM sodium carbonate and read immediately on a Spectramax Gemini XS fluorometer. The metal cations tested were ZnCl₂

(Sigma), CoCl_2 (Sigma), MgCl_2 (JT Baker), FeCl_2 (Aldrich), MnCl_2 (JT Baker), NiCl_2 (Sigma), and CuCl_2 (JT Baker), as well as EDTA (Boehringer), a compound that sequesters metal ions in solution, and compared to a reaction containing no additional metal cation or EDTA (Figure 2.5).

The Inhibition Characteristics of Drosophila Golgi Mannosidase IIb

To determine the inhibition characteristics of dGMIIb, the enzyme was assayed in 20 mM NaH_2PO_4 , 10 mM citric acid, pH 6.0, 1 mM CoCl_2 , a range of 4 MU-Man from 0.1875 mM – 3 mM, and varying concentrations of swainsonine (SWA) (Sigma), 1,4-di-deoxy-mannitol (DIM) (Sigma), kifunensine (KIF) (Toronto Research Chemicals), and deoxy-mannojirimycin (DMNJ) (Toronto Research Chemicals). The reactions were prepared in 96 well flat-bottomed plates on ice, incubated at 37°C for 1 hour, and stopped with 150 mM sodium carbonate, pH 12.7. The fluorescence was quantitated on a Spectramax Gemini XS fluorometer. All fluorescence values are compared to a 4MU standard curve to determine the nmoles of 4MU-Man cleaved per minute.

K_m and K_i data were obtained for each enzyme by varying concentrations of 4MU-Man substrate at different inhibitor concentrations. Lineweaver-Burk reciprocal plots ($1/v$ vs. $1/[S]$) were used to derive kinetic constants using a replot of the slopes of each individual reciprocal plot versus inhibitor concentration (Segal 1993). dGMIIb, dGMII and hLysMan were assayed at pH 6.0, 5.0 and 4.0, respectively (Table 2.2).

Natural Substrate for Drosophila Golgi Mannosidase IIb

To perform kinetic analysis using natural substrates, Man₉GlcNAc₂ was isolated from soybean agglutinin as previously described (Karaveg, Siriwardena et al. 2005) and was used to generate Man₅GlcNAc₂ by incubation with ERManI and GolgiManIA. GlcNAcMan₅GlcNAc₂ was generated by incubation with GlcNAcTI, which transfers a GlcNAc to the α 1,6 mannose branch onto Man₅GlcNAc₂-N-linked glycan. Pyridylamine (PA) tagged high mannose oligosaccharides were generated by reductive amination of the oligosaccharide-reducing end with 2-aminopyridine (Hase 1994; Karaveg, Siriwardena et al. 2005). PA-tagged oligosaccharides were detected by fluorescence after separation on an amine column and compared to standards.

dGMIIb enzymatic reactions were assembled on ice in 1.5 mL microfuge tubes. The enzymatic reactions contained 20 mM NaH₂PO₄, 10 mM citric acid (pH 6.0), 1 mM CoCl₂, 10 μ M GlcNAcMan₅GlcNAc₂-PA or Man₅GlcNAc₂-PA, 40 μ M swainsonine (Sigma) and/or 2 μ M PUGNAc (Toronto Research Chemicals). Four conditions were tested with each substrate and enzyme: 1) enzyme with no inhibitor, 2) enzyme with swainsonine, 3) enzyme with PUGNAc, and 4) enzyme with swainsonine and PUGNAc. These enzymatic reactions were incubated at 37°C for 1 – 4 hours and then stopped by boiling for 8-10 minutes. dGMII and hLysMan were tested under the same conditions, minus CoCl₂, and at their respective pH optimums.

The cleavage of high mannose substrates was detected by HPLC to assess the natural substrate specificity of dGMIIb, and confirm the natural

substrate specificity of dGMII and hLysMan as controls. The enzymatic reaction solutions were injected into an amine column (Alltech Brava™ NH₂, particle size: 5 μm, surface area: 195 m²/g) under isocratic buffer conditions of 55% acetonitrile and 45% 0.1 M sodium phosphate buffer, pH 4.0 (Figure 2.6).

To determine the K_ms of the three enzymes with their preferred natural substrates, the assays were assembled with 20 mM NaH₂PO₄, 10 mM citric acid at the pH corresponding to the optimum pH for the enzyme being tested (pH 6.0 for dGMIIb, pH 5.0 for dGMII and pH 4.0 for hLysMan), 1 mM CoCl₂ (*Dm Golgi Man IIb* only), and varying concentrations of GlcNAcMan₅GlcNAc₂-PA or Man₅GlcNAc₂-PA from 10 μM – 200 μM. dGMII and dGMIIb were incubated for 1 hour at 37°C and stopped with boiling for 8 – 10 minutes. hLysMan was incubated for 4 hours at 37°C and stopped with boiling for 8 – 10 minutes. The samples were injected into the amine column under isocratic buffer conditions of 55% acetonitrile and 45% 0.1 M sodium phosphate at pH 4.0. The K_m data was analyzed using Sigma Plot under Michaelis Menten conditions (Table 2.3).

Homology Modeling Using DeepView / Swiss PdbViewer

Three dimensional models of primary sequences of dGMIIb (NP_650494) and SfMII (AAB62719) were built based on the solved structure of dGMII (3CZN) as a template structure (or scaffold) in Swiss PdbViewer (Guex and Peitsch 1997). Using Swiss PdbViewer, the dGMII structure was loaded as a template structure and the target sequence (primary protein sequence to be modeled) was

loaded into the program and initially aligned to the template sequence within the program. The preliminary 3D structure was then submitted to the Swiss Model server. Log files of the failed modeling attempts were used to edit the target sequence and eliminate problematic loop regions. The edited target sequence was then resubmitted for modeling until a successful 3D model was produced. The flanking residues of regions where amino acids were deleted to construct the final 3D model can be seen in the sequence alignment (Figure 2.7.1) and models (Figures 2.7.1 and 2.7.2) highlighted in red.

Swiss PdbViewer was also used to superimpose the previously solved structure of bLysMan (1O7D) to the dGMII structure (3CZN) for structural comparison using the Magic Fit option. Magic Fit compares primary sequences of the two molecules using PAM matrix (PAM 200), which selects the best matching fragments of amino acid pairs and based on that selection, superimposes the molecules. MacPymol was used for the analysis of the aligned structures and homology models as well as for image production.

REFERENCES

- Bischoff, J., K. Moremen, et al. (1990). "Isolation, characterization, and expression of cDNA encoding a rat liver endoplasmic reticulum alpha-mannosidase." J Biol Chem **265**(28): 17110-7.
- Bonay, P. and R. C. Hughes (1991). "Purification and characterization of a novel broad-specificity (alpha 1----2, alpha 1----3 and alpha 1----6) mannosidase from rat liver." Eur J Biochem **197**(1): 229-38.
- Chen, W., J. Roth, et al. (1992). "Subcellular distribution in rat liver of a novel broad-specificity (alpha 1----2, alpha 1----3 and alpha 1----6) mannosidase active on oligomannose glycans." Eur J Biochem **205**(1): 399-407.
- Bourne, Y. and B. Henrissat (2001). "Glycoside hydrolases and glycosyltransferases: families and functional modules." Curr Opin Struct Biol **11**(5): 593-600.
- Chen, W., D. A. Kuntz, et al. (2006). "Synthesis, enzymatic activity, and X-ray crystallography of an unusual class of amino acids." Bioorg Med Chem **14**(24): 8332-40.
- Chen, W. and B. M. Pinto (2007). "Synthesis of aza- and thia-spiroheterocycles and attempted synthesis of spiro sulfonium compounds related to salacinol." Carbohydr Res **342**(15): 2163-72.
- Dennis, J. W., M. Granovsky, et al. (1999). "Glycoprotein glycosylation and cancer progression." Biochim Biophys Acta **1473**(1): 21-34.

- Englebienne, P., H. Fiaux, et al. (2007). "Evaluation of docking programs for predicting binding of Golgi alpha-mannosidase II inhibitors: a comparison with crystallography." Proteins **69**(1): 160-76.
- Grard, T., V. Herman, et al. (1996). "Oligomannosides or oligosaccharide-lipids as potential substrates for rat liver cytosolic alpha-D-mannosidase." Biochem J **316 (Pt 3)**: 787-92.
- Guex, N. and M. C. Peitsch (1997). "SWISS-MODEL and the Swiss-PdbViewer: an environment for comparative protein modeling." Electrophoresis **18**(15): 2714-23.
- Hase, S. (1994). "High-performance liquid chromatography of pyridylaminated saccharides." Methods Enzymol **230**: 225-37.
- Henrissat, B. (1991). "A classification of glycosyl hydrolases based on amino acid sequence similarities." Biochem J **280 (Pt 2)**: 309-16.
- Henrissat, B. (1998). "Glycosidase families." Biochem Soc Trans **26**(2): 153-6.
- Henrissat, B. and A. Bairoch (1993). "New families in the classification of glycosyl hydrolases based on amino acid sequence similarities." Biochem J **293 (Pt 3)**: 781-8.
- Henrissat, B. and A. Bairoch (1996). "Updating the sequence-based classification of glycosyl hydrolases." Biochem J **316 (Pt 2)**: 695-6.
- Henrissat, B. and G. Davies (1997). "Structural and sequence-based classification of glycoside hydrolases." Curr Opin Struct Biol **7**(5): 637-44.
- Karaveg, K., A. Siriwardena, et al. (2005). "Mechanism of class 1 (glycosylhydrolase family 47) {alpha}-mannosidases involved in N-glycan

- processing and endoplasmic reticulum quality control." J Biol Chem **280**(16): 16197-207.
- Kawar, Z., K. Karaveg, et al. (2001). "Insect cells encode a class II alpha-mannosidase with unique properties." J Biol Chem **276**(19): 16335-40.
- Kawatkar, S. P., D. A. Kuntz, et al. (2006). "Structural basis of the inhibition of golgi alpha-mannosidase II by mannosatin A and the role of the thiomethyl moiety in ligand-protein interactions." J Am Chem Soc **128**(25): 8310-9.
- Kumar, N. S., D. A. Kuntz, et al. (2008). "Binding of sulfonium-ion analogues of di-epi-swainsonine and 8-epi-lentiginosine to Drosophila Golgi alpha-mannosidase II: the role of water in inhibitor binding." Proteins **71**(3): 1484-96.
- Kuntz, D. A., C. A. Tarling, et al. (2008). "Structural analysis of Golgi alpha-mannosidase II inhibitors identified from a focused glycosidase inhibitor screen." Biochemistry **47**(38): 10058-68.
- Kuntz, D. A., W. Zhong, et al. (2009). "The molecular basis of inhibition of Golgi alpha-mannosidase II by mannosatin A." Chembiochem **10**(2): 268-77.
- Li, B., S. P. Kawatkar, et al. (2004). "Inhibition of Golgi mannosidase II with mannosatin A analogues: synthesis, biological evaluation, and structure-activity relationship studies." Chembiochem **5**(9): 1220-7.
- Liao, Y. F., A. Lal, et al. (1996). "Cloning, expression, purification, and characterization of the human broad specificity lysosomal acid alpha-mannosidase." J Biol Chem **271**(45): 28348-58.

- Mcllvaine, T. C. (1921). Journal of Biological Chemistry **49**: 183-186.
- Merkle, R. K., Y. Zhang, et al. (1997). "Cloning, expression, purification, and characterization of the murine lysosomal acid alpha-mannosidase." Biochim Biophys Acta **1336**(2): 132-46.
- Misago, M., Y. F. Liao, et al. (1995). "Molecular cloning and expression of cDNAs encoding human alpha-mannosidase II and a previously unrecognized alpha-mannosidase IIx isozyme." Proc Natl Acad Sci U S A **92**(25): 11766-70.
- Monis, E., P. Bonay, et al. (1987). "Characterization of a mannosidase acting on alpha 1----3- and alpha 1----6-linked mannose residues of oligomannosidic intermediates of glycoprotein processing." Eur J Biochem **168**(2): 287-94.
- Moremen, K. W. (2000). -Mannosidases in Asparagine linked Oligosaccharide Processing and Catabolism, Wiley and Sons.
- Moremen, K. W. (2002). "Golgi alpha-mannosidase II deficiency in vertebrate systems: implications for asparagine-linked oligosaccharide processing in mammals." Biochim Biophys Acta **1573**(3): 225-35.
- Moremen, K. W. and O. Touster (1986). "Topology of mannosidase II in rat liver Golgi membranes and release of the catalytic domain by selective proteolysis." J Biol Chem **261**(23): 10945-51.
- Moremen, K. W., O. Touster, et al. (1991). "Novel purification of the catalytic domain of Golgi alpha-mannosidase II. Characterization and comparison with the intact enzyme." J Biol Chem **266**(25): 16876-85.

- Nilssen, O., T. Berg, et al. (1997). "alpha-Mannosidosis: functional cloning of the lysosomal alpha-mannosidase cDNA and identification of a mutation in two affected siblings." Hum Mol Genet **6**(5): 717-26.
- Numao, S., D. A. Kuntz, et al. (2003). "Insights into the mechanism of Drosophila melanogaster Golgi alpha-mannosidase II through the structural analysis of covalent reaction intermediates." J Biol Chem **278**(48): 48074-83.
- Oh-Eda, M., H. Nakagawa, et al. (2001). "Overexpression of the Golgi-localized enzyme alpha-mannosidase IIx in Chinese hamster ovary cells results in the conversion of hexamannosyl-N-acetylchitobiose to tetramannosyl-N-acetylchitobiose in the N-glycan-processing pathway." Eur J Biochem **268**(5): 1280-8.
- Park, C., L. Meng, et al. (2005). "Characterization of a human core-specific lysosomal {alpha}1,6-mannosidase involved in N-glycan catabolism." J Biol Chem **280**(44): 37204-16.
- Schmidt, A., A. Schlacher, et al. (1998). "Structure of the xylanase from *Penicillium simplicissimum*." Protein Sci **7**(10): 2081-8.
- Segal, I. H. (1993). Enzyme Kinetics: Behavior and Analysis of Rapid Equilibrium and Steady-State Enzyme Systems, John Wiley & Sons, Inc.
- Shah, N., D. A. Kuntz, et al. (2003). "Comparison of kifunensine and 1-deoxymannojirimycin binding to class I and II alpha-mannosidases demonstrates different saccharide distortions in inverting and retaining catalytic mechanisms." Biochemistry **42**(47): 13812-6.

- Shah, N., D. A. Kuntz, et al. (2008). "Golgi alpha-mannosidase II cleaves two sugars sequentially in the same catalytic site." Proc Natl Acad Sci U S A **105**(28): 9570-5.
- Siriwardena, A., H. Strachan, et al. (2005). "Potent and selective inhibition of class II alpha-D-mannosidase activity by a bicyclic sulfonium salt." ChemBiochem **6**(5): 845-8.
- Tulsiani, D. R., T. M. Harris, et al. (1982). "Swainsonine inhibits the biosynthesis of complex glycoproteins by inhibition of Golgi mannosidase II." J Biol Chem **257**(14): 7936-9.
- Vallee, F., F. Lipari, et al. (2000). "Crystal structure of a class I alpha1,2-mannosidase involved in N-glycan processing and endoplasmic reticulum quality control." Embo J **19**(4): 581-8.
- van den Elsen, J. M., D. A. Kuntz, et al. (2001). "Structure of Golgi alpha-mannosidase II: a target for inhibition of growth and metastasis of cancer cells." Embo J **20**(12): 3008-17.
- Wen, X., Y. Yuan, et al. (2005). "A combined STD-NMR/molecular modeling protocol for predicting the binding modes of the glycosidase inhibitors kifunensine and salacinol to Golgi alpha-mannosidase II." Biochemistry **44**(18): 6729-37.
- Weng, S. and R. G. Spiro (1993). "Demonstration that a kifunensine-resistant alpha-mannosidase with a unique processing action on N-linked oligosaccharides occurs in rat liver endoplasmic reticulum and various cultured cells." J Biol Chem **268**(34): 25656-63.

- Weng, S. and R. G. Spiro (1996). "Endoplasmic reticulum kifunensine-resistant alpha-mannosidase is enzymatically and immunologically related to the cytosolic alpha-mannosidase." Arch Biochem Biophys **325**(1): 113-23.
- Winchester, B., S. al Daher, et al. (1993). "The structural basis of the inhibition of human alpha-mannosidases by azafuranose analogues of mannose." Biochem J **290 (Pt 3)**: 743-9.
- Yamashiro, K., H. Itoh, et al. (1997). "Purification and characterization of neutral alpha-mannosidase from hen oviduct: studies on the activation mechanism of Co²⁺." J Biochem (Tokyo) **122**(6): 1174-81.
- Zhong, W., D. A. Kuntz, et al. (2008). "Probing the substrate specificity of Golgi alpha-mannosidase II by use of synthetic oligosaccharides and a catalytic nucleophile mutant." J Am Chem Soc **130**(28): 8975-83.

CHAPTER 3

DISCUSSION

We have shown that *Drosophila melanogaster* Golgi Mannosidase IIb (dGMIIb) is a ~140-145 kDa GH38 α -mannosidase with characteristics similar to other enzymes in this family. These characteristics include a relatively large protein molecular weight, a region of conserved sequence predominantly associated with catalytic domain residues, the ability to cleave mannose residues from the non-reducing terminus of N-glycans, sensitivity to furanose transition state analogues like swainsonine (SWA) and 1,4-dideoxy-1,4-imino-D-mannitol (DIM), and a cation requirement for catabolism (Henrissat and Bairoch 1996). Sequence analysis of the PFAM signature peptide sequence called Glyco_hydro_38, that exists in the N-terminal region of GH38 mannosidases (Henrissat 1998), revealed that *Drosophila melanogaster* has protein representatives in the Golgi Mannosidase and Broad Specificity Lysosomal Mannosidase clades (with a larger representation in the latter clade), but does not have representatives in the Heterogeneous Ancestral or recently defined Core Specific Lysosomal Mannosidase clade. dGMIIb is a member of the Golgi Mannosidase clade rooted closely to *Spodoptera frugiperda* Golgi Mannosidase II (SfMII), a previously characterized Golgi mannosidase (Kawar, Karaveg et al.

2001). dGMIIb is similar in substrate specificity to SfMII in that it preferentially cleaves $\text{Man}_5\text{GlcNAc}_2\text{-PA}$ to $\text{Man}_3\text{GlcNAc}_2\text{-PA}$, but cleaves $\text{GlcNAcMan}_5\text{GlcNAc}_2\text{-PA}$ with poor efficiency, is stimulated by cobalt, is sensitive to inhibition by swainsonine, and has a neutral pH optimum. This enzyme is also sensitive to DIM and more weakly inhibited by kifunensine (KIF) and deoxymannojirimycin (DMNJ), which has not been tested with SfMII. Thus, dGMII is likely an ortholog of SfMII.

Most processed N-linked glycans found in insects are paucimannosidic, or truncated high mannose structures. These glycans consist of a tri- or tetra-mannosylchitobiosyl core structure that often includes core fucosylation ($\text{Man}_4\text{GlcNAc}_2$ (M4N2) or $\text{Man}_3\text{GlcNAc}_2$ (M3N2) with or without an α 1,6-linked fucose (F^6) and/or an α 1,3-linked fucose (F^3)). The steps required in creating these paucimannosidic glycans require the prior action of GnTI (Sarkar, Leventis et al. 2006).

Due to the fact that the majority of paucimannosidic glycans do not have a non-reducing terminal GlcNAc residue, an N-Acetylglucosaminidase was hypothesized to be involved in N-linked glycan processing in flies. A protein termed FDL was found to hydrolyze GlcNAc (N) specifically attached to the α 1,3-linked mannose of the core pentasaccharide N2M3N2 as well as NM3N2 (Leonard, Rendic et al. 2006). NM3N2F^6 (where GlcNAc is attached to the α 1,3-linked mannose branch) is a major glycan in FDL null flies. The residual amount of M3N2 and M3N2F^6 paucimannosidic glycans in both FDL null and GnTI null flies implicates a GnTI independent mannosidase. We believe that dGMIIb is the

GnTI independent enzyme in the N-glycan processing pathway, which can bypass the GMII step (although with reduced efficiency) and is the cause of residual paucimannosidic glycans seen in these mutants. Further research must be conducted to confirm this hypothesis in null flies. However, the data indicate that dGMIIb can cleave $\text{Man}_5\text{GlcNAc}_2$ to $\text{Man}_3\text{GlcNAc}_2$ independent of the action of GnTI.

There are a variety of genetic tools available that can be used in determining the importance or purpose of dGMIIb in *Drosophila melanogaster*. Transgenic fly stocks with P-element insertions can be obtained from *Drosophila* stock centers (Tweedie, Ashburner et al. 2009) to create populations that represent a mutation in the gene that encodes dGMIIb. P-element insertions can create a disruption in the transcription of *dGMIIb* or may be used to create excision mutants that can eliminate the whole gene. These mutations could lead to a loss of function of the dGMIIb protein creating a dGMIIb null phenotype. A dGMIIb null may cause a loss of paucimannosidic glycans. However, assuming that dGMIIb is an alternate bypass to dGMII, creating a null organism may produce a minor overall affect on the phenotype. The change seen in the null phenotype would depend on where and when dGMIIb is expressed. The creation of single and double null organisms (dGMIIb, dGMII, dGMIIb/dGMII, dGMIIb/GnTI, dGMIIb/FDL) would lead to a better conclusion of whether or not dGMIIb is the alternative bypass to GMII in *Drosophila*. The disappearance of paucimannosidic structures in double null organisms followed by a reappearance of paucimannosidic structures with the overexpression of dGMIIb would confirm

that dGMIIb is the alternate bypass to dGMII and is responsible for the residual paucimannosidic structures seen in GnTI and FDL null flies. RNAi transgenic flies are also available from *Drosophila* stock centers (Dietzl, Chen et al. 2007) which can be used to determine loss of function phenotypes of dGMIIb. RNAi transgenics can silence the transcription of a gene in a tissue specific manner when paired with promoters that are specific for activating elements only available in certain tissues.

dGMIIb is an ortholog of the well-characterized *Drosophila* Golgi Mannosidase II (dGMII). The preferred natural substrate for dGMII is GlcNAcMan₅GlcNAc₂ asparagine (N)-linked to proteins, whereas the preferred natural substrate for dGMIIb is Man₅GlcNAc₂. *Drosophila melanogaster* Golgi α -mannosidase II (dGMII) cloning and sequence analysis was first performed in the Roberts' lab (Foster, Yudkin et al. 1995) and further characterized for enzymatic characteristics (Rabouille, Kuntz et al. 1999). The dGMII sequence was cloned into a pProtA expression vector to create a Prot-dGMII fusion and the presence of α -mannosidase activity was verified using the synthetic substrate pNP-Man for the enzymes bound to the IgG sepharose beads. The optimal pH for dGMII was found to be 5.7 in these studies, which is similar to other GMIIs (Kaushal, Szumilo et al. 1990; Moremen, Touster et al. 1991; Ren, Castellino et al. 1997). dGMII was strongly inhibited by SWA (IC₅₀ = 12 - 20 nM). dGMII was found to have no metal ion dependency or activation when tested with MgCl₂, CaCl₂, MnCl₂, ZnSO₄, NiSO₄, BaCl₂, LiCl₂, and NaCl up to 10 mM – EDTA also had no effect on activity under these same conditions. However, dGMII was strongly

inhibited by CuSO_4 with an IC_{50} of 25 μM . In our studies, CuCl_2 had little to no effect on the activity of dGMII. This may be explained by the different assay conditions used in the two different studies, such as stripping of the enzyme with EDTA before performing metal ion analysis, using pNP-Man as a synthetic substrate instead of 4MU-Man, using a fusion protein bound to beads versus using a non-bound, non-fusion of the protein, or using CuSO_4 instead of CuCl_2 . During purification in our studies there was a 15% increase in total activity seen after the first Phenyl Sepharose purification step, which may be explained by removal of inhibiting contaminants including 500 μM CuSO_4 in the conditioned induction media.

dGMII was recently crystallized as a nucleophilic mutant (D204A) with its natural substrate $\text{GlcNAcMan}_5\text{GlcNAc}$ bound in a cleft made up of three sugar binding sites for the large flexible glycan; the active site, the holding site, and the anchoring site (Shah, Kuntz et al. 2008). There is a high sequence conservation of active site residues in GH38 enzymes, which suggests a similar mechanism for hydrolyzing mannose residues. The high sequence conservation, similar mechanisms of action, and similar inhibition characteristics provide difficulty for finding selective inhibitors. The key to developing selective GH38 mannosidase inhibitors is a more complete understanding of the unique substrate specificities of the enzyme isoforms. For GMII, this means fully characterizing the holding and anchoring sites in substrate recognition and contrasting these substrate binding elements with related enzymes that have different substrate specificities. The dGMIIb structural model generated in this body of work displays a significant

difference in the “anchoring site” compared to the dGMII co-crystal structure. Although the dGMIIb model appears to have a pocket in the vicinity of the “anchoring site”, it does not have key residues found in dGMII that either directly interact with the GlcNAc residue (His273) or stabilize the GlcNAc residue (Tyr267) in the anchoring site. Site directed mutagenesis of dGMIIb and dGMII could be performed to confirm amino acid residues involved in anchoring GlcNAc. A mutation of dGMIIb to include the His and Tyr residue thought to be important in GlcNAc binding in dGMII may lead to a change in substrate specificity from $\text{Man}_5\text{GlcNAc}_2$ to $\text{GlcNAcMan}_5\text{GlcNAc}_2$, dGMII’s natural substrate. These residues could also be mutated in dGMII to show a loss of function by either mutating the residues to small, truncated residues like Ala, or large, bulky residues like Trp, that would result in a loss of hydrogen bonding due to the absence or obstruction of the anchoring site preventing GlcNAc binding. X-ray crystallization of dGMIIb would also contribute to our understanding of the differences between dGMIIb and dGMII’s substrate specificity in the anchoring region. The differences in this region could be key in providing the unique substrate specificity for dGMII in glycan processing. Characterization of inhibitors based on the differences between dGMIIb and dGMII in the anchoring site could then be tested against human GMII and human LysMan to aid in constructing a specific inhibitor for human GMII for use in cancer therapeutics..

REFERENCES

- Dietzl, G., D. Chen, et al. (2007). "A genome-wide transgenic RNAi library for conditional gene inactivation in *Drosophila*." Nature **448**(7150): 151-6.
- Foster, J. M., B. Yudkin, et al. (1995). "Cloning and sequence analysis of GmII, a *Drosophila melanogaster* homologue of the cDNA encoding murine Golgi alpha-mannosidase II." Gene **154**(2): 183-6.
- Henrissat, B. (1998). "Glycosidase families." Biochem Soc Trans **26**(2): 153-6.
- Henrissat, B. and A. Bairoch (1996). "Updating the sequence-based classification of glycosyl hydrolases." Biochem J **316 (Pt 2)**: 695-6.
- Kaushal, G. P., T. Szumilo, et al. (1990). "Purification to homogeneity and properties of mannosidase II from mung bean seedlings." Biochemistry **29**(8): 2168-76.
- Kawar, Z., K. Karaveg, et al. (2001). "Insect cells encode a class II alpha-mannosidase with unique properties." J Biol Chem **276**(19): 16335-40.
- Leonard, R., D. Rendic, et al. (2006). "The *Drosophila* fused lobes gene encodes an N-acetylglucosaminidase involved in N-glycan processing." J Biol Chem **281**(8): 4867-75.
- Moremen, K. W., O. Touster, et al. (1991). "Novel purification of the catalytic domain of Golgi alpha-mannosidase II. Characterization and comparison with the intact enzyme." J Biol Chem **266**(25): 16876-85.
- Rabouille, C., D. A. Kuntz, et al. (1999). "The *Drosophila* GMII gene encodes a Golgi alpha-mannosidase II." J Cell Sci **112 (Pt 19)**: 3319-30.

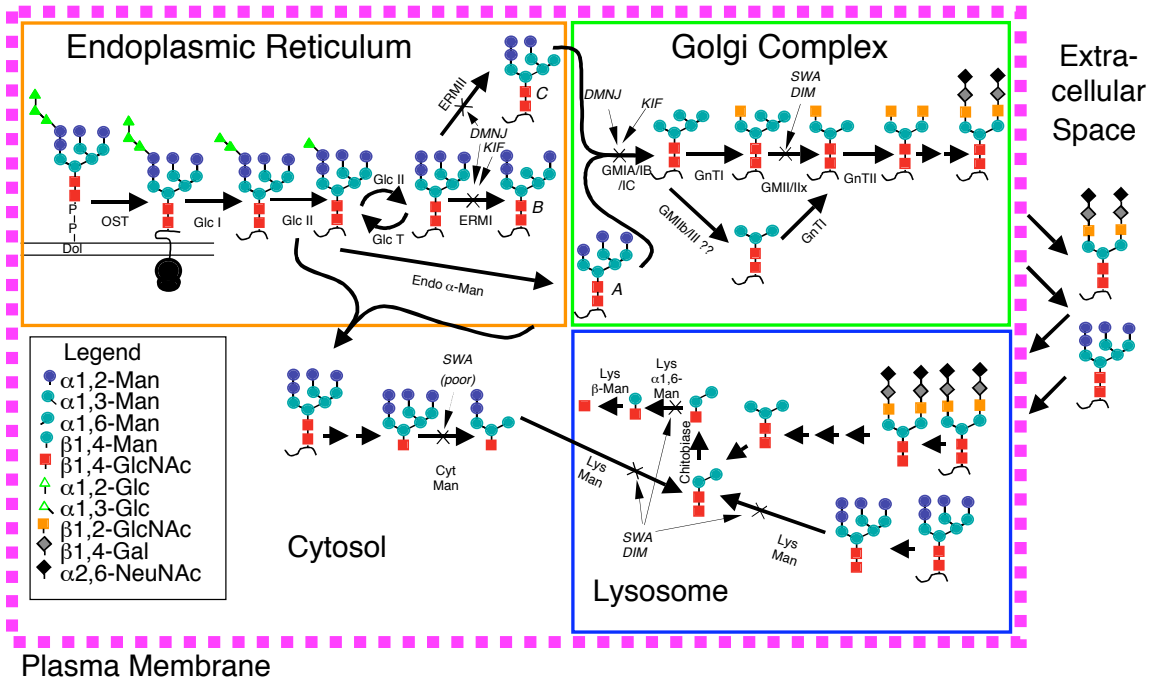
- Ren, J., F. J. Castellino, et al. (1997). "Purification and properties of alpha-mannosidase II from Golgi-like membranes of baculovirus-infected *Spodoptera frugiperda* (IPLB-SF-21AE) cells." Biochem J **324 (Pt 3)**: 951-6.
- Sarkar, M., P. A. Leventis, et al. (2006). "Null mutations in *Drosophila* N-acetylglucosaminyltransferase I produce defects in locomotion and a reduced life span." J Biol Chem **281**(18): 12776-85.
- Shah, N., D. A. Kuntz, et al. (2008). "Golgi alpha-mannosidase II cleaves two sugars sequentially in the same catalytic site." Proc Natl Acad Sci U S A **105**(28): 9570-5.
- Tweedie, S., M. Ashburner, et al. (2009). "FlyBase: enhancing *Drosophila* Gene Ontology annotations." Nucleic Acids Res **37**(Database issue): D555-9.

Figure 1.1: Partial Scheme for Mammalian N-linked Biosynthesis and Catabolism

This figure represents a subset of steps in mammalian N-linked biosynthesis and catabolism. A $\text{Glc}_3\text{Man}_9\text{GlcNAc}_2$ is transferred from a dolichol lipid linked precursor to a newly formed protein in the Endoplasmic Reticulum (ER) (orange solid line). The glycan then undergoes a series of glucose and mannose trimming steps to produce a $\text{Man}_8\text{GlcNAc}_2$ structure. The glycan is cleaved further in the Golgi complex (green solid line) by Golgi Mannosidase IA/IB/IC to a $\text{Man}_5\text{GlcNAc}_2$ structure. At this point, GlcNAc transferase I adds one GlcNAc residue to the α -1,3 core mannose branch, and in doing so creates the substrate for Golgi Mannosidase II, an enzyme important to this body of work. There have been implications of a Golgi mannosidase IIb that can cleave the $\text{Man}_5\text{GlcNAc}_2$ glycan without the addition of a GlcNAc residue, but so far this function has only been found in insects. Golgi mannosidase II cleaves $\text{GlcNAcMan}_5\text{GlcNAc}_2$ to a $\text{GlcNAcMan}_3\text{GlcNAc}_2$ structure, which is then further modified in the Golgi by other glycosyltransferases. Proteins that fail to fold properly in the ER are transferred to the cytosol, enclosed by the dotted pink line representing the plasma membrane, where a cytosolic mannosidase cleaves 4 mannose residues to create a $\text{Man}_5\text{GlcNAc}_2$ glycan from a $\text{Man}_9\text{GlcNAc}_2$ glycan. The lysosome (solid blue line) catabolizes glycans from the cytosol and extracellular space into simple sugars. Lysosomal mannosidase can cleave $\text{Man}_9\text{GlcNAc}_2$ to $\text{Man}_2\text{GlcNAc}_2$ but prefers the $\text{Man}_5\text{GlcNAc}_2$ glycan as a substrate. The $\text{Man}_2\text{GlcNAc}_2$ is degraded into simple sugars by a chitobiase, α 1,6 lysosomal mannosidase, and lysosomal β mannosidase, respectively. Enzymes are abbreviated as follows: OST, oligosaccharide transferase; Glc I, glucosidase I; Glc II, glucosidase II, Glc T, glycosyltransferase; UDP-Glc, glycoprotein glucosyltransferase; ER Man I, ER mannosidase I; GMIA/IB, Golgi mannosidases IA and IB; GnTI, GlcNAc transferase I; GMII, Golgi mannosidase II; GMIIb/III, Golgi mannosidase IIb or III. Processing inhibitors that block enzyme reactions are indicated by an X and a thin arrow with the following abbreviations: DMNJ, 1-deoxymannojirimycin; KIF, kifunensine; SWA, swainsonine; DIM, 1-4-di-deoxymannitol. The legend in the lower left indicates oligosaccharide residues and their linkages.

1.1

Glycoprotein Biosynthesis



Glycoprotein Catabolism

Table 1.1: Characteristics of Eukaryotic Processing and Catabolic α -Mannosidases.

This table shows known characteristics for the collection of mammalian and selected *Drosophila* GH38 processing and catabolic α -mannosidases. α -Mannose linkages cleaved by each enzyme is indicated as linkage specificity. The limit digestion product is the end product of enzymatic cleavage for each enzyme. Glycans are abbreviated as follows: M_xN_x, where x equals the number of residues of mannose (M) or N-Acetylglucosamine (N). Enzymes are abbreviated as follows: ERMII, ER Mannosidase II; GMII, Golgi mannosidase II; GMIIx, Golgi Mannosidase IIx; dGMIIb, *Drosophila melanogaster* Golgi Mannosidase IIb; dGMII, *Drosophila melanogaster* Golgi Mannosidase; Cyt Man, Cytosolic Mannosidase; Lys Man, Lysosomal Mannosidase; α 1,6-Lys Man, α 1,6-Lysosomal Mannosidase. Processing are inhibitors abbreviated as follows: DMNJ, 1-deoxymannojirimycin; DIM, 1-4-di-deoxy-mannitol, KIF, kifunensine; SWA, swainsonine.

| Eukaryotic Processing and Catabolic Class II α-Mannosidases | | | | | | | | |
|--|-------------------------------|--------------------------------|--------------------------------|--------------------------------|-------------------------------|-------------------------------|-------------------------------|-----------------------------|
| Characteristics | ERMII (rat) | GMII (rat, human) | GMIIx (mouse) | dGMII (fruit fly) | dGMIIb (fruit fly) | Cyt Man (rat) | Lys Man (human) | α 1,6-LysMan (human) |
| Linkage specificity | α 1,2-Man | α 1,3/1,6-Man | α 1,3/1,6-Man | α 1,3/1,6-Man | α 1,3/1,6-Man | α 1,2/1,3/1,6-Man | α 1,2/1,3/1,6-Man | α 1,6-Man |
| Limit digestion product | M ₈ N ₂ | NM ₃ N ₂ | NM ₃ N ₂ | NM ₃ N ₂ | M ₃ N ₂ | M ₈ N ₂ | M ₂ N ₂ | MN |
| Glycosidase Mechanism | ? | retaining | ? | retaining | ? | ? | retaining | ? |
| Localization | ER | Golgi | Golgi | Golgi | Golgi | Cytosol | Lysosome | Lysosome |
| Metal Requirement | none | Zinc | Cobalt activates | Zinc | Cobalt activates | Cobalt activates | none | Cobalt activates |
| Inhibitors | DMNJ, DIM | SWA, DIM | SWA, DIM | SWA, DIM | SWA, DIM | DMNJ, DIM, SWA | SWA, DIM | SWA, DIM |
| Synthetic Substrates | 4MU-Man | 4MU-Man | 4MU-Man | 4MU-Man | 4MU-Man | 4MU-Man | 4MU-Man | 4MU-Man |
| pH Optimum | 6.0-6.5 | 5.0-5.5 | 5.6 | 5.0-5.5 | 5.5-6.0 | 6.0 | 4.0-4.5 | 4.6 |

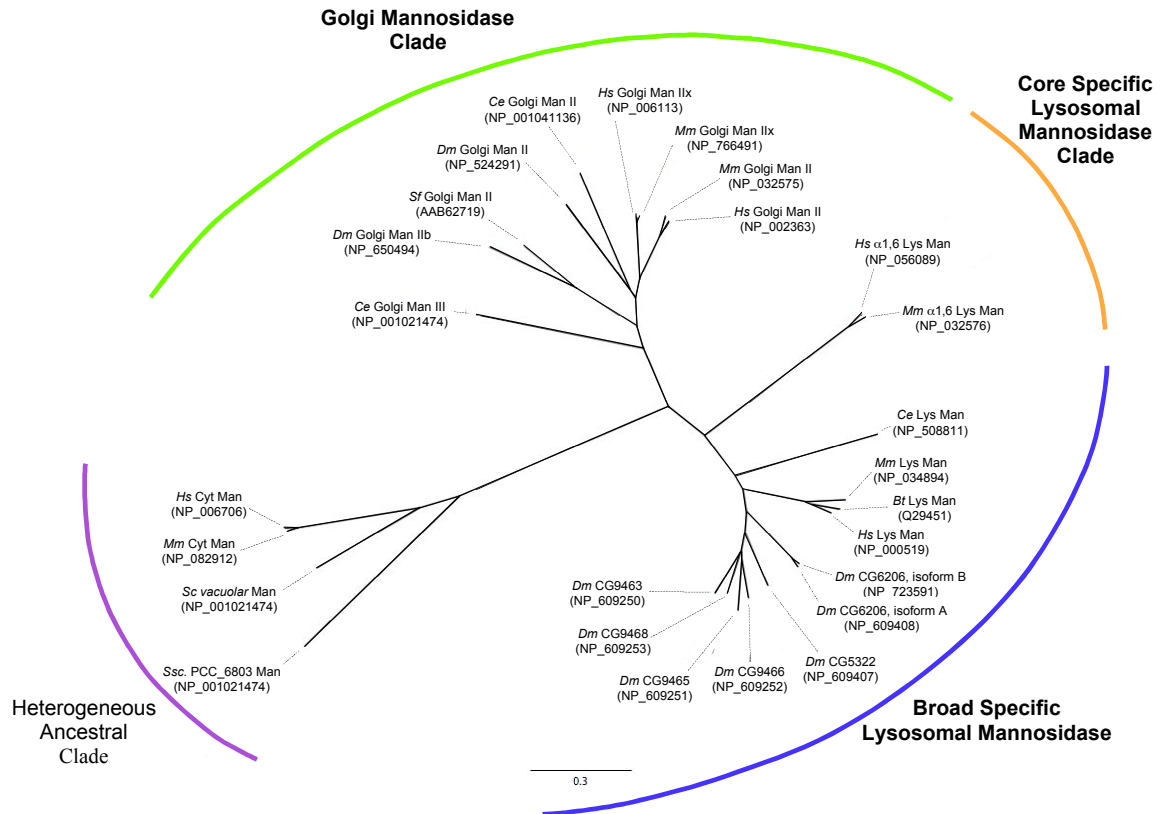


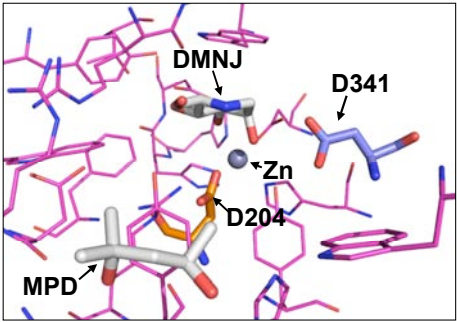
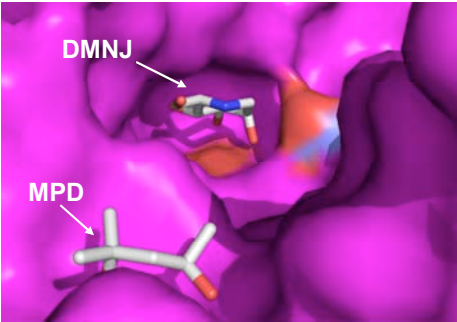
Figure 1.2: Dendrogram of Selected Glycosyl Hydrolase Family 38 Enzymes.

Sequence alignments of GH38 Family members were performed using the ClustalW program and displayed as an unrooted dendrogram using Geneious 4.6.7 Pro/Basic. Genbank accession numbers are shown in parenthesis at the end of each branch. The Golgi Mannosidase clade is represented by a green line, the Core Specific Lysosomal Mannosidase clade is represented by an orange line, the Broad Specificity Lysosomal Mannosidase clade is represented by a blue line, and the Heterogeneous Ancestral clade is represented by a purple line. Abbreviations are as follows: Man, Mannose; Golgi, Golgi Apparatus; ER, Endoplasmic Reticulum; Cyt, Cytosolic; Dm, *Drosophila melanogaster*; Hs, *Homo sapiens*; Bt, *Bos taurus*; Mm, *Mus musculus*; Ce, *Caenorhabditis elegans*; Sf, *Spodotera frugiperda*; Sc, *Saccharomyces cerevisiae*; Ssp, *Sulfolobus solfataricus P2*.

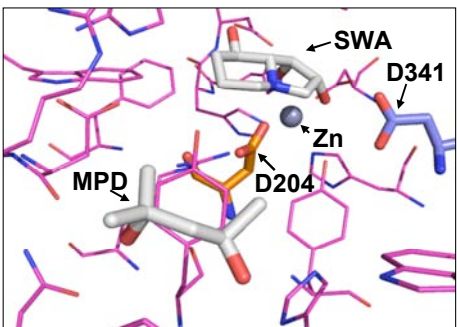
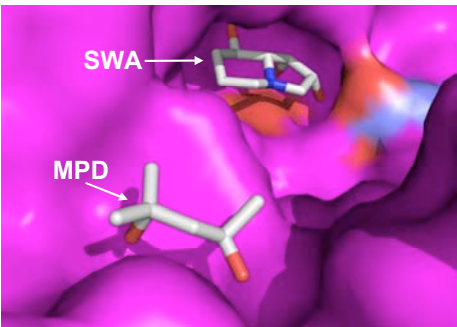
Figure 1.3: Co-crystal Structures of dGMII with Small Inhibitors

Each figure displays a co-crystal of dGMII with a bound ligand in the active site or substrate recognition site. DGMII is colored magenta. The binding site is represented in surface (left) and residues with atoms within 5 Å are represented as lines (right). All atoms of DMNJ, SWA, MPD, and 5FGulF are colored grey and represented as sticks. Zn²⁺ is represented by a dark grey sphere. The catalytic nucleophile, Asp204, is colored orange and represented in stick form. The catalytic acid/base, Asp341, is colored blue. Figure 1.3.1 and 1.3.2 are co-crystals with bound dGMII inhibitors, DMNJ (PDB ID: 1HXK) and SWA (PDB ID: 1HWW) (van den Elsen, Kuntz et al. 2001), respectively. These inhibitors are involved in ionic interactions with the Zn²⁺ ion, which coordinates with the nucleophile, water and surrounding residues to aid in catalysis. MPD is a cryoprotectant captured in the putative anchoring/GlcNAc-binding site. Figure 1.3.3 is a co-crystal of the fluorescent transition state inhibitor, 5FGulF (PDB ID: 1QWN), covalently bound to the catalytic nucleophilic residue, D204 (Numao, Kuntz et al. 2003). This structure demonstrates the covalent glycosyl intermediate transition state for dGMII.

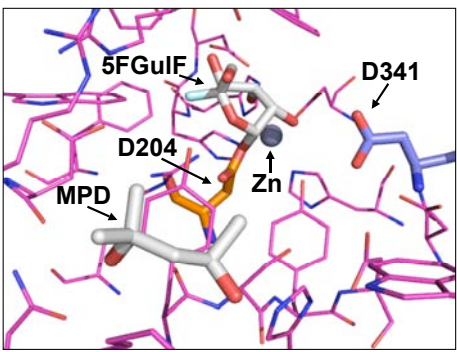
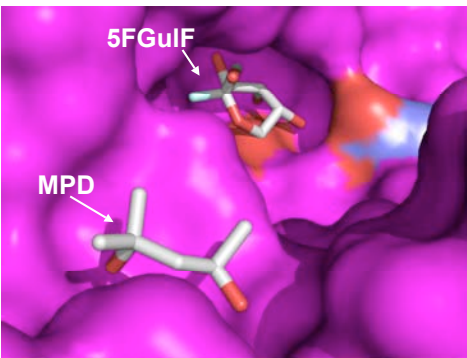
1.3.1



1.3.2



1.3.3



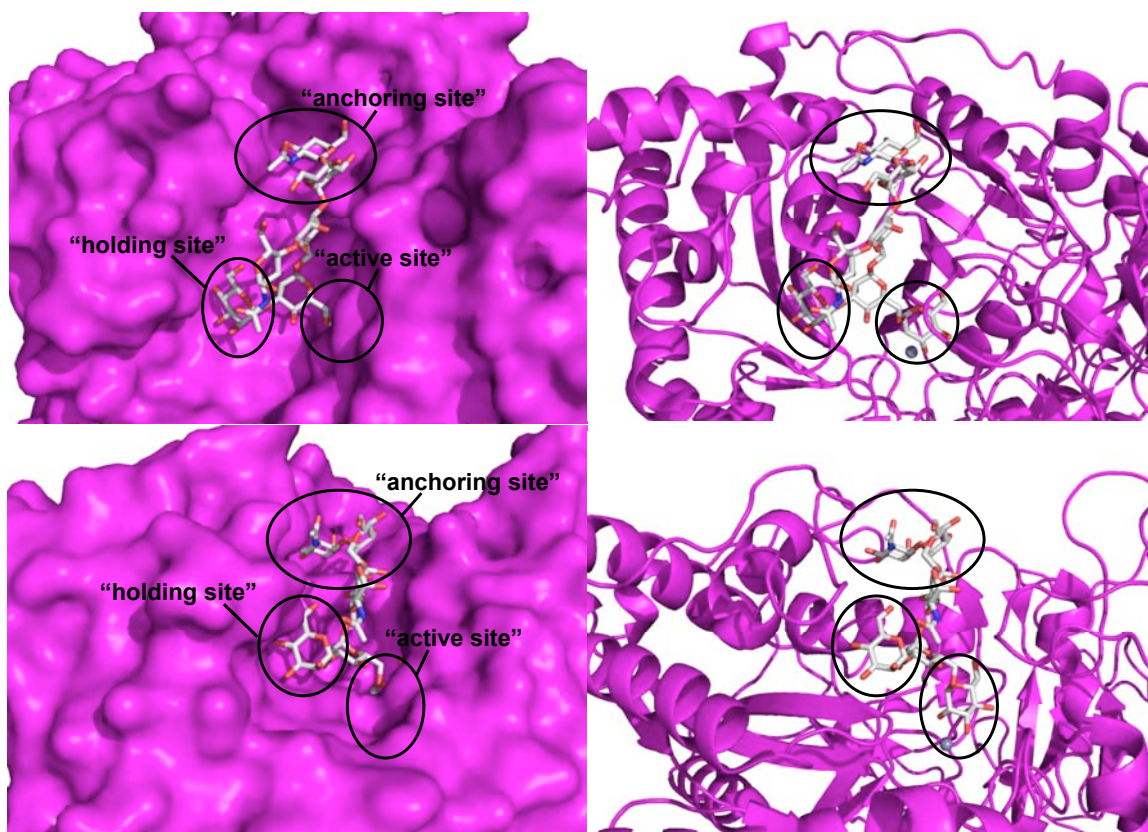


Figure 1.4: Three Binding Pockets for Specific Substrate Interactions with dGMII

Figure 1.4 shows dGMII (magenta) in a surface representation (left) and a cartoon representation (right) in two different orientations to highlight the three binding regions for the GlcNAcMan₅GlcNAc ligand (grey stick figure) for dGMII. A Zn⁺² cation is represented as a dark grey sphere occupying the active site. The “anchoring region”, “holding site”, and “active site” are circled in black and labeled for reference in the right-hand surface representation of dGMII.

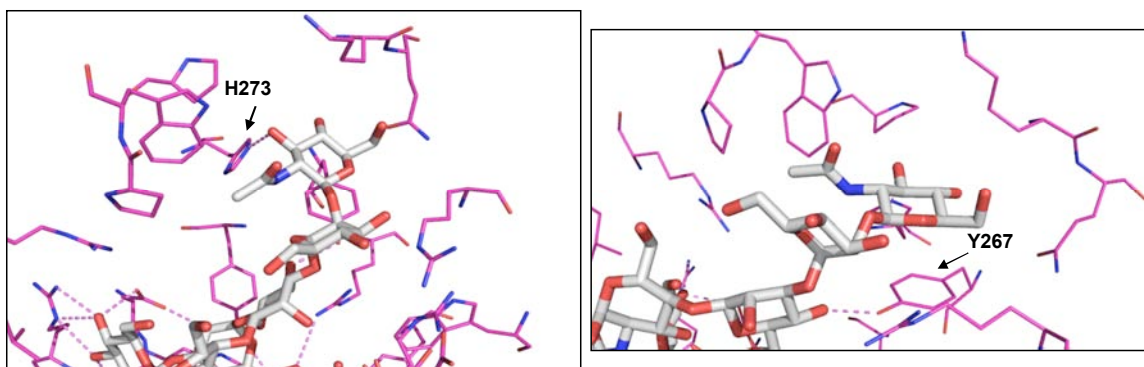


Figure 1.5: The Anchoring Site

Two different orientations display the GlcNAc residue of dGMII's substrate bound in the anchoring site of the co-crystal (3CZN). All residues with atoms within 4 Å. are represented as lines and direct polar contacts between the ligand and protein are indicated by violet dashes. This figure shows the important interactions of H273 and Y267 (indicated by black arrows) and their contribution to the anchoring of the GlcNAc residue. Both proline and tryptophan residues are visible in the upper left hand corner of the left figure and at the top of the right figure, which contribute to the stabilization of the key H273 residue directly involved in hydrogen bonding interactions with GlcNAc.

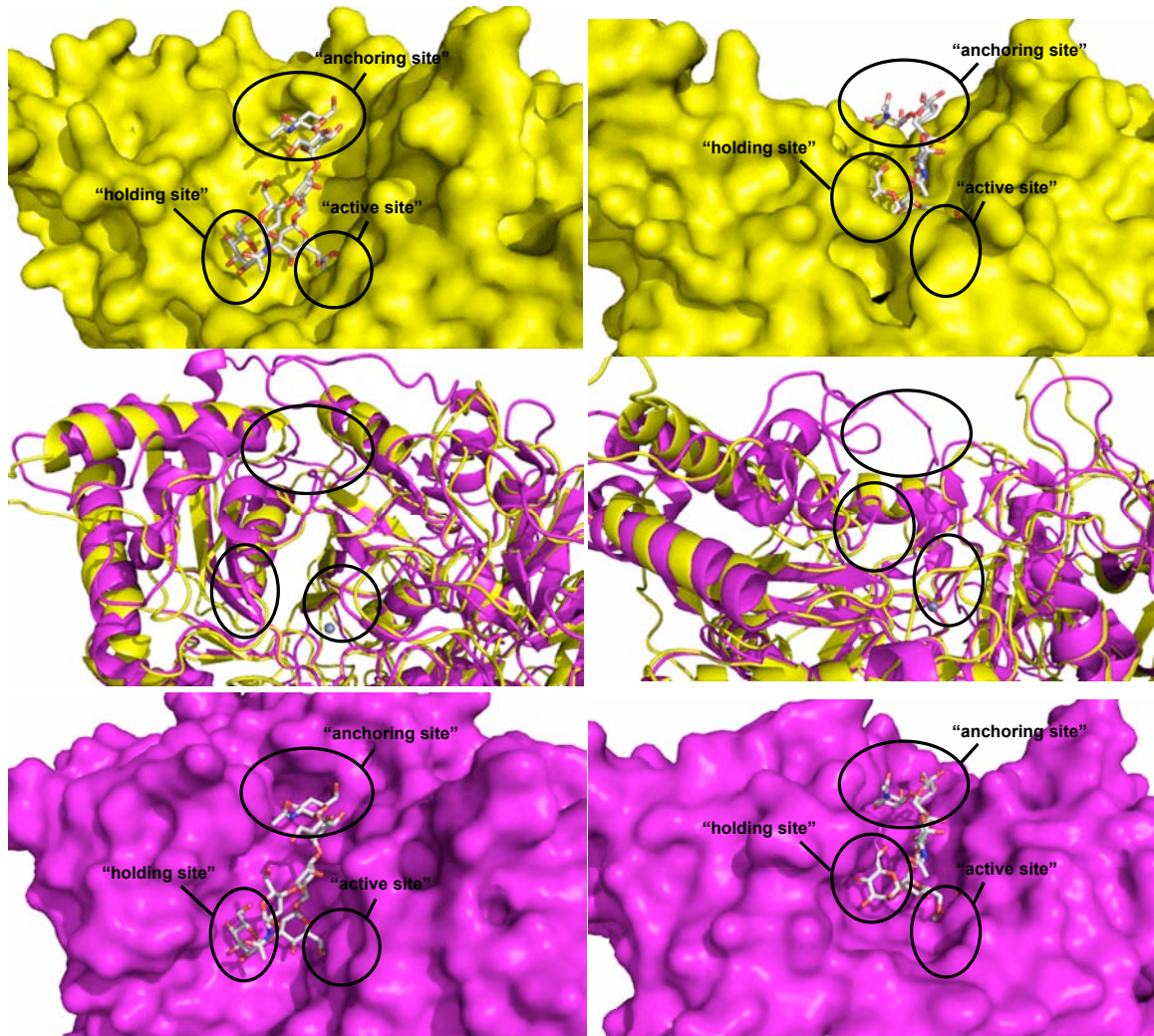
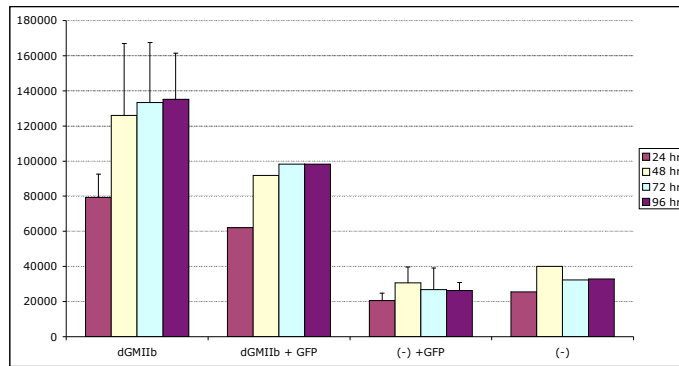


Figure 1.6: Superimposed bLysMan and dGMII

Figure 1.6 shows bLysMan (yellow) and dGMII (magenta) in a surface representations (top and bottom, respectively) and a superimposed cartoon representation (middle) in two different orientations to highlight the three binding regions in the binding pocket of GlcNAcMan₅GlcNAc (grey stick figure) for dGMII. A Zn⁺² cation is represented as a dark grey sphere occupying the active site. The “anchoring region”, “holding site”, and “active site” are circled in black and labeled for reference in the upper and lower panels of the surface representations of the proteins. This figure illustrates the striking difference in the regions of dGMII’s substrate anchoring site.

2.1.1



2.1.2

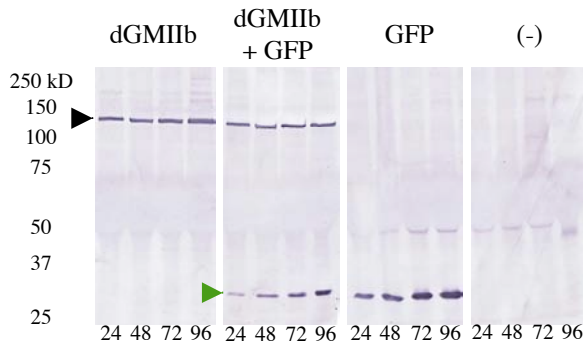


Figure 2.1: 4MU-Man Activity Over Induction Period of Four Days

Figure 2.1.1 shows a bar graph where each grouping of bars represents a co-transfection monitored every 24 hours over a 96 hour period. The legend to the right of the bar graph indicates each time point. DNA plasmid preps used for co-transfections are labeled dGMI Ib for pMT-BiP-V5H/dGMI Ib and GFP for pMT-BiP-V5H/GFP. Transfection controls are indicated by (-) where no dGMI Ib DNA was added to the transfections. All transfections include pCoBlast that imparts antibiotic resistance. Co-transfections involving GFP are indicated by “GFP”. Error bars reflect standard deviations between duplicate transfections. Figure 2.1.2 is a western blot used to visualize the samples shown in figure 2.1.1. A His-AP conjugate antibody was used to detect the His tag in dGMI Ib (black arrow) and GFP (green arrow). The molecular weight marker is depicted in kD units on the left side of the blots labeled “M” in the appropriate lane.

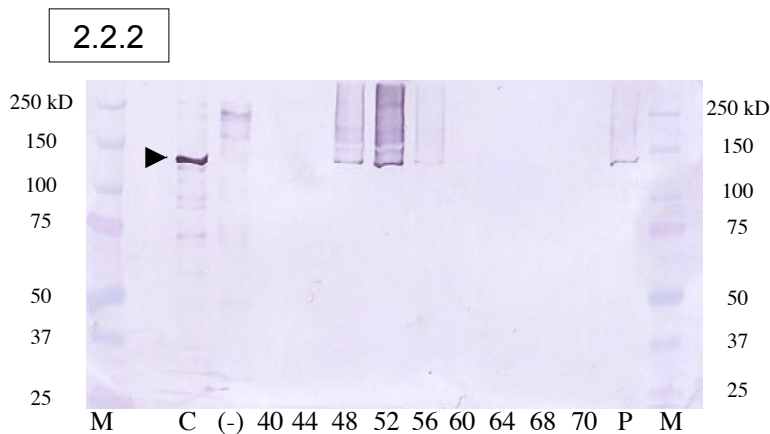
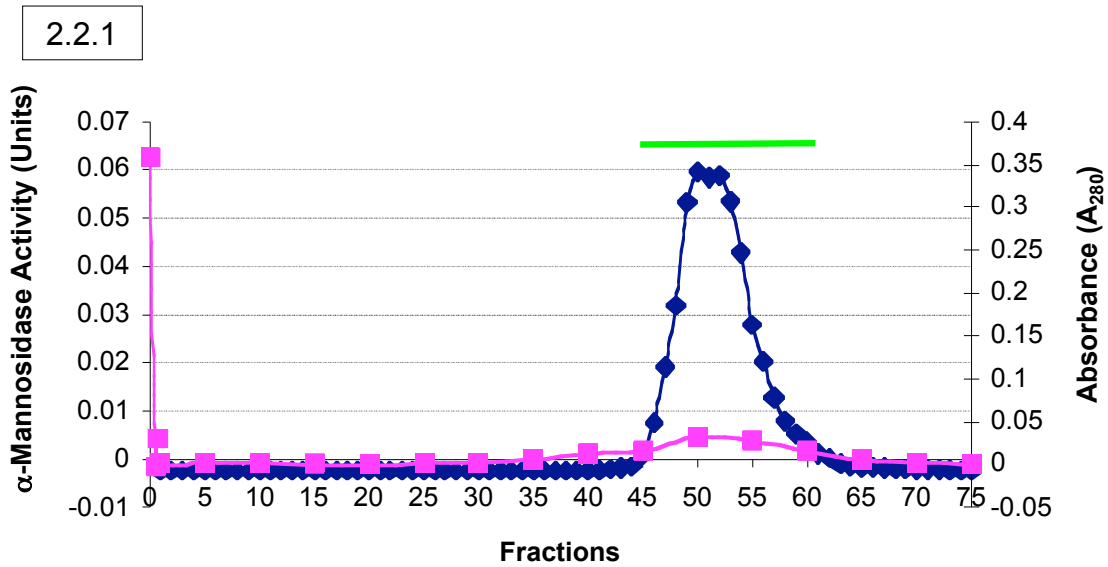
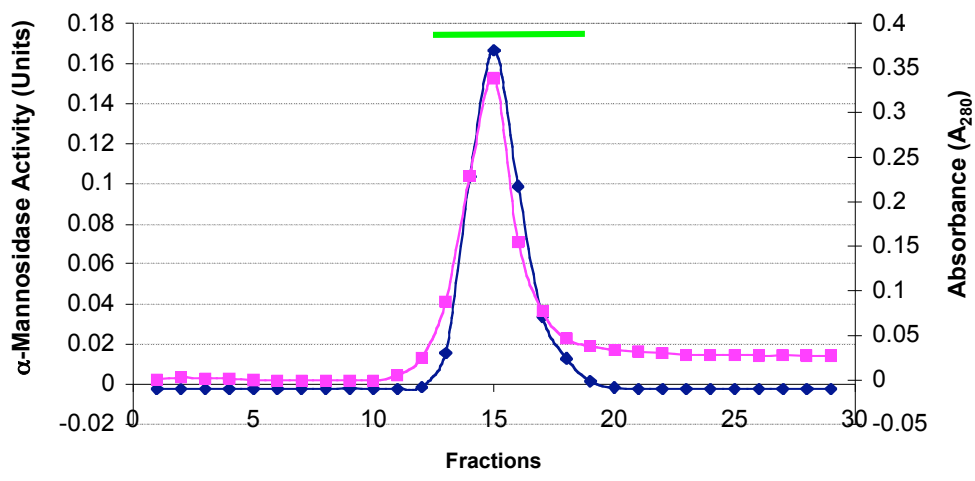


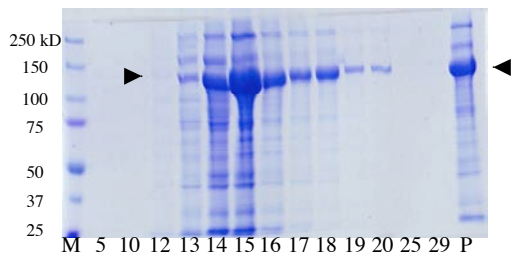
Figure 2.2: Phenyl Sepharose Purification

Figure 2.2.1 is a graph of UV absorbance units (blue diamond line) and mannosidase activity units (pink square line) of each fraction as the protein eluted off of the Phenyl Sepharose column. Fractions collected are indicated by a green line. Figure 2.2.2 is a Western blot with a His-AP conjugate used to visualize the His tag in the dGMIIb construct (black arrow). The numbers below each lane are representative of fractions collected. Abbreviations are as follows: M, molecular weight marker; C, crude protein sample; P, pooled fractions.

2.3.1



2.3.2



2.3.3

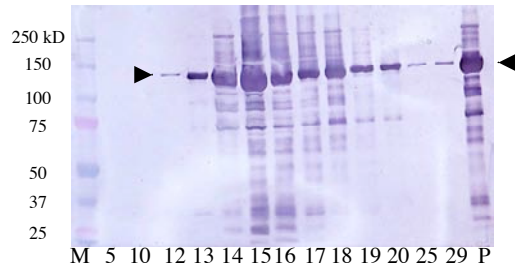


Figure 2.3: Nickel-NTA Purification.

Figure 2.3.1 is a graph of UV absorbance units (blue diamond line) and mannosidase activity units (pink square line) of each fraction as the protein eluted off of the Nickel-NTA column. Fractions collected are indicated by a green line. Figure 2.3.2 is a Coomassie Blue stained SDS-PAGE gel. The dGMIIb construct is indicated by a black arrow. Figure 2.3.3 is a western blot with a His-AP conjugate used to visualize the His tag in the dGMIIb construct (black arrow). The numbers under each lane in 2.3.2 and 2.3.3 are representative of fractions collected. Abbreviations for 2.3.2 and 2.3.3 are as follows: M, molecular weight marker; C, crude protein sample; P, pooled fractions.

Table 2.1 : Protein Purification Table.

This table displays each step of protein purification; how much total protein was present, the units of mannosidase activity (nmoles/min), specific activity, percent yield of starting sample and the fold purification by this purification method. The steps are abbreviated as follows: Crude, secreted dGMIIb into S2 Schneider's medium; PS Pool, fractions pooled after purification using a Phenyl Sepharose column; Ni Pool, fractions pooled after purification using a Nickel-NTA column.

| Step | Protein (mg) | Mannosidase Activity (Units) | Specific Activity (Units/mg) | Yield (%) | Purification (-fold) |
|---------|--------------|------------------------------|------------------------------|-----------|----------------------|
| Crude | 6470 | 263.90 | 0.04 | 100 | 1 |
| PS Pool | 1106 | 302.40 | 0.27 | 115 | 6.70 |
| Ni Pool | 18.33 | 28.29 | 1.5 | 11 | 38 |

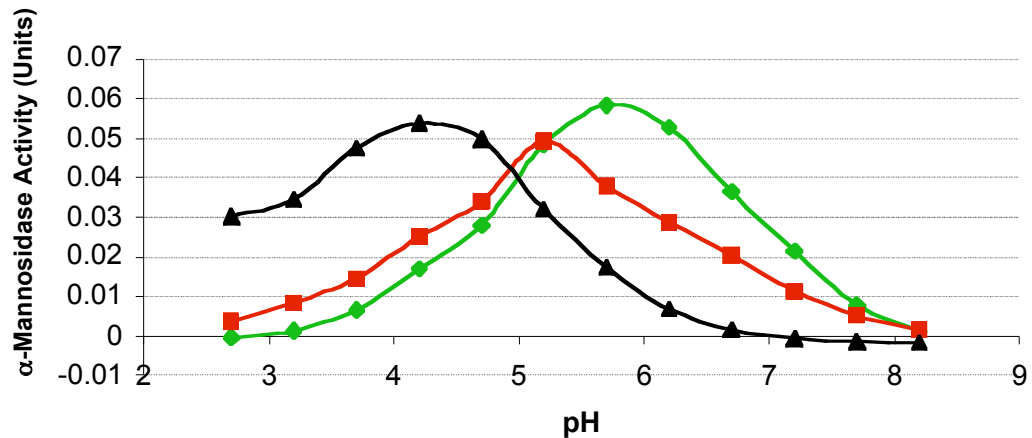
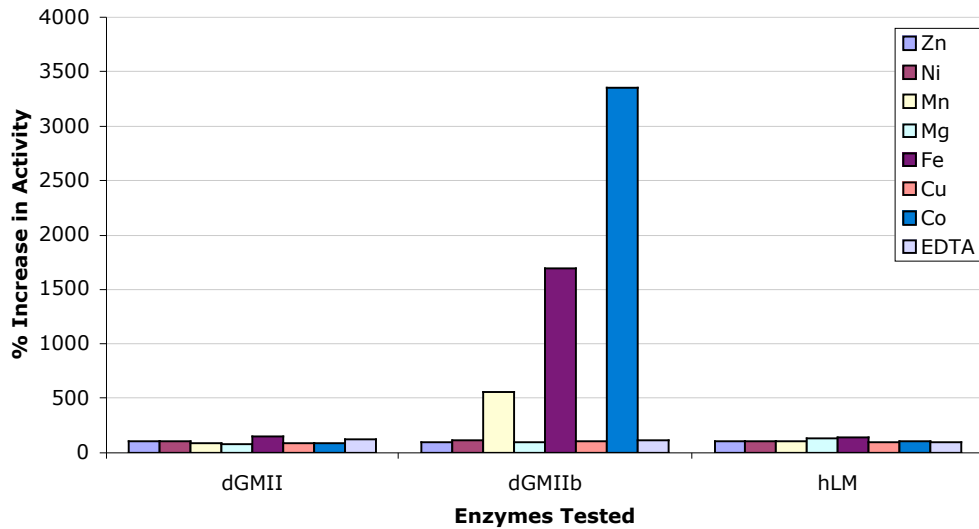


Figure 2.4: Determination of Optimum pH for Catalytic Activity.

This figure shows the cleavage of the synthetic substrate 4-methylumbelliferyl- α -D-mannopyranoside (4MU Man) over a pH range of 2.5 to 8 pH units by three different enzymes to determine the optimal pH for each enzyme. Each enzyme tested is colored as follows: dGMIIb, *Drosophila Melanogaster* Golgi mannosidase IIb (green diamond); dGMII, *Drosophila Melanogaster* Golgi Mannosidase II (red square); hLysMan, *Homo Sapiens* Lysosomal Mannosidase (black triangle). The optimal pH for each of the enzymes is 5.5 ± 0.2 , 5.0 ± 0.2 , 4.0 ± 0.2 , respectively.

2.5.1



2.5.2

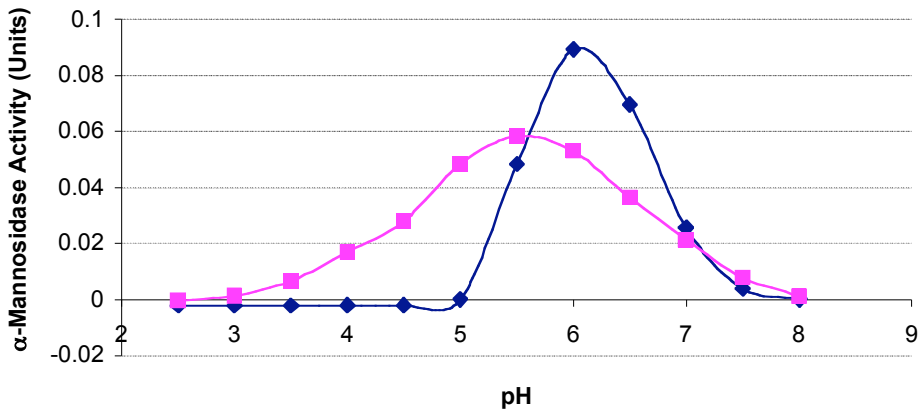


Figure 2.5: Metal Cation Requirement.

Figure 2.5.1 is a bar graph depicting the enhancement or inhibition of mannosidase activity of *Drosophila* Mannosidase II (dGMII), *Drosophila* Mannosidase IIb (dGMIIb) and human lysosomal mannosidase (hLM) with different metal cations indicated in the legend to the right of the bar graph. dGMIIb activity is enhanced by manganese (yellow bar), iron (brown bar), and cobalt (blue bar). The enhancement of dGMIIb activity by cobalt shifts its pH optimum from 5.5 ± 0.2 (pink square) to 6.0 ± 0.2 (blue diamond) as seen in figure 2.5.2.

Table 2.2: K_m and K_i Data with 4MU-Man Substrate and Selected Inhibitors.

Abbreviations are as follows: dGMII, *Drosophila melanogaster* Golgi mannosidase II; dGMIIb, *Drosophila melanogaster* Golgi Mannosidase IIb; hLysMan, *Homo Sapiens* lysosomal mannosidase; SWA, swainsonine; DIM, 1,4-di-deoxy-1,4-imino-D-mannitol; KIF, kifunensine; DMNJ, deoxymannojirimycin. dGMIIb is more sensitive to SWA and DIM than dGMII and hLysMan. dGMIIb is more sensitive to KIF than dGMII, but has comparable sensitivity with hLysMan. dGMIIb is more sensitive to DMNJ than dGMII or hLysMan.

| Inhibitor | Enzyme | | |
|-----------|--------------------------|--------------------------|--------------------------|
| | dGMII | dGMIIb | hLysMan |
| | $K_m = 4.90 \pm 2.60$ mM | $K_m = 0.90 \pm 0.10$ mM | $K_m = 0.80 \pm 0.40$ mM |
| SWA | $K_i = 0.30$ μ M | $K_i = 0.07$ μ M | $K_i = 0.50$ μ M |
| DIM | $K_i = 2.30$ μ M | $K_i = 0.03$ μ M | $K_i = 4.90$ μ M |
| KIF | $K_i = 2.30$ mM | $K_i = 28$ μ M | $K_i = 34$ μ M |
| DMNJ | $K_i = 580$ μ M | $K_i = 73$ μ M | $K_i = 625$ μ M |

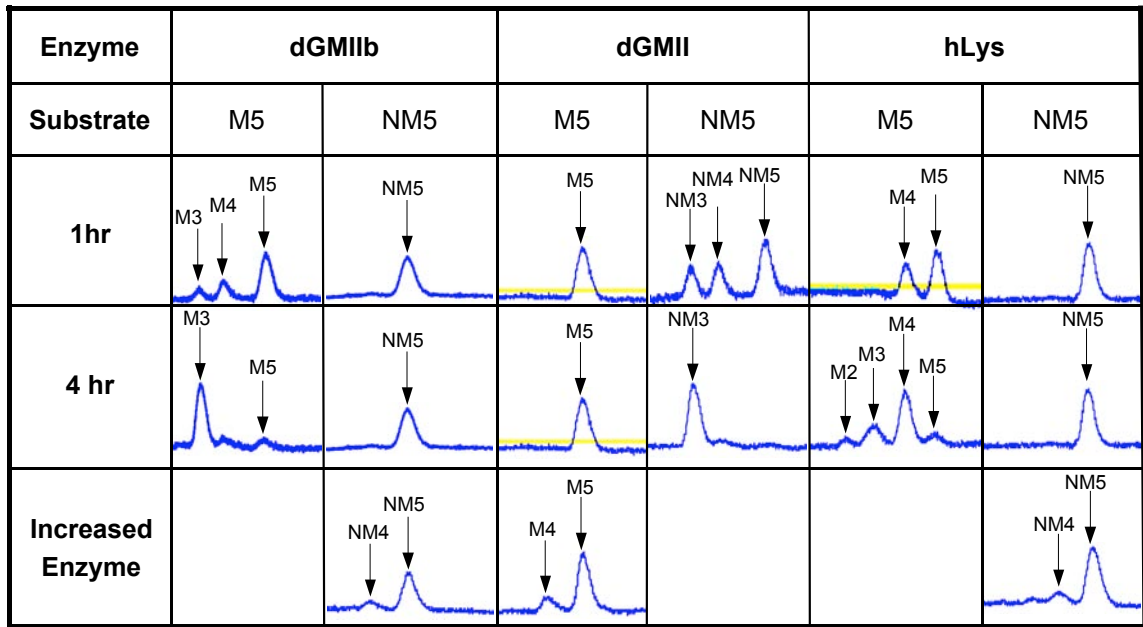


Figure 2.6: HPLC Chromatograms Depicting Natural Substrate Cleavage

All three proteins; dGMIIb (*Drosophila melanogaster* Golgi Mannosidase IIb), dGMII (*Drosophila melanogaster* Golgi mannosidase II), and hLys (*Homo Sapiens* lysosomal mannosidase) were incubated at 37 °C for 1 and 4 hours (hrs) with PA-tagged natural substrates M5 (Man₅GlcNAc₂-PA) and NM5 (GlcNAcMan₅GlcNAc₂-PA). Boiling for 8 – 10 minutes stopped the enzymatic reactions. Degradation products were separated on an amine column by HPLC. dGMIIb cleaved M5 after 1 and 4 hrs, but did not cleave NM5 under the same conditions. dGMII cleaved NM5 after 1 and 4 hrs but did not cleave M5 under the same conditions. hLys cleaved M5 after 1 and 4 hrs, but did not cleave NM5 under the same conditions. The natural substrate preferences for dGMIIb, dGMII, and hLys are M5, NM5, and M5, respectively. Substrates not preferred by each enzyme could be cleaved when the enzyme amount was increased as seen in the last row of chromatographic data. All data have been normalized to the appropriate substrate standards per assay. All data have been tested against the mannosidase inhibitor, swainsonine, and the hexosaminidase inhibitor, PUGNAc, to ensure cleavage shown is not the result of a hexosaminidase or mannosidase contaminant in the protein solutions. Abbreviations of substrates and cleavage products are as follows: M5, Man₅GlcNAc₂-PA; M4, Man₄GlcNAc₂-PA, M3, Man₃GlcNAc₂-PA; M2, Man₂GlcNAc₂-PA, NM5, GlcNAcMan₅GlcNAc₂-PA, NM4; GlcNAcMan₄GlcNAc₂-PA; NM3, GlcNAcMan₃GlcNAc₂-PA.

Table 2.3: K_m Data with Natural Substrates.

The data in the table above shows the K_m for each enzyme using its preferred substrate as indicated. The normalized K_m ratio of NM5N2-PA or M5N2-PA Affinity (x1000) is the K_m value of each enzyme with its preferred natural substrate normalized to the K_m value obtained with the synthetic substrate 4MU-Man, multiplied by 1000 for ease of comparison. The data indicate that while each enzyme has a similar affinity for its respective natural substrate, the affinity for the 4MU-Man synthetic substrate is significantly lower for dGMII. Abbreviations are as follows: dGMII, *Drosophila melanogaster* Golgi mannosidase II; dGMIIb, *Drosophila melanogaster* Golgi Mannosidase IIb; hLysMan, *Homo Sapiens* lysosomal mannosidase; M5N2, Man₅GlcNAc₂-PA; NM5N2, GlcNAcMan₅GlcNAc₂-PA.

| Enzyme | K_m (μ M) | Substrate | Normalized Ratio of NM5N2-PA or M5N2-PA Affinity (x1000) |
|---------|------------------|-----------|--|
| dGMIIb | 77.40 | M5N2 | 0.43 |
| dGMII | 89.60 | NM5N2 | 26.80 |
| hLysMan | 85.80 | M5N2 | 0.15 |

Table 2.4: Comparison of Natural Substrate Catalytic Turnover Normalized to 4MU-Man Synthetic Substrate.

The data in this table compares the rate of catalytic turnover for each enzyme using the indicated natural substrate, normalized to mannosidase activity with 4MU-Man. The normalized ratio of NM5N2-PA/M5N2-PA activity was calculated with the following equation $((\text{NM5N2-PA}/4\text{MU-Man})1000) / ((\text{M5N2-PA}/4\text{MU-Man})1000)$. dGMII appears to have the highest affinity towards its natural substrate in this normalized data which is believed to be imparted by GlcNAc binding. Abbreviations are as follows: dGMII, *Drosophila melanogaster* Golgi mannosidase II; dGMIIb, *Drosophila melanogaster* Golgi Mannosidase IIb; hLysMan, *Homo Sapiens* lysosomal mannosidase; M5N2, Man₅GlcNAc₂-PA; NM5N2, GlcNAcMan₅GlcNAc₂-PA, 4MU-Man, 4-methylumbelliferyl- α -D-mannopyranoside.

| Enzyme | Substrate | | Normalized Ratio of NM5N2-PA/M5N2-PA Activity |
|---------|----------------------------|---------------------------|---|
| | NM5N2-PA / 4MU-Man (x1000) | M5N2-PA / 4MU-Man (x1000) | |
| dGMII | 280 | 0.33000 | 848.50000 |
| dGMIIb | 0.00021 | 0.00160 | 0.13125 |
| hLysMan | 0.00560 | 1.90000 | 0.00295 |

Figure 2.7: Homolgy Modeling of dGMIIb and SfMII

Figure 2.7.1 represents a sequence alignment of the crystallized dGMII (magenta), bLysMan, and homology models dGMIIb (green) and SfMII (cyan). Residues highlighted red represent deletions made in the primary target sequence for modeling. Figure 2.7.2 are cartoon representatives of the final homology models; dGMIIb (green) and SfMII (cyan). Red spheres represent the α carbons of amino acid residues flanking the deletion sites. GlcNAcMan₅GlcNAc (grey sticks) is displayed in the putative binding region in the models based on the bound ligand in the dGMII structure. An active site Zn⁺² is represented by a dark grey sphere.

2.7.1

| | | | | | | |
|---------|-----|-------------|------------|------------|------------|---------------|
| dGMII | 31 | CQDVVQD | VPNVVQMLE | LYDRMSFKDI | DGGVVKQGW | IKYDPLKYNA |
| dGMIIb | 117 | YELIQSN | TNITASEEHS | KPDFQPEWMR | SKEYWDRGFE | ERFDAQKKDK |
| SfMII | 70 | DOCPALKESE | ADIDTVAIYP | TDFQPSWLR | TKEFWDKSFE | DRYERIHNDT |
| blysman | 51 | | | | | GYKTCPKV |
| . | | | | | | |
| dGMII | 78 | HHK-LKVFV | PHSHNDPGWI | QTFEEYY--- | ----QHDTKH | -ILSNALRHL |
| dGMIIb | 164 | QRPLKIIVV | PHSHNDPGWL | KTFTNYF--- | ----QSDSRQ | -ILNLLVTKM |
| SfMII | 120 | TRPRLKVIIV | PHSHNDPGWL | KTFEQYF--- | ----EWKTKN | -IINNIVNKL |
| blysman | 59 | KPDMLNVHLV | PTHDDVQWL | KTVDQYFYGI | YNNIQPAGVQ | YILDSVISSL |
| | | *..* | ***.* | *** | *..* | . . . * . . . |
| dGMII | 119 | HDNPEMKFIW | AEISYFARFY | HDLGENKKLQ | MKSIVKNGQL | EFVTGGWVMP |
| dGMIIb | 206 | QEYTDMTFIW | SEISFLQLWW | DQAHPTKQRA | LKRLIDAGRI | EITTTGGWVMT |
| SfMII | 162 | HOYPNMTFIW | TEISFLNAW | ERSHPVKQKA | LKKLIKEGRL | EITTTGGWVMP |
| blysman | 109 | LANPTRRFIY | VEIAFFSRWW | RQQTNATQKI | VRELVRQGR | EFANGGWVMN |
| | | ** | ***.. | | * | *. ***** |
| dGMII | 169 | DEANSHWRNV | LLQLTEGQW | LKQFM--NVT | PTASWAIAPF | GHSPTMPYIL |
| dGMIIb | 256 | DEANVHIYPM | LDQLIEGHQW | LKNNL--NVT | PKVGSIDPF | GHGSTVYPYLL |
| SfMII | 212 | DEACTHIYAL | IDQFIEGHWW | VKTNL--GVI | PKTGSIDPF | GHGATVYPYLL |
| blysman | 159 | DEATTHYGAI | IDQMTLGLRF | LEETFGSDGR | PRVAWHIDPF | GHSREQASLF |
| | | *** | * | . . * | * . * * ** | ** |
| dGMII | 217 | QKSGFKNMLI | ORTHYSVKKE | LAQOROLEFL | WRQIW----D | NKGDTA-LFT |
| dGMIIb | 304 | SGANFEGTII | QRIHYAWKQW | FARQOSGDFI | WKPYWRSRKD | KDSEAGSLLT |
| SfMII | 260 | DQSGLEGTII | QRIHYAWKQW | LAERQIEEFY | WLASWATTKP | -----SMIV |
| blysman | 209 | AQMFGDGFPP | GRLDYQDKK- | -VRKKTLOM- | -EQVWRASTS | LKPPTADLFT |
| | | . . . | * * * | . . . | * | . . . |
| dGMII | 262 | HMMPFYSDI | PHTCGDPKV | CCQDFKRMG | SFGLSCPWKV | PPRTISQNV |
| dGMIIb | 354 | HNMPFDIYSI | KGSCGPHFPI | CLNFDFRKIP | --GEYTEYSV | KAQFITDDNL |
| SfMII | 304 | HNQPFDIYSI | KSTCGPHPSI | CLSFDFRKIP | --GEYSEYTA | KHEDITEHNL |
| blysman | 255 | SVLP-NMYN- | -----PPEGL | CWDMLCADKP | --V--VEDTR | SPEYNAKELV |
| | | * | * | * . * | . . . | . . . |
| dGMII | 312 | AARSDLLVDQ | WKKKAELYRT | NVLLIPLGDD | FRFKQNTQEW | VQRVNYERLF |
| dGMIIb | 402 | ESKAQLLEQ | YARTASLFP | NVALIPVGDD | FRYNKDREVD | QOQYNYKKLI |
| SfMII | 352 | HSKAKTLIEE | YDRIGSLTPH | NVVLVPLGDD | FRYEYSVEFD | AQYVNYMKMF |
| blysman | 294 | ----RYFLKL | ATDQGLYRT | KHTVMTMGSD | FQYENA---N | TWFKNLDKLI |
| | | . . . | . * | . . . * * | *.. | . * . . . |
| dGMII | 362 | EHI-NSQAHF | NVQAQFGTLQ | EYFDAQHQA | RAGQAEFPTL | SGDFFTYADR |
| dGMIIb | 452 | DHIMANRRLY | NADIRFGTPS | DYFEAIKERM | KDHTPGFPTF | KGDFVYSDI |
| SfMII | 402 | NYINAHKEIF | NADVQFGTPL | DYFNAMKERH | QN----IPSL | KGDFVYSDI |
| blysman | 337 | QLVNPAIR--- | -VNVLYSTPA | CY---LWE-L | NKANLSWSVK | KDDFFPYAD- |
| | | . . . | ..* | * . . | . . . | *** * . * |
| dGMII | 411 | -SD---NYWS | GYTSPRYHK | RMDRVLHMYV | RAAEML---- | --SAWS-WD |
| dGMIIb | 502 | FSEGRPAYWS | GYFTTRPFYK | LLSSELEHQL | RSAEIVFTLA | YNTARQAKRE |
| SfMII | 448 | FSE----YWS | GYTTRPYQK | ILAROFEHQL | RSAEILFTLV | SNYIROMGRO |
| blysman | 383 | ---GPYFWT | GYFSSRPALK | RYERLSYNFL | QVCNQLEALA | GPGDSAPLNE |
| | | . * | ***..** | * | | |
| dGMII | 450 | GMA----RIE | ER----LEQA | RRELSLFQHH | DGITGTAKTH | VVDYEQRMQ |
| dGMIIb | 552 | NAI----KIY | EKNYELIINA | RRNLGLFQHH | DAITGTSKAA | VMRDYAMRLF |
| SfMII | 494 | GEFGASEKKL | EKSQEQLIYA | RRNLGLFQHH | DAITGTSKSS | VMQDYGTKLF |
| blysman | 439 | AMAVLQHHDA | VSGTSRQHVA | NDYARQLSEG | WRPCEVLMNS | ALAHLSGLKE |
| | | . . . | * | . . . | . . . | . . . |

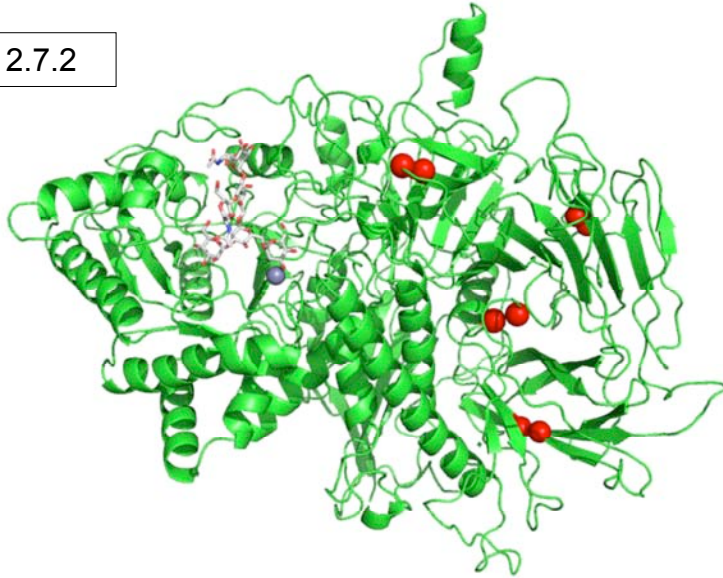
2.7.1

| | | | | | | |
|---------|------|------------|------------|------------|------------------------|------------------------|
| dGMII | 492 | EALKACQVMV | QOSVYRLLTk | -----PSIY | SPDFSFsYFT | LDDSRWPGSG |
| dGMIIb | 598 | ESTQNmvkMQ | ESCLELLLOK | GQPRH-HGFL | LSEFERDNFN | KLPRKMP IAN |
| SfMII | 544 | TSlyHCIRLQ | EAALtTIMLP | DOSLHSQSII | QSEVEWETYG | KPPKKLOVSF |
| blysman | 489 | DFAFCRKLNI | SICPLtQTAE | RFQVIVYNPL | GRKVDWMVRL | PVSKHVYLvK |
| . | | | | | | |
| dGMII | 536 | VEDSRtTIIL | GED----ILP | SKHVVMHNTL | PHWREQLVDF | YVSSPFVS-V |
| dGMIIb | 647 | GDESTPTVPA | GEGGAGGSSS | SGSVVLYNSL | AQKRLE VVTL | RVQHPNVKIV |
| SfMII | 594 | IDKKK----- | ----- | ---VILFNPL | AETRTEVVTV | RSNTSNIRVY |
| blysman | 539 | DPGGKIVPSD | VVTIPSSDSQ | ELLFSALVPA | VGFSIYSVSQ | MPRDLVIQNE |
| * | | | | | | |
| dGMII | 581 | TDLANNPVEA | QVSPVWS--- | WHHDILTktI | -----HPOGS | TTKYRIIFKA |
| dGMIIb | 697 | NDKGVELNHI | QINPVWNITD | TYEQGLGTSV | SGTVGRIRTS | TRQFEVMFVA |
| SfMII | 626 | DTHKRKHVLY | QIMP--SITI | ---QDNGKSI | -----VSDT | T--FDIMFVA |
| blysman | 611 | YLRARFDpNT | GLLMELENLL | LLPVRQAFYw | YNASTGNNLS | SOASGAYIFR |
| . | | | | | | |
| dGMII | 623 | RVPPMGLATY | VLtISD---S | KPEHTSYASN | LLLRKNPTSL | PLGQYPEDVK |
| dGMIIb | 747 | ELEPLSLStY | RVQDEVNFk | RNIATiYcDD | CTESQPASVS | PPEEIESPT |
| SfMII | 663 | TIPPLTSISY | KLQ-EHTNTS | HHCv-IFcNN | CEQYQKSNV- | ----- |
| blysman | 664 | PNQNKPLFVS | HWAQThLVKA | SLVQEVHQNf | SAWCSQVVRL | YPRQRHLELE |
| . | | | | | | |
| dGMII | 670 | FG-DPREIS- | --LRVNGGPT | -LAFSEQ-GL | LKSIQLTQDS | PHVPVHFk-F |
| dGMIIb | 797 | SVFEARGKPA | GDIQLENPHM | -LlFDEKSGF | LKTITRKNQK | KELLKPLQCN |
| SfMII | 700 | --FQIKMMP | GDIQLENAVL | KLLVNRNTGF | LRQVYRKDIR | KRTVv----D |
| blysman | 714 | WTVGPIPVGD | GWGKEVISRF | DTALATRGLF | YtDSNGREIL | ERRRNYRPTW |
| . | | | | | | |
| dGMII | 713 | LKYGV-RSHG | DRSGAYLFLP | NGPASPVE-- | ----LGQ--- | PV---VLVTK |
| dGMIIb | 846 | IKFAAYRSAQ | FHSGAYLFkT | DPEQSEAEKE | VLEGYTD--- | MR---IIITS |
| SfMII | 744 | VQFGAYQSAQ | RHSGAYLFM- | -PHYDSPEKN | VLHPYTNQNN | MQDDNIIIVS |
| blysman | 764 | KLNQTEPVAG | NYYPVNSRIY | ITDGNMQLTV | LtDRSQGGSS | LRDGSLELMV |
| . | | | | | | |
| dGMII | 750 | GKLESSVSVG | LPSVvhQTI- | ---MRG---- | GAPeIRNLVD | IGSLDN---T |
| dGMIIb | 890 | GPIASDVtVI | YGPFLAHTVR | IFNTRTh-LD | AAIYVENDID | FEPppK---T |
| SfMII | 792 | GPISTEITTM | YLPFLVHTIR | IYNVPDPVLS | RAILLETdVD | FEAPPKNRET |
| blysman | 814 | HRRLlKDDAR | GVGEPLNKEG | SGLWVRGRHL | VLLDKKETAA | ARHRLQAEME |
| . | | | | | | |
| dGMII | 789 | EIVMRLETHI | DSGD----- | ----- | -----IFYT | DLNGLQFIKR |
| dGMIIb | 936 | ELFMRFVTNI | DNIAQAPMQR | DPLKEPVDAA | TMPELpVFYS | DONGFOYHER |
| SfMII | 842 | ELFMRLQTDI | QN----- | ----- | --GDIPEFYT | DONGFOYQKR |
| blysman | 864 | VLAPQVVLAQ | GPRTQFSGLR | RELPPSVRLL | TlARWGPETL | LLRLEHQFAV |
| . | | | | | | |
| dGMII | 817 | RRLDKLPLQA | NYYPiPSGMF | IEDANTRlTL | LtGQPLGGSS | LASGELEIMQ |
| dGMIIb | 986 | IKVPAIGIEG | NYFPITSGAF | IQDSRLRLTL | LtTHAQGAAS | YEPGQLEVML |
| SfMII | 872 | VKVNLGIEA | NYYPITTMAC | LQDETRlTL | LtNHAQGAAA | YEPGRLEVML |
| blysman | 924 | GEDSGRNlSS | PVtLDLtnLF | SAFTITNLRE | TtLAANQLLA | YASRLQWTTD |
| . | | | | | | |
| dGMII | 867 | DRRLASDDER | GLGQGVLDNK | PVLHIYRLVL | EKVNN---CV | RPSKLHPAG- |
| dGMIIb | 1036 | DRRTLYDDYR | GMGEGVDSR | LTRHKFWLLV | EDLPG---GQ | HVTQPPSYK- |
| SfMII | 922 | DRRTLYDDFR | GIGEGVVDNK | PtTFQNWILI | ESMPGVTRAK | RDTSEPGFKF |
| blysman | 988 | ATITLQPMEl | RTFLASVQW | | | |
| . | | | | | | |
| dGMII | 913 | ----- | -----YlTS | AAHKASQSLl | DPLDKFIFAE | NEWIGAQOGF |
| dGMIIb | 1082 | ----- | -----VLSQ | QAQQLANALR | YPPNLYFVSN | LEQPELAAAL |
| SfMII | 972 | VNERRFGPGQ | KESPYQVPSQ | TADYLSRMFN | YpVNvYLVDT | SEVGEIEVK- |

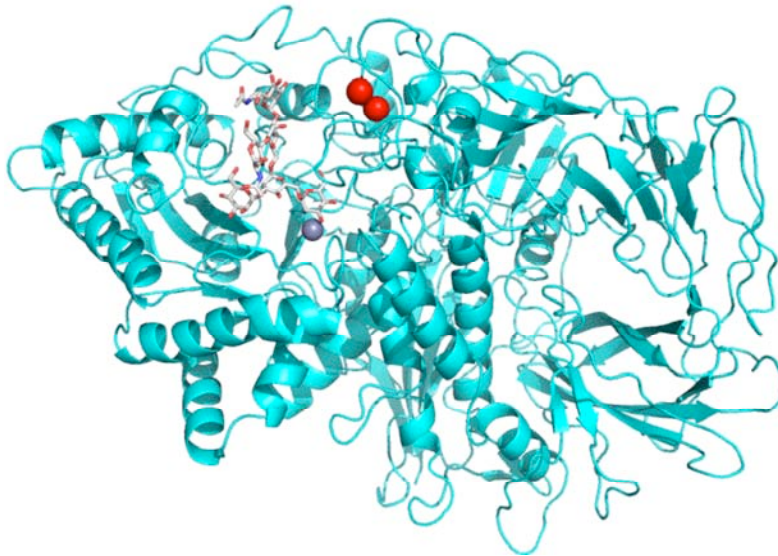
| | | | | | | |
|--------|------|------------|------------|------------|------------|------------|
| dGMII | 947 | GGDHPSARED | LDVSMRRLT | KSSAKTORVG | YVLHRTNLMQ | CGTPEEHTQK |
| dGMIIb | 1116 | LPLVRLLPKG | PLPCDVHLTT | LRTLSDPELQ | LFPSASALLV | LHRQGFDCSV |
| SfMII | 1021 | -PYQSFLQ-- | SFPPGIHLVT | LRTITDDVLE | LFPSNESYMV | LHRPGYSCAV |

| | | | | | | |
|--------|------|------------|------------|------------|------------|------------|
| dGMII | 997 | LDVCHLLPNV | ARCERTTLTF | LQNLHLDGM | VAPEVCPMET | AAYVSSHs |
| dGMIIb | 1166 | SAGRELSMEA | ICPLSSKGLG | NVQLGRSLH | TIATSLTGT | EOKSSRES-- |
| SfMII | 1068 | GEKPVAKSPK | FSSKTRFNGL | NIQNITAVSL | TG- | |

2.7.2



dGMIIb



SfMII

2.8.1

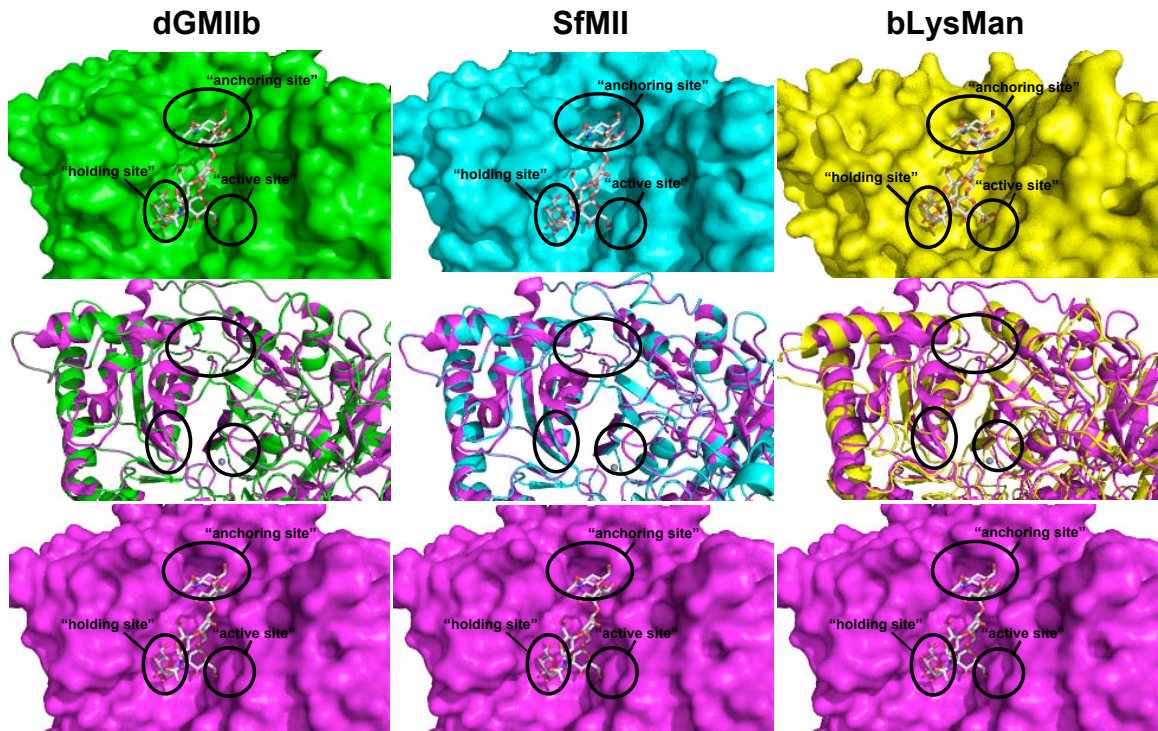


Figure 2.8.1: Comparison of Binding Regions in Homology Models and Superimposed Structure

Figure 2.8.1 shows one orientation of dGMIIb (green), SfMII (cyan), bLysMan (yellow) and dGMII (magenta) in surface representations (top and bottom, left to right, respectively) and a superimposed cartoon representation (middle, left to right respectively) to highlight the three binding regions in the dGMII binding pocket of GlcNAcMan₅GlcNAc (grey stick figure). A Zn⁺² cation is represented as a dark grey sphere occupying the active site. The “anchoring region”, “holding site”, and “active site” are circled in black and labeled for reference in the upper and lower panels in the surface representations of the proteins. This figure illustrates differences in the regions of dGMII’s substrate binding site.

2.8.2

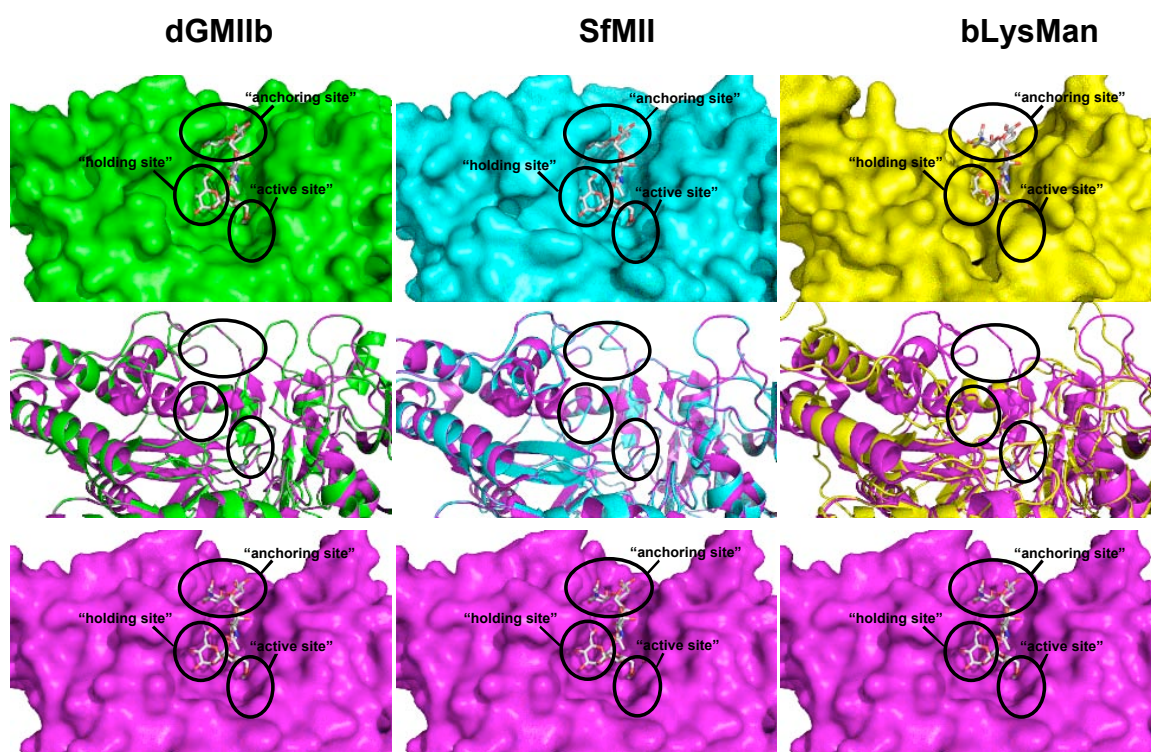


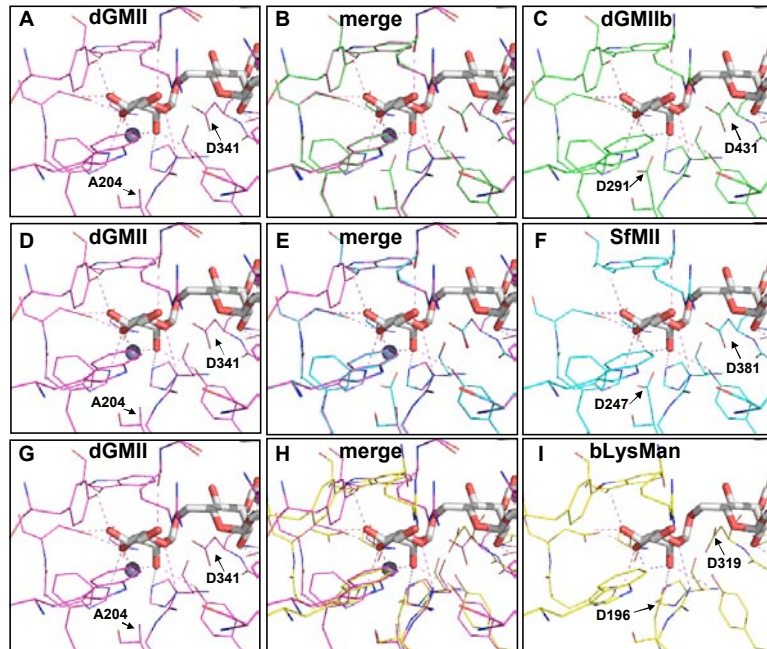
Figure 2.8.2: Comparison of Binding Regions in Homology Models and Superimposed Structure

Figure 2.8.2 shows another orientation of dGMIIb (green), SfMII (cyan), bLysMan (yellow) and dGMII (magenta) in surface representations (top and bottom, left to right, respectively) and a superimposed cartoon representation (middle, left to right respectively) to highlight the three binding regions in the dGMII binding pocket of GlcNAcMan₅GlcNAc (grey stick figure). A Zn⁺² cation is represented as a dark grey sphere occupying the active site. The “anchoring region”, “holding site”, and “active site” are circled in black and labeled for reference in the upper and lower panels in the surface representations of the proteins. This figure illustrates differences in the regions of dGMII’s substrate binding site.

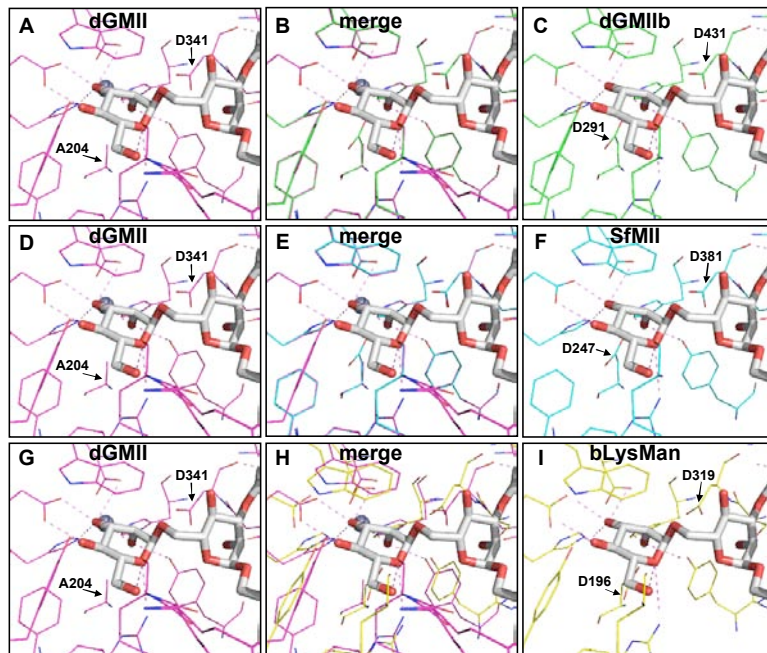
Figure 2.9: The Active Site

In these two sets of panels the active site is shown with the bound or superimposed substrate (grey sticks) in two orientations (2.9.1 and 2.9.2) and all residues (lines: dGMII, magenta; dGMIIb, green; SfMII, cyan; bLysMan, yellow) with atoms within 4 Å away from the substrate. The panels are occupied as follows: A, D, G, dGMII; B, dGMII/dGMIIb merge; C, dGMIIb; E, dGMII/SfMII merge; F, SfMII; H, dGMII/bLysMan merge; I, bLysMan. The active site is the most highly conserved region between all four proteins. Each protein has a representative Asp nucleophile and an Asp catalytic acid base. Zn is represented by a dark grey sphere and occupies bLysMan's active site in its crystal structure (not shown). Hydrogen bonding and ionic interactions are represented by violet dashes are indicative of the interactions in the dGMII structure only, but shown in all figures for ease of comparison.

2.9.1



2.9.2



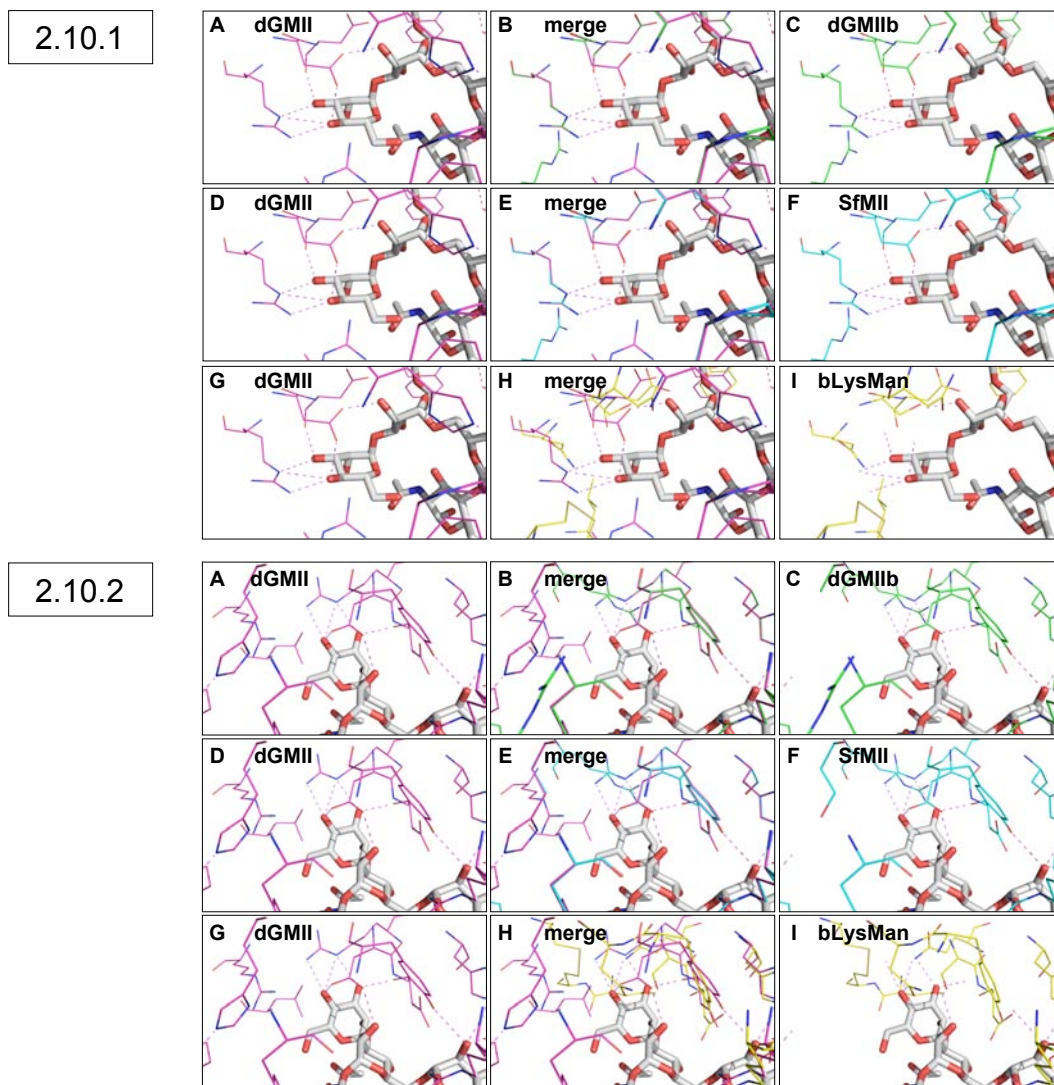


Figure 2.10: The Holding Site

In these two sets of panels the holding site is shown with the bound substrate (grey sticks) in two orientations (2.10.1 and 2.10.2) and all residues (lines: dGMII, magenta; dGMIIb, green; SfMII, cyan; bLysMan, yellow) with atoms within 4 Å away from the substrate. The panels are occupied as follows: A, D, G, dGMII; B, dGMII/dGMIIb merge; C, dGMIIb; E, dGMII/SfMII merge; F, SfMII; H, dGMII/bLysMan merge; I, bLysMan. In these two sets of panels the α 1,6 linked mannose, second in line for cleavage is stabilized by hydrogen bonding interactions (violet dashes). The holding site is well conserved between dGMII, dGMIIb, and SfMII, but not bLysMan. Hydrogen bonding interactions represented by violet dashes are indicative of the interactions in the dGMII structure only, but shown in all figures for ease of comparison.

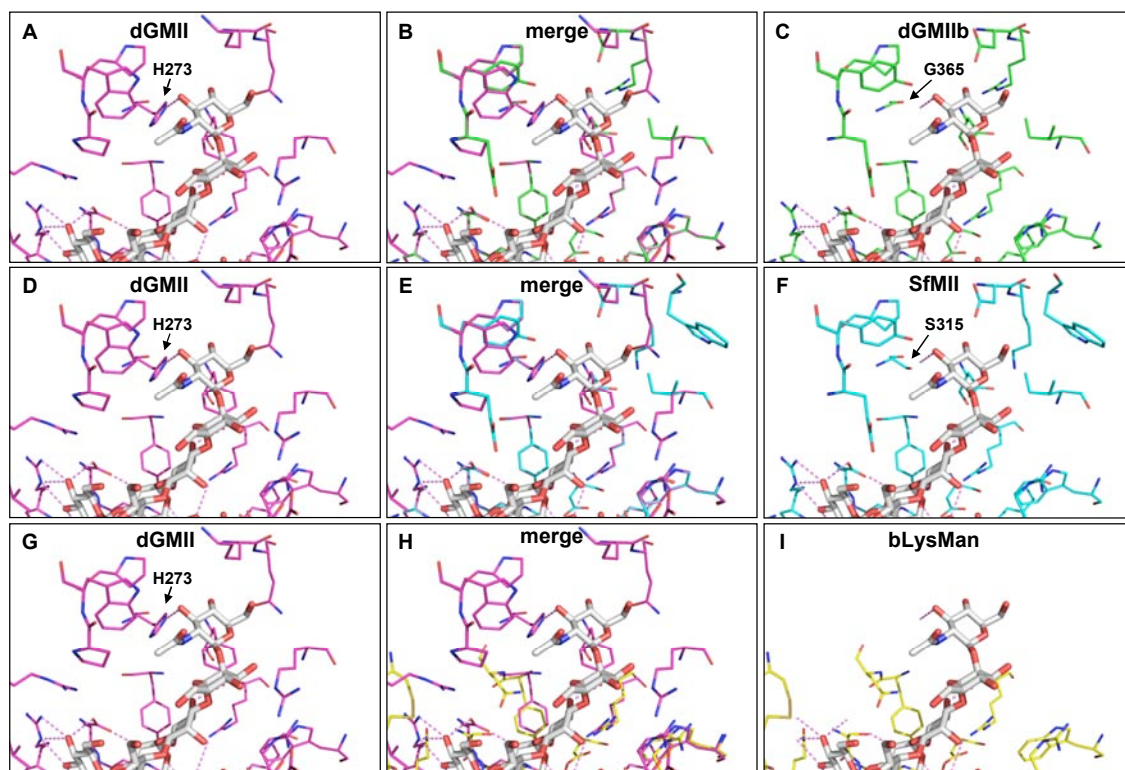


Figure 2.11.1: The Anchoring Site

In this first set of panels the anchoring site is shown with the bound substrate (grey sticks) and all residues (lines: dGMII, magenta; dGMIIb, green; SfMII, cyan; bLysMan, yellow) with atoms within 4 Å away from the substrate. The panels are occupied as follows: A, D, G, dGMII; B, dGMII/dGMIIb merge; C, dGMIIb; E, dGMII/SfMII merge; F, SfMII; H, dGMII/bLysMan merge; I, bLysMan. This first set of panels is oriented to display the His273 residue directly involved in hydrogen bonding with the GlcNAc residue of the bound substrate. The anchoring site is the least conserved between all four proteins. Both dGMIIb and SfMII have residues in this region that seem to make up a pocket, but the important His residue is absent in both of these proteins and is made up of much shorter amino acid residues (Gly and Ser, respectively). The bLysMan is not only lacking a His, but appears to not have a pocket in this region at all. Hydrogen bonding interactions represented by violet dashes are indicative of the interactions in the dGMII structure only, but shown in all figures for ease of comparison.

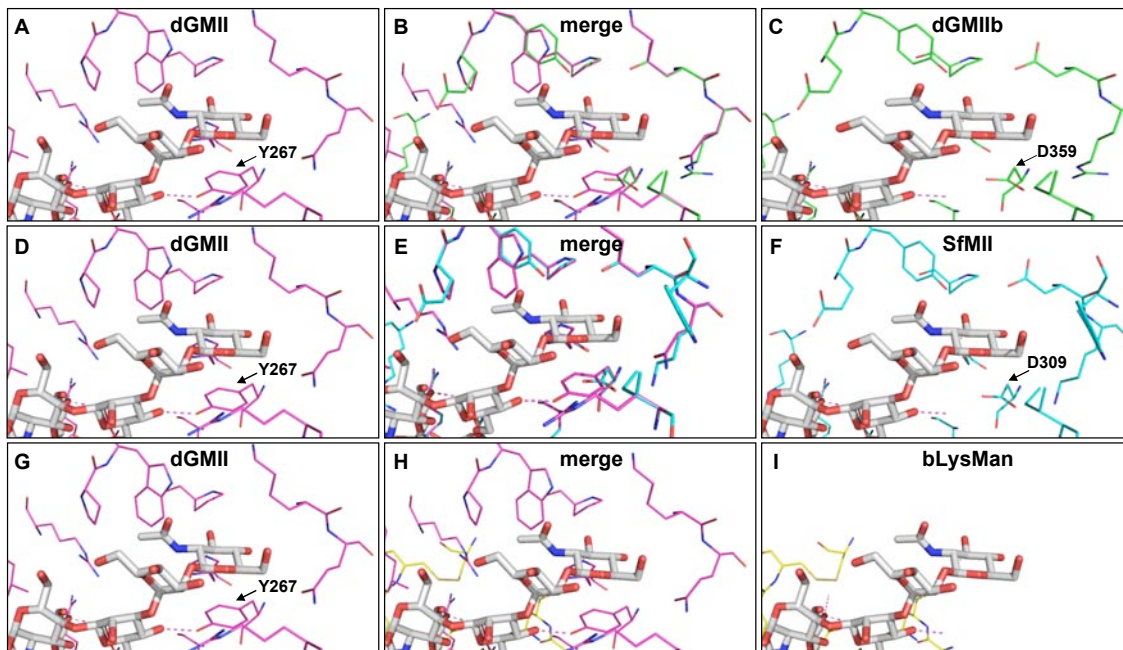


Figure 2.11.2: The Anchoring Site

In this second set of panels the anchoring site is shown with the bound substrate (grey sticks) and all residues (lines: dGMII, magenta; dGMIIb, green; SfMII, cyan; bLysMan, yellow) with atoms within 4 Å away from the substrate. The panels are occupied as follows: A, D, G, dGMII; B, dGMII/dGMIIb merge; C, dGMIIb; E, dGMII/SfMII merge; F, SfMII; H, dGMII/bLysMan merge; I, bLysMan. This set of panels is oriented to display the Tyr267 residue directly involved in hydrogen bonding with the core mannose residue of the substrate and most likely involved in stacking interaction with the GlcNAc residue. The anchoring site is the least conserved between all four proteins. dGMIIb and SfMII have an Asp residue in this region instead of an Tyr, which is too far away from both of the sugar residues in the ligand. The bLysMan is once again lacking residues of the anchoring site. Hydrogen bonding interactions represented by violet dashes are indicative of the interactions in the dGMII structure only, but shown in all figures for ease of comparison.

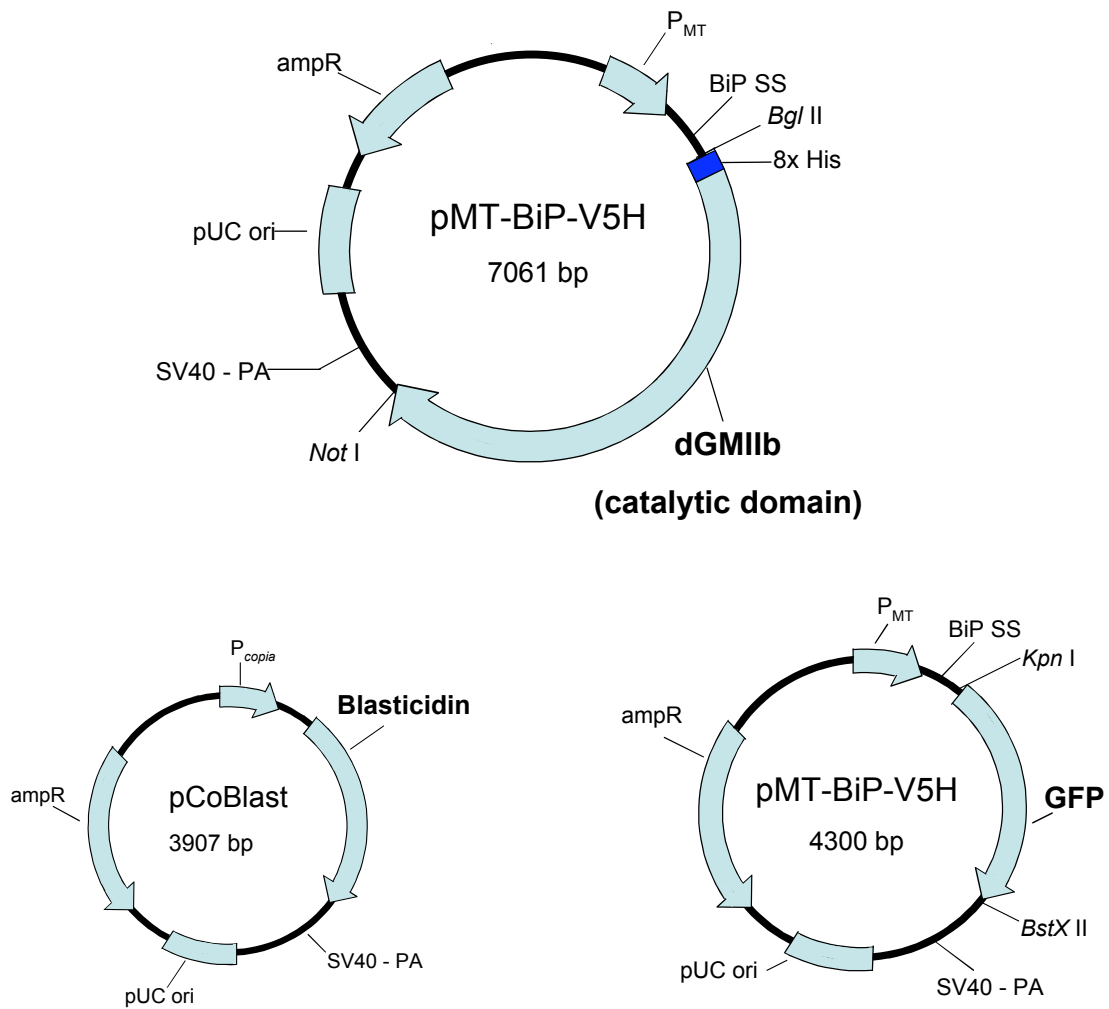


Figure 2.12: Constructs Used for Expression.

The constructs above were co-transfected into S2 cell lines using a calcium phosphate transfection method. The GeneArt construct, pMT-BiP-V5H/dGMIIB contains a metallothionine promoter (P_{MT}), BiP Secretion signal sequence (BiP SS), and an 8x His tag (bright blue segment) incorporated into the dGMIIB sequence. The pCoBlast construct imparts blasticidin antibiotic resistance. The pMT/BiP/V5-His/GFP vector has an inducible GFP with a His tag for fluorescent or antibody detection.